



**UNIVERSIDAD DE INVESTIGACIÓN DE
TECNOLOGÍA EXPERIMENTAL YACHAY**

Escuela de Ciencias de la Tierra, Energía y Ambiente

**TÍTULO: PHYSIOGRAPHIC CONTROLS OF RUNOFF
RESPONSE OF MICRO-CATCHMENTS IN THE MIRA
WATERSHED (ECUADOR)**

Trabajo de integración curricular presentado como requisito para la
obtención del título de Geología.

Autor:

Gordillo Urresta Jonathan Patricio

Tutor:

Ph. D. Pineda Ordóñez Luis Eduardo

Urcuquí, agosto 2019

Urcuquí, 21 de agosto de 2019

SECRETARÍA GENERAL
 (Vicerrectorado Académico/Cancillería)
ESCUELA DE CIENCIAS DE LA TIERRA, ENERGÍA Y AMBIENTE
CARRERA DE GEOLOGÍA
ACTA DE DEFENSA No. UITEY-GEO-2019-00001-AD

En la ciudad de San Miguel de Urcuquí, Provincia de Imbabura, a los 21 días del mes de agosto de 2019, a las 09:00 horas, en el Aula AI-102 de la Universidad de Investigación de Tecnología Experimental Yachay y ante el Tribunal Calificador, integrado por los docentes:

Presidente Tribunal de Defensa	<u>Dr. GOMEZ PAREDES, JORGE ESTEBAN Ph.D.</u>
Miembro No Tutor	<u>Mgs. AGUIRRE SIACHOQUE, LUIS FELIPE</u>
Tutor	<u>Dr. PINEDA ORDOÑEZ, LUIS EDUARDO Ph.D.</u>

Se presenta el(la) señor(ita) estudiante **GORDILLO URRESTA, JONATHAN PATRICIO**, con cédula de identidad No. 1003159280, de la **ESCUELA DE CIENCIAS DE LA TIERRA, ENERGÍA Y AMBIENTE**, de la Carrera de **GEOLOGÍA**, aprobada por el Consejo de Educación Superior (CES), mediante Resolución **RPC-SE-10-No.031-2016**, con el objeto de rendir la sustentación de su trabajo de titulación denominado: **Physiographic controls of runoff response of micro-catchments in Mira watershed (Ecuador)**,. previa a la obtención del título de **GEOLOGO/A**.

El citado trabajo de titulación, fue debidamente aprobado por el(los) docente(s):

Tutor	<u>Dr. PINEDA ORDOÑEZ, LUIS EDUARDO Ph.D.</u>
--------------	---

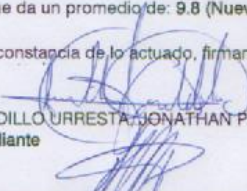
Y recibió las observaciones de los otros miembros del Tribunal Calificador, las mismas que han sido incorporadas por el(la) estudiante.

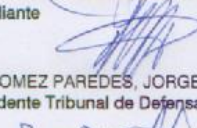
Previamente cumplidos los requisitos legales y reglamentarios, el trabajo de titulación fue sustentado por el(la) estudiante y examinado por los miembros del Tribunal Calificador. Escuchada la sustentación del trabajo de titulación, que integró la exposición de el(la) estudiante sobre el contenido de la misma y las preguntas formuladas por los miembros del Tribunal, se califica la sustentación del trabajo de titulación con las siguientes calificaciones:

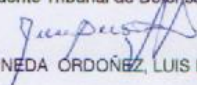
Tipo	Docente	Calificación
Presidente Tribunal De Defensa	Dr. GOMEZ PAREDES, JORGE ESTEBAN Ph.D.	9,9
Miembro Tribunal De Defensa	Mgs. AGUIRRE SIACHOQUE, LUIS FELIPE	9,7
Tutor	Dr. PINEDA ORDOÑEZ, LUIS EDUARDO Ph.D.	10,0

Lo que da un promedio de: **9.8 (Nueve punto Ocho)**, sobre 10 (diez), equivalente a: **APROBADO**

Para constancia de lo actuado, firman los miembros del Tribunal Calificador, el/la estudiante y el/la secretario ad-hoc.


GORDILLO URRESTA, JONATHAN PATRICIO
Estudiante


Dr. GOMEZ PAREDES, JORGE ESTEBAN Ph.D.
Presidente Tribunal de Defensa


Dr. PINEDA ORDOÑEZ, LUIS EDUARDO Ph.D.
Tutor



[Signature]
 Mgs. AGUIRRE SIACHOQUE, LUIS FELIPE
 Miembro No Tutor

[Signature]
 TERAN ROSALES, ANDREA YOLANDA
 Secretario Ad-hoc

SECRETARÍA GENERAL
 (Instituto Académico/Instituto)
 ESCUELA DE CIENCIAS DE LA TIERRA, ENERGÍA Y AMBIENTE
 CARRERA DE GEOLOGÍA
 ACTA DE DEFENSA Nº. UTU-GEO-2019-0001-40

En la ciudad de San Miguel de Utcubamba, Provincia de Imbabura, a los 21 días del mes de agosto de 2019, a las 10:00 horas, en la Aula A1-102 de la Universidad de Investigación de Tecnología Experimental Yachay y ante el Tribunal Calificador,

Presidencia Tribunal de Defensa: D. GONZALEZ PAREDES, JORGE ESTEBAN P.R.D.
 Miembro No Tutor: Mgs. AGUIRRE SIACHOQUE LUIS FELIPE
 Tutor: D. PINEDA GONZALEZ LUIS EDUARDO P.R.D.

Se presenta el/la señor/la estudiante GONZALEZ LUIS FELIPE, JONATHAN PATRICIO con cédula de identidad No. 100123890, de la ESCUELA DE CIENCIAS DE LA TIERRA, ENERGÍA Y AMBIENTE de la Carrera de GEOLOGÍA, convocados por el Consejo de Educación Superior (CES) mediante Resolución RUC-25-10-16-021-2018, con el objeto de rendir la evaluación de su trabajo de titulación denominado: "Fisiografía del control de ruidos en respuesta de micro-estructuras en la zona de estudio", previa a la obtención del título de GEOLOGÍA.

En el acto de la evaluación, los estudiantes expusieron su trabajo de titulación.

Y recibió las observaciones de los otros miembros del Tribunal Calificador, las mismas que han sido respondidas por el/la estudiante.

Finalmente cumplidos los requisitos legales y reglamentarios, el trabajo de titulación fue sustentado por el/la estudiante y examinado por los miembros del Tribunal Calificador. Basándose en la sustentación del trabajo de titulación, que incluyó la exposición de el/la estudiante sobre el contenido de la misma y las preguntas formuladas por los miembros del Tribunal, se otorga la sustentación del trabajo de titulación con las siguientes calificaciones:

Nombre	Calificación
Presidencia Tribunal de Defensa: D. GONZALEZ PAREDES, JORGE ESTEBAN P.R.D.	2.0
Miembro No Tutor: Mgs. AGUIRRE SIACHOQUE LUIS FELIPE	2.0
Tutor: D. PINEDA GONZALEZ LUIS EDUARDO P.R.D.	2.0

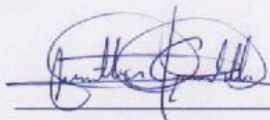
Lo que se da por promulgado. Se firmó en la ciudad de San Miguel de Utcubamba, a los 21 días del mes de agosto de 2019, a las 10:00 horas, en la Aula A1-102 de la Universidad de Investigación de Tecnología Experimental Yachay y ante el Tribunal Calificador, con la siguiente firma:

[Signature]
 GONZALEZ LUIS FELIPE, JONATHAN PATRICIO
 Estudiante
 D. GONZALEZ PAREDES, JORGE ESTEBAN P.R.D.
 Presidencia Tribunal de Defensa
[Signature]
 D. PINEDA GONZALEZ LUIS EDUARDO P.R.D.
 Tutor

AUTORÍA

Yo, **Jonathan Patricio Gordillo Urresta**, con CI 1003159280 declaro que las ideas, juicios, valoraciones, interpretaciones, consultas bibliográficas, definiciones y conceptualizaciones expuestas en el presente trabajo; así cómo, los procedimientos y herramientas utilizadas en la investigación, son de absoluta responsabilidad de el/la autora (a) del trabajo de integración curricular. Así mismo, me acojo a los reglamentos internos de la Universidad de Investigación de Tecnología Experimental Yachay.

Urcuquí, agosto 2019



Jonathan Patricio Gordillo Urresta

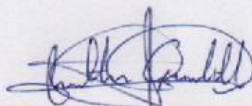
CI: 1003159280

AUTORIZACIÓN DE PUBLICACIÓN

Yo, **Jonathan Patricio Gordillo Urresta**, con cédula de identidad 1003159280, cedo a la Universidad de Tecnología Experimental Yachay, los derechos de publicación de la presente obra, sin que deba haber un reconocimiento económico por este concepto. Declaro además que el texto del presente trabajo de titulación no podrá ser cedido a ninguna empresa editorial para su publicación u otros fines, sin contar previamente con la autorización escrita de la Universidad.

Asimismo, autorizo a la Universidad que realice la digitalización y publicación de este trabajo de integración curricular en el repositorio virtual, de conformidad a lo dispuesto en el Art. 144 de la Ley Orgánica de Educación Superior.

Urququí, agosto 2019.



Jonathan Patricio Gordillo Urresta

CI: 1003159280

Dedicatoria

Siempre me he sentido maravillado por el apoyo de mi familia, se han preocupado de mí desde el momento en que llegué a este mundo, me han formado para saber cómo luchar y salir victorioso ante las diversas adversidades de la vida. Muchos años después, sus enseñanzas no cesan, y aquí estoy, con un nuevo logro exitosamente conseguido, mi proyecto de tesis. El presente estudio se lo dedico al Sr. Diego José Gordillo y la Sra. Meri Floralba Urresta Rivera por haberme forjado como la persona que soy en la actualidad, muchos de mis logros se los debo a ustedes, incluido este. Igualmente, dedico de manera muy especial a mi hermano Diego Fernando Gordillo Urresta pues fue el principal modelo a seguir para la construcción de mi vida profesional ya que sentó en mí las bases de responsabilidad y deseos de superación. En él tengo el espejo en el cual deseo reflejarme pues sus virtudes infinitas y su gran corazón me llevan a admirarlo cada día más.

Gracias padre, madre y hermano.

Jonathan Patricio Gordillo Urresta

Agradecimiento

Deseo expresar mi sincero agradecimiento a todas las personas que, a través de su apoyo científico y humano, han colaborado en el desarrollo de esta investigación. Primero, quiero agradecer a las instituciones públicas ecuatorianas que hicieron posible este trabajo a través de la provisión de datos: Instituto Nacional de Meteorología e Hidrología (para datos hidrometeorológicos). El Ministerio de Agricultura, Ganadería y Pesca (para mapas temáticos) y el Instituto Geográfico Militar (para información cartográfica).

Estoy muy agradecido con mi tutor de tesis, el Dr. Luis Eduardo Pineda Ordóñez, por la orientación académica, el apoyo y la discusión crítica que me permitieron emprender este trabajo de investigación, que finalmente llegó a una conclusión exitosa. Finalmente, deseo agradecer a mi familia por su comprensión, comunicación constante y apoyo diario. A mis padres que siempre han estado a mi lado compartiendo mi felicidad y mis angustias, y de una manera muy especial, a mi hermano por el estímulo para superarme día a día siendo el apoyo incondicional donde encontré la fuerza para llegar al final de este camino.

Jonathan Patricio Gordillo Urresta

Resumen

La cuenca de Mira suministra agua dulce para la agricultura y el consumo humano en el norte de Ecuador, pero estos servicios de agua están amenazados por el cambio ambiental y climático global. En la actualidad, esta región carece de estudios hidrológicos, que son esenciales para el uso sostenible de los recursos hídricos. El objetivo de este estudio es caracterizar la variabilidad de la escorrentía en la cuenca del Mira e investigar los controles fisiográficos que condicionan el comportamiento y la dinámica de la escorrentía. A través del análisis de datos hidrometeorológicos a largo plazo, la escorrentía en la cuenca del río Mira muestra dos regímenes de variabilidad, que se asocian principalmente con la distribución de las precipitaciones durante todo el año. En el noreste de la cuenca, la magnitud del flujo está condicionada por las características del paisaje que controlan la dinámica temporal de la respuesta de la escorrentía. El alto índice de follaje y la composición orgánica del suelo benefician el proceso de infiltración y el almacenamiento de agua subterránea, respectivamente. Por el contrario, el aumento de la temperatura durante la estación más seca acentúa la evapotranspiración activa que limita la infiltración en la superficie del suelo en el suroeste de la cuenca Mira. Por esta razón, el flujo se ve afectado por la evapotranspiración a nivel de la superficie y del subsuelo, de modo que las contribuciones finales al flujo base exceden las del flujo rápido. En conclusión, la generación de escorrentía en la cuenca del río Mira se controla mediante la interacción de varias características climáticas y fisiográficas que son específicas del sitio y la cuenca.

Palabras Clave: Flujo rápido y lento, evapotranspiración, índices de flujo.

Abstract

The Mira catchment supplies fresh water for agriculture and human consumption in northern Ecuador, but these water services are threatened by global environmental and climate change. At present, this region lacks hydrological studies, that are essential for the sustainable use of water resources. The objective of this study is to characterize runoff variability in the Mira watershed and to investigate the physiographic controls that condition the behavior and dynamics of runoff. Through the analysis of long-term hydro-meteorological data, the runoff in the Mira river basin shows two regimens of variability, which are primarily associated with the rainfall distribution throughout the year. In the northeast of the basin, the magnitude of the flow is conditioned by landscape features that control the temporal dynamics of the runoff response. The high foliage index and the organic composition of the soil benefit the infiltration process and the underground water storage respectively. By contrast, the increase in temperature during driest season accentuates the active evapotranspiration limiting the infiltration in the ground surface in the southwest of the Mira basin. For this reason, the flow is affected by evapotranspiration at the surface and subsurface level, so that the final contributions to the base flow exceed those of the quick flow. In conclusion, the generation of runoff in the Mira river basin is controlled by the interplay of several climatic and physiographic characteristics which are site and catchment specific.

Key Words: Quick and slow flow, evapotranspiration, flow indices.

This undergraduate thesis has been approved in partial fulfillment of the requirements for the Degree of BACHELOR OF SCIENCE in Geology.

Thesis Advisor: Luis Eduardo Pineda Ordóñez, Ph.D.
School of Earth Sciences, Energy and Environment

Thesis Co-Advisor: Paúl Nelson Arellano Mora, Ph.D.
School of Earth Sciences, Energy and Environment

Committee Member: Luis Felipe Aguirre Siachoque, M.Sc.
School of Earth Sciences, Energy and Environment

Committee Member: Jorge Esteban Gómez Paredes, Ph.D.
School of Earth Sciences, Energy and Environment

Committee Member: Andrea Yolanda Terán
School of Earth Sciences, Energy and Environment

SUMMARY	1
I. INTRODUCTION	2
II. PROBLEM STATEMENT	3
III. OBJECTIVES.....	4
IV. STUDY AREA	4
4.1 GENERAL DESCRIPTION	4
4.2 GEOGRAPHIC CHARCATERISTICS	4
4.2.1 Lithology	6
4.2.1.1 Geodynamics.....	6
4.2.1.2 Tectonic evolution	6
4.2.1.3 Structural geology	7
4.3 RELIEF	8
4.4 CLIMATE.....	10
4.4.1 Temperature	10
4.4.2 Precipitation.....	10
4.5 SOIL	10
4.5.1 Soil classification	11
4.5.2 Land use	13
4.6 WATER RESOURCES	15
4.6.1 Catchment drainage.....	15
V. MATERIALS AND METHODS.....	15
5.1 MATERIALS.....	16
5.1.1 Data.....	16
5.1.1.1 Geographic Information	16
5.1.1.2 Hydro-meteorological information	16
5.1.2 Characteristics of the study area	17
5.1.2.1 Location.....	17
5.1.2.2 Physiographic characteristics of the basin.....	17
5.2 METHODS	24
5.2.1 Stream flow analysis and data processing.....	24
5.2.1.1 Time series data format and quality control.....	24
5.2.1.2 Hydrological annual cycle	25
5.2.2 Hydrograph separation component.....	26

5.2.3 Computation of catchment physiographic characteristics	29
5.2.4 Computation of flow indices	31
5.2.5 Analysis of physiographic controls of flow characteristics	33
5.2.6 Correlation analysis	34
5.2.6.1 Pearson correlation	34
5.2.6.2 Spearman correlation	35
VI. RESULTS AND DISCUSSION	36
6.1 CATCHMENTS DESCRIPTORS	36
6.2 QUICK/SLOW FLOW RATIO RELATIONSHIP	36
6.3 PHYSIOGRAPHIC CONTROLS OF FLOW CHARACTERISTICS	39
6.3.1 Group of sub-basins G1	39
6.3.2 Group of sub-basins G2	43
6.4 FLOOD HYDROGRAPH ANALYSIS	47
6.4.1 Group of sub-basins G1	47
6.4.2 Group of sub-basins G2	48
VII. CONCLUSION.....	49
7.1 SPATIAL VARIABILITY OF RUNOFF	49
7.2 AT CATCHMENT SCALE.....	50
VIII. FURTHER RESEARCH.....	51
IX. ACKNOWLEDGEMENTS	52
X. BIBLIOGRAPHY	53
XI. APPENDIX.....	57
11.1 TABLES	57
11.2 SEASONAL BASEFLOW ANALYSIS	59
11.3 CORRELATION MATRICES	70

SUMMARY

Water is a key economic and ecological resource in Andean tropical ecosystems. Meeting the increasing demand of water due to population growth and agricultural activities requires knowledge on the hydrological functioning of catchments. The Mira catchment supplies fresh water for agriculture and human consumption in northern Ecuador, but these water services are threatened by global environmental and climate change. At present, this region lacks hydrological studies, that are essential for the sustainable use of water resources. Furthermore, this catchment provides an important case study for advancing the understanding of hydrological processes in the Andes, a region that embraces a variety of landscapes such as dry valleys, cloud forest, and cold wetland zones. The objective of this study is to characterize runoff variability in the Mira watershed and to investigate the physiographic controls that condition the behavior and dynamics of runoff.

Through the analysis of long-term hydro-meteorological data, the runoff in the Mira river basin shows two regimens of variability, which are primarily associated with the rainfall distribution throughout the year. In the northeast of the basin, the magnitude of the flow is conditioned by landscape features that control the temporal dynamics of the runoff response. The high foliage index and the organic composition of the soil benefit the infiltration process and the underground water storage respectively. The infiltration is limited by well-consolidated rocks, when the saturation limit of the vadose zone is reached. Thus, steep slopes and high levels of infiltration through densely vegetated areas suggest a lateral movement of the flow following a Hortonian-like mechanism. By contrast, the distribution of annual rainfall in the southwest of the Mira basin, conditions the generation of surface runoff in the driest season. The decrease in rainfall after an increase in temperature accentuates the active evapotranspiration limiting the infiltration in the ground surface. Pyroclastic deposits and andesitic lavas restrict this infiltration. For this reason, the flow is affected by evapotranspiration at the surface and subsurface level, so that the final contributions to the base flow exceed those of the quick flow. In conclusion, the generation of runoff in the Mira river basin is controlled by the interplay of several climatic and physiographic characteristics which are site and catchment specific.

I. INTRODUCTION

In Ecuador, water resources are increasingly threatened by a growing water demand for industrial and economic activities, such as agriculture, industrial mining and hydropower, which is further aggravated by environmental and climate change. Despite this trend, the Ecuadorian population consumes in average 43,500 m³ of water per year, and the total amount of rainfall per person is three times the world average of 10,800 m³ (Consejo Nacional de Recursos Hídricos, 2002, quoted in Albán et al., 2004). This is considerably higher than the per capita water availability of other regions.

Most of the fresh water resources in Ecuador originate in the Andes which cross the country from north to south, shaping a series of intersecting catchments west and east of the Andes. The Ecuadorian territory is thus divided into 31 hydrological systems and has a total number of 79 river basins (Consejo Nacional de Recursos Hídricos, 2002). These systems lay on two Andean slopes, the first one draining into the Pacific Ocean (24 river basins) and the second one into the Amazonia (7 river basins). This national hydrological network yields c.a. 110 billions of m³ to the Pacific Ocean and 290 billions of m³ to the Amazonas (Consejo Nacional de Recursos Hídricos, 2002). In addition to the great country-wide contribution and support that these catchments provide to industrial and economic activities, each of these catchments provides different and localized water services, such as runoff regulation, ecological functioning, flood prevention, lake and aquifer recharge, soil erosion prevention and sediment control.

The Mira catchment in the Pacific slope of the Northern Andes supplies water services to a variety of sectorial users. For example, 12% of the catchment-wide total demand is allocated to water for human consumption, 84% for agriculture activities and 4% for industry (Tosse & Iza, 2017). It also hosts a variety of land forms and ecosystems including mountain glaciers; cold wetland zones, locally known as paramo; lakes; humid forest and desiccated valleys.

To ensure the ecological functioning of these environments and so the provision of hydrological services, both in quantity and quality, under increasing anthropogenic pressure, water authorities, managers and stakeholders need to set and implement management and conservation. This in turn requires to increase the knowledge on the hydrological functioning

of these catchments. The latter can only be achieved by studying the catchment hydrological behavior, processes, and its dependency on environmental factors controlling the timing and spatially distribution of catchment runoff.

II. PROBLEM STATEMENT

Hydrologic studies help to understand the rainfall-runoff relationships in order to improve water resources management. However, knowledge about how this cycle functions in high elevation zones is limited, due to a complex interaction between climatic and geological factors. According to Crespo et al. (2011), the runoff relationship in micro-catchments in the Andes is mainly controlled by the amount of precipitation and soil properties. In addition, preexisting soil water content may contribute to the streamflow, especially the amount of baseflow (Crespo et al., 2011). Finally, vegetation is another factor that influences catchment hydrological functioning because of the degradation and over exploitation of soils (Molina et al., 2007).

In general, the abrupt topography of the Andean region is characterized by the convergence of several climatic systems which generate very extreme hydroclimatic gradients (Crespo et al., 2011). In the Mira basin, rainfall can exceed approximately 6000 mm in areas close to the Lita and Blanco rivers (INAMHI, 2005) generating strong gradients in catchment atmospheric water inputs. This, together with varying temperatures and diversity of soil types and vegetation covers, influences runoff generating mechanisms. This results in a great variety of environments which show different behaviors in relatively short distances, ranging from humid forests to mountainous areas and dry tropical valleys. Furthermore, human activities such as, agriculture continuously affect soil cover, affecting the natural cycle of runoff. In the Mira basin, the lumped water yield is approx. $7,729 \text{ hm}^3$, which is equivalent to 1120 mm of rainfall depth available to support agricultural activities, human consumption and industry in the basin (Tosse & Iza, 2017). The water yield varies across micro-catchments owing to the spatial variation of climatic and geological factors.

The lack of knowledge on the rainfall-runoff relationship of the important Mira Basin, as well as on some of the main factors that affect such relationship, constitutes an obstacle for the implementation of adequate water management strategies, which are urgently needed to

meet both human and ecosystem requirements. This investigation focuses on the study of the climatic and physiographic factors that control runoff generation and dynamics in selected micro-catchments of the Mira basin, and attempts to be a benchmark study for catchments in the Northern Ecuadorian Andes.

III. OBJECTIVES

The objective of this study is to determine to which extent the runoff components (surface, interflow, and baseflow) are being conditioned by climate, geology, land cover, and soil properties in selected micro-catchments of the Mira basin according to a 30-year record of hydro-meteorological data.

The specific objectives are:

- To characterize hydrological regimens and their components in ten micro-catchments of the Mira basin.
- To identify the climatic and physiographic controls of runoff and their components.

IV. STUDY AREA

4.1 GENERAL DESCRIPTION

The Mira river basin is located in the North of the Imbabura Province, but also covers areas of the Carchi and Esmeraldas Provinces in Ecuador, as well as areas of Nariño in Colombia. The Mira basin located at the north of Ecuador (coordinates 78°34,3'W- 77°38,9'W and 0°7,4'N / 1°14,7'N) has an area of 6904 km². It is limited by the Napo river basin to the East, and the southwest edges of the Esmeraldas river basin. The Mira river basin is divided into 2 sub-basins: i) the Mira river sub-basin with an area of 6538 km² and ii) the Carchi river sub-basin with an area equal to approx. 366 km². The study focuses on 10 different sub-basins, upstream of the hydrological station H0011, Lita, (Fig. 1) delineated taking into consideration the long-term availability (~30 years) of hydrological gauge stations.

4.2 GEOGRAPHIC CHARACTERISTICS

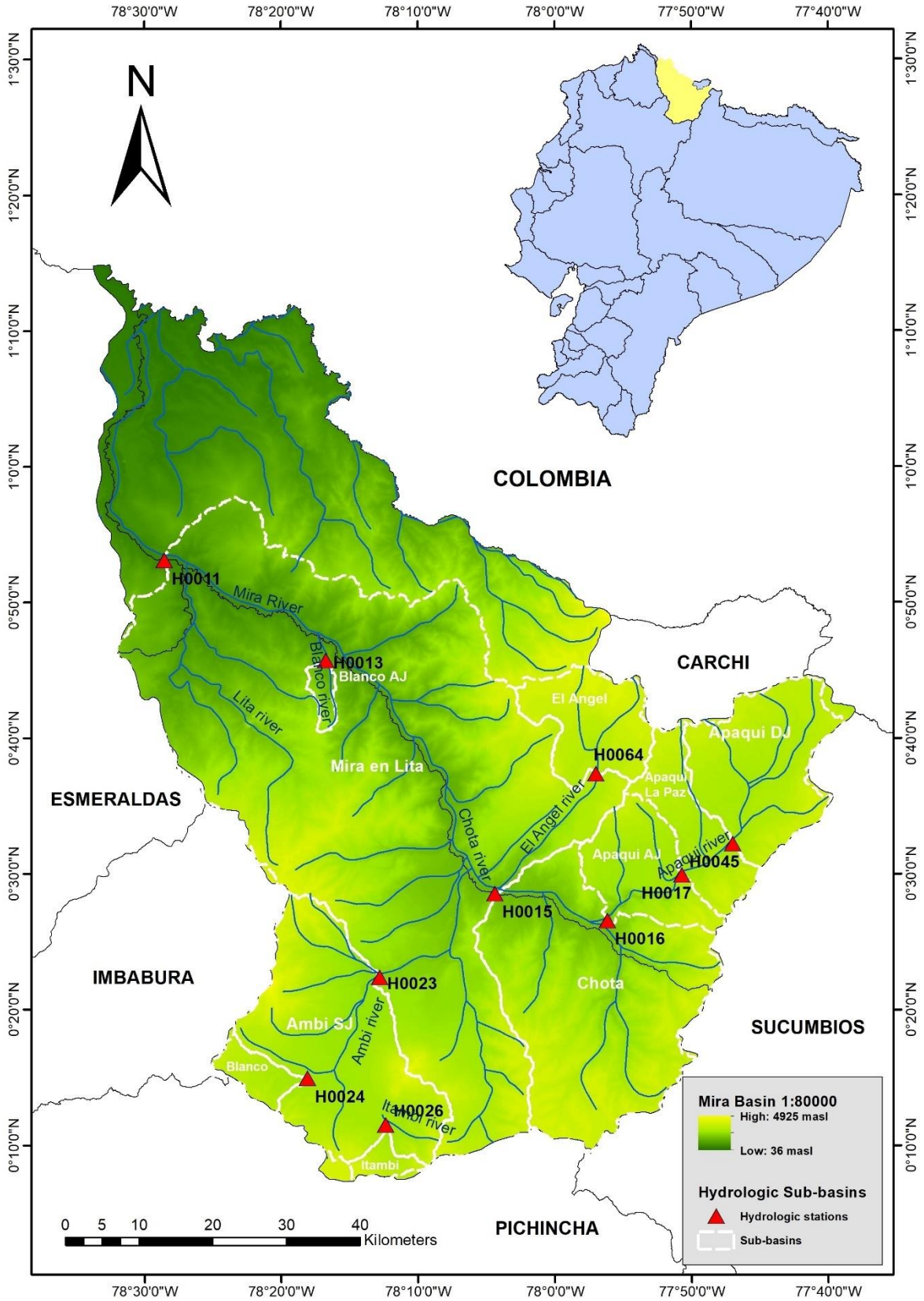


Fig. 1. Study area showing delineated sub-basins and hydrological stations.

4.2.1 Lithology

4.2.1.1 Geodynamics

The northern Andes of Ecuador is divided into two major mountain regions: The Western and Eastern Cordillera. The geo-dynamics that governs this area is generated from the convergence of the Nazca plate under the South American block from the Oligocene (Alvarado, 2012). The direction of the convergence is E-W (N81 ° E and N120 ° E), with a speed of 70 to 57 mm / year (Pardo-Casas & Molnar, 1987).

On the other hand, the Carnegie seismic mountain range perform an important function in the geodynamics of the country. According to Gutscher et al. (1999), this mountain range was formed on the Nazca plate 1 Ma, extending in an E-W direction from the Galápagos hot spot until hitting the South American plate. The Carnegie mountain range exerts a transpressional force that deforms the Andes by means of the convergence with the South American block.

4.2.1.2 Tectonic evolution

The Western Cordillera (WC) is formed by Pallatanga and San Juan Units (Vallejo et al., 2006). The Pallatanga unit is composed of basalts, dolerites, pillow lavas of oceanic plateau, while the San Juan unit basically consists of gabbroic and ultramafic mafic clusters of the same geochemical origin (Spikings et al., 2001).

Rocks belonging to the Cretaceous underlie intra-oceanic island arc sequences (Vallejo et al., 2009). The geological formations of the study area are deposited near a volcanic source and distant from a continental one, associated with the beginning of subduction, below the plateau of the Caribbean (Vallejo et al., 2009). Turbiditic sequences are derived from the Cordillera Real and the South American Craton, belonging to the Upper Campanian - Maastrichtian period. The blockage of the subduction zone and the deformation of the continental margin are produced by the collision of the Caribbean Plate with the South American Plate in the early Maastrichtian (70 Ma), producing a rotation of 20 °-50 ° (Vallejo et al., 2006).

A collision between the South American Plate and the Caribbean Plateau resulted in a rapid exhumation of the Cordillera Real (Spikings et al., 2001, 2005). A new volcanic arc towards the east emerged, which gave rise to the Late Maastrichtian Silant Unit deposited in a terrestrial environment with calcoalkaline affinity (Vallejo, 2006).

4.2.1.3 Structural geology

The geology of the WC from 0° to 1° N, presents a complex structure controlled by series of faults in the NE-SW direction which represents the lateral limits of the geological units. In addition, faults that cross the terroir with an E-W heading close to the batholiths are observed (Boland et al., 2000). Intense fracturing, presence of veins and development of breccias represent large areas of ductile deformation in the study area. Such deformation is associated with intense fracturing and growth of calcite veins.

The eastern structural limit of the WC is marked by the Pallatanga fault system (McCourt et al., 1997). This mega-fault, with NE-SW orientation, is characterized by showing a configuration of faults that dip in the same direction. To the east, two main zones of ductile deformation have been identified: the Mulaute Shear Zone (Hughes and Bermúdez, 1997) with NE-SW direction and the Naranjal Shear Zone (Boland et al., 2000). The boundary between the Mulaute zone and western deposits of the mountain range is marked by the Toachi-Toacazo fault (Hugues & Bermúdez, 1997).

The Mulaute Shear Zone extends through an 8 km-wide belt with penetrative cleavage and is characterized by slate deposits and fine-grained siltstones. The middle of the belt presents coarse-grained sediments with ductile deformation appearing as an intercalation of sediments with rocks without alteration. On the other hand, Naranjal Shear Zone presents a penetrative cleavage in igneous rocks and is characterize by deposits with high content of amphibole. In addition, it is crossed by Rio Bravo and Barbudo, with a width of up to 2 km. Although the age of the deformation is unknown, this sector of the mountain range must be prior to the location of the *Batolito de Santiago* to the south, which is not deformed and has an age of 44-35 Ma. Therefore, it is expected that this area maintains a certain temporal relationship.

Prominent formations in the study area are: the Silante unit (HSI), the Naranjal unit (KNA), the Macuchi unit (EM), the Chota group (MCh), Volcanics and Alluvial deposits (Spencer,

2011) (Fig. 2). The Silante Unit is limited to the northern sector of the study area and is characterized by conglomerates and canalized breccias, supported matrix conglomerates deposited by lahatic flows, red mudstone, shale, and violet tuffs (Vallejo et al., 2009). Naranjal unit is characterized as a volcanic sequence of arc affinity of islands and oceanic plateau (Vallejo et al., 2006). This unit is restricted to the northern sector and is composed of a sequence of basaltic and andesite lava pillows, interspersed with sedimentary rocks (Vallejo et al., 2006). One of the most dispersed sequences in the study area is the Macuchi unit, which is defined as a sequence of volcanic rocks of Calcoalkaline and Toleitic composition from a volcanic arc. It consists of pillow basaltic lava, lithic tuffs of basaltic and andesitic composition, basaltic breccias, andesitic intrusions, volcanic material re-deposited in turbiditic layers and cherts (Vallejo et al., 2006). The Chota group emerges along the Chota River and on the Ibarra road. It consists of massive gray sandstones and matrix conglomerates supported with well-rounded clasts of shales, cherts and weakly foliate granitoids; besides intercalations of shales and siltstones (Boland et al, 2000). Finally, there are volcanic deposits of Miocene to Holocene age formed by the main volcanic centers: Cayambe, Imbabura, Cuicocha and Pululahua, as well as holocene alluvial occur along the great fluvial valleys, mainly the rivers Mira, Lita and San Juan.

4.3 RELIEF

The general relief of the Mira river basin is characterized by the presence of mountainous systems that show typical morphological features of volcanic origin. The most outstanding ones are the Chiles volcano in the Carchi Province, and Imbabura and Cotacachi volcanos in Imbabura Province. They have an average high of 4500 m. On their foothills rest numerous lakes such as Yahuarcocha, San Pablo, Cuicocha and Mojanda, among others minor ones. The north of the study area around Chiles volcano and El Ángel paramo decrease to the south, shaping wide terraces and plateaus such as the Chota and Mira valleys. At this point, some ridges converge to form the stream bed for Mataqui and Ambi rivers which drain to the Chota and Mira rivers. This latter serves as a division between the western WC and the southeastern basin, bordering it until the ranges cross the Colombian border. Finally, the tributary river San Juan is the last member of this configuration which is born in the WC from Chiles volcano and drain to the Mira river before crossing to Colombian territory.

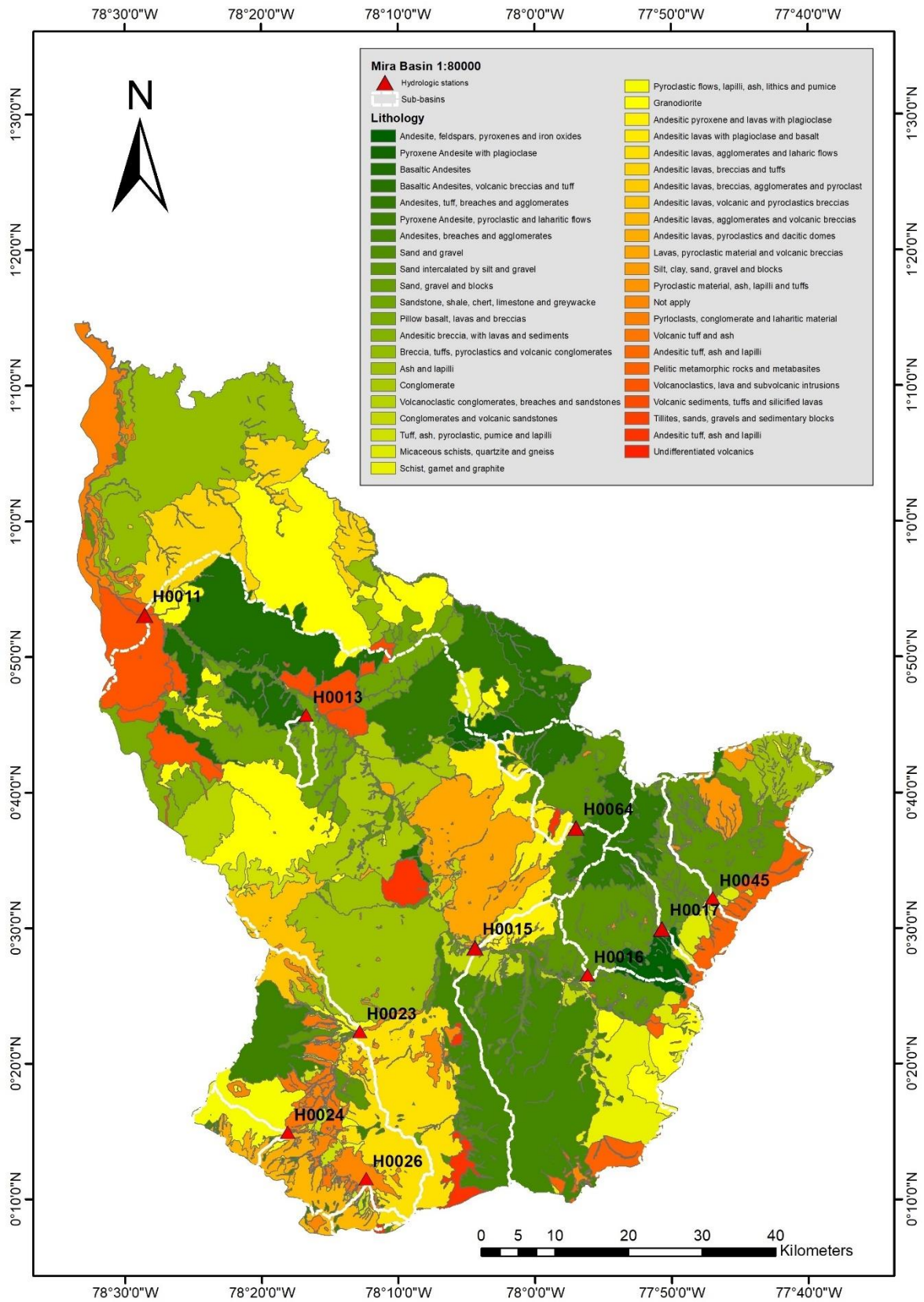


Fig. 2. Lithological map in the Mira river basin with sub-basins in the study area.

4.4 CLIMATE

The Mira river basin is located on the Pacific-Andean watershed. Climatic differences (mostly precipitation) are related to, firstly, elevation gradients and the displacement of the inter-tropical convergence zone, and secondly to the moist contribution from the Pacific Ocean and Amazon basin. This generates marked dry and wet seasons, particularly in valleys.

4.4.1 Temperature

The annual temperature varies throughout the year. The headwaters of the catchment record low temperatures that reach 9 °C. However, temperature increase inversely with altitude down to bottom valleys, with up to 20 to 23 °C, and approximately 17 °C for the dry season.

4.4.2 Precipitation

The annual mean precipitation of the Mira river basin varies from 600 to 3000 mm and the mean annual rainfall depth is 1473 mm (INAMHI, 2005). It is temporally and spatially variable. Annual rainfall is low in the middle zone and high in the northwestern and southern regions of the basin. It is possible to distinguish two climatic seasons: two dry period within October and May and a wet period from June to September. There is a bimodal behavior of precipitation with two peaks in October and March and one minimum in July.

The inter-Andean zone is highly variable with respect to climate. The highest points are cold and wet areas with low but lasting precipitations. At intermediate zones temperature increases and precipitation becomes more intense. However, weather characteristics drastically change at low valleys like Chota, in which a dry climate and low precipitation (below 300 mm per day) are prevalent.

4.5 SOIL

In general, the Northern Ecuador is characterized by volcanic deposits with sediments interlayered in zones near rivers. The material presents ideal conditions to keep water, a characteristic that increases in zones with low vegetation.

4.5.1 Soil classification

In general, soils in the study area are derived from volcanic rocks and granite. These are kaolinitic, clayey, compact, not very permeable, poorly drained, of low fertility, acid pH, eroded, reddish brown, compacted and shallow. Andisols are black soils that develop from volcanic deposits or pyroclastic materials, so they show little to moderate evolution (Fig. 3). These soils are subject to frequent rejuvenation due to the proximity to volcanoes. In addition, they are well structured soils and are enriched with organic nutritional materials. Therefore, these are characterized by good drains and have good moisture retention. On the other hand, inceptisols are young soils that show the development of horizons (Fig. 3). These are characterized by having a rapid formation genesis, with processes of translocation of materials or extreme weathering. This type of soil has very variable physical and chemical properties such as: soil from poorly drained to well drained, textures from sandy to clayey, pH from slightly acidic to slightly alkaline, with base saturation greater than or less than 60%. These properties have been strategically used by agriculture.

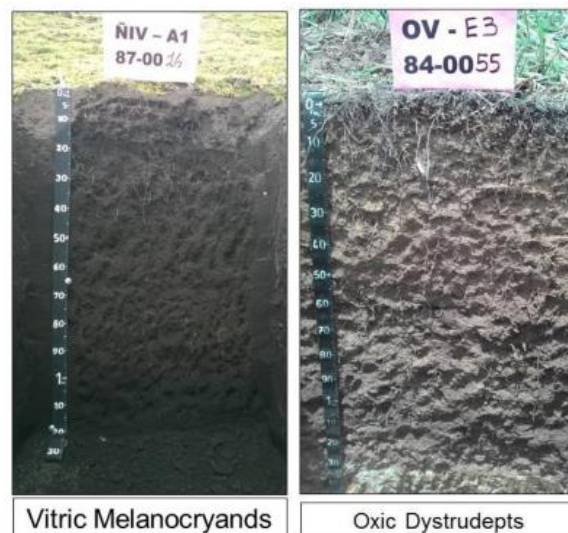


Fig. 3. Andisol (Vitric Melanocryands, left) and Inceptisol (Oxic Dystrudepts, right). (SIGTIERRAS, 2017)

The soil classification was based on the soil map developed by Ministerio de Agricultura, Ganadería y Pesca (MAGAP) (MAGAP, n.d). The main type of soils in this study's area are Andisols bordering the Mira basin and Inceptisols in the central zone of the valley (Fig. 4).

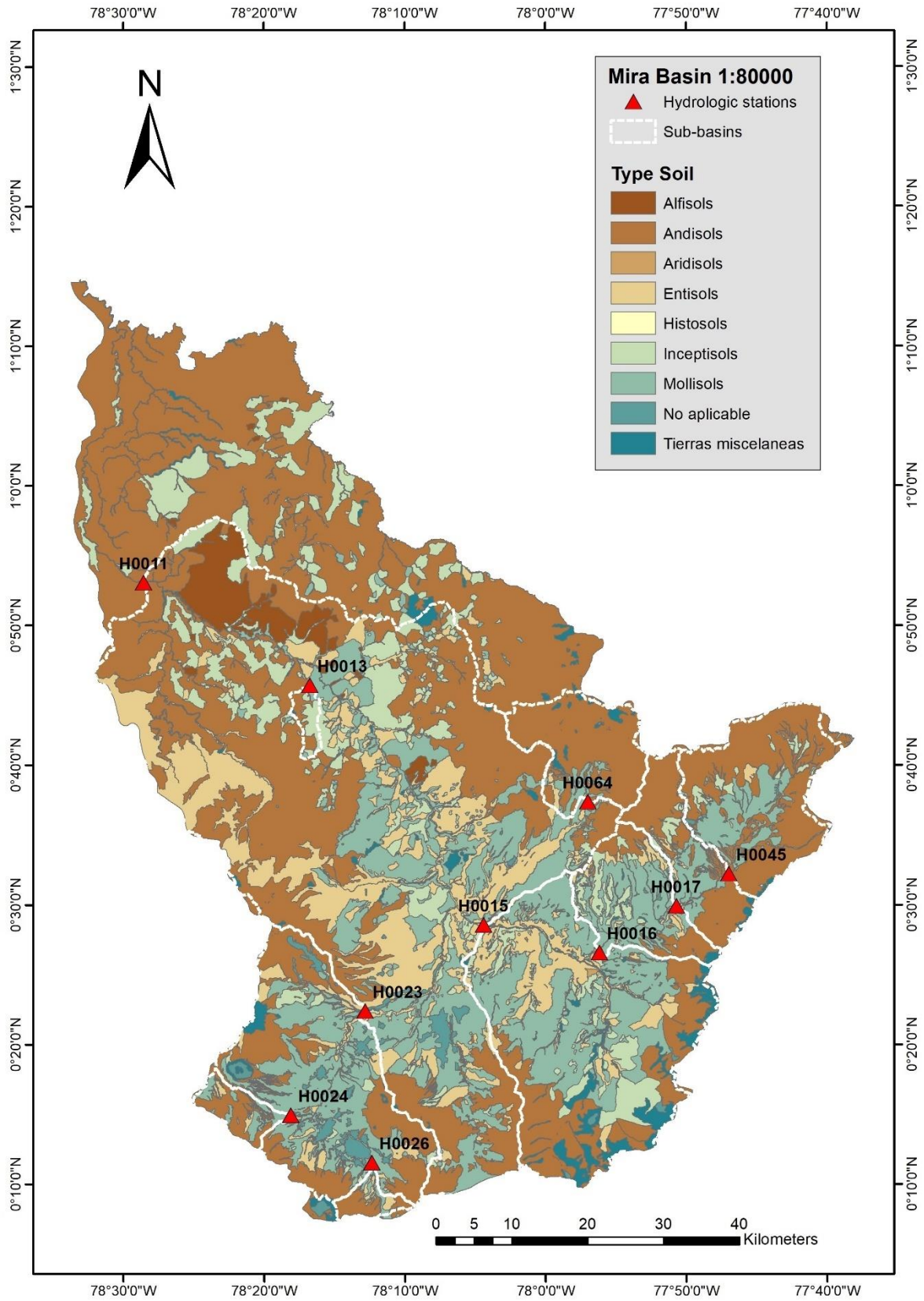


Fig. 4. Map of soil types in the Mira river basin with sub- basins in the study area.

4.5.2 Land use

According to the Ecuadorian Censo Agropecuario (INEC, 2000) in Imbabura Province, land for agriculture is mainly used for crops, such as beans, corn and sugarcane, followed by the production of wheat and barley, and then by very little percentage of potatoes and bananas. Thus, the main production of Imbabura and Carchi Provinces relates to cereals, followed by legumes. However, in the nearby region, at the border with the Carchi Province, there is poor land use regulation, which results in an inappropriate land use for farming activities (INEC, 2000)

Other important land uses in the Mira river basin are conservation and protection zones. These zones correspond to remaining native forest and paramos (Fig. 5). Paramos are cold zones that play a very important role in regulating water flows (Podwojewski, 1999). In paramos, soils have pyroclastic deposits which are the result of continuous eruptions and collapse of various volcanic edifices. In general, these soils are classified as andisols and vitrosols, however their properties vary according to pedogenetic factors as naturalness, age, composition and climatic conditions (Podwojewski, 1999). According to Podwojewski, paramos show a high-water retention capacity, from 60 % up to 200%. Due to this level of water retention, these zones regulate hydric flows through storage in wet season and releasing water during dry seasons.

Nevertheless, the disappearing of vegetation coverage in the north of Ecuador, due to variety of factors, leads to a dramatic increase of runoff which hinders the regulatory capacity of paramos (Podwojewski, 1999). This process is linked to the development of hydrophobic substances that provoke the irreversible desiccation of volcanic soils which lose their ability of water retention (Podwojewski, 1999). The decrease of permeability leads to the formation of arid zones that suffer laminar erosion converting north zones of highland in Ecuador in great desertic extensions.

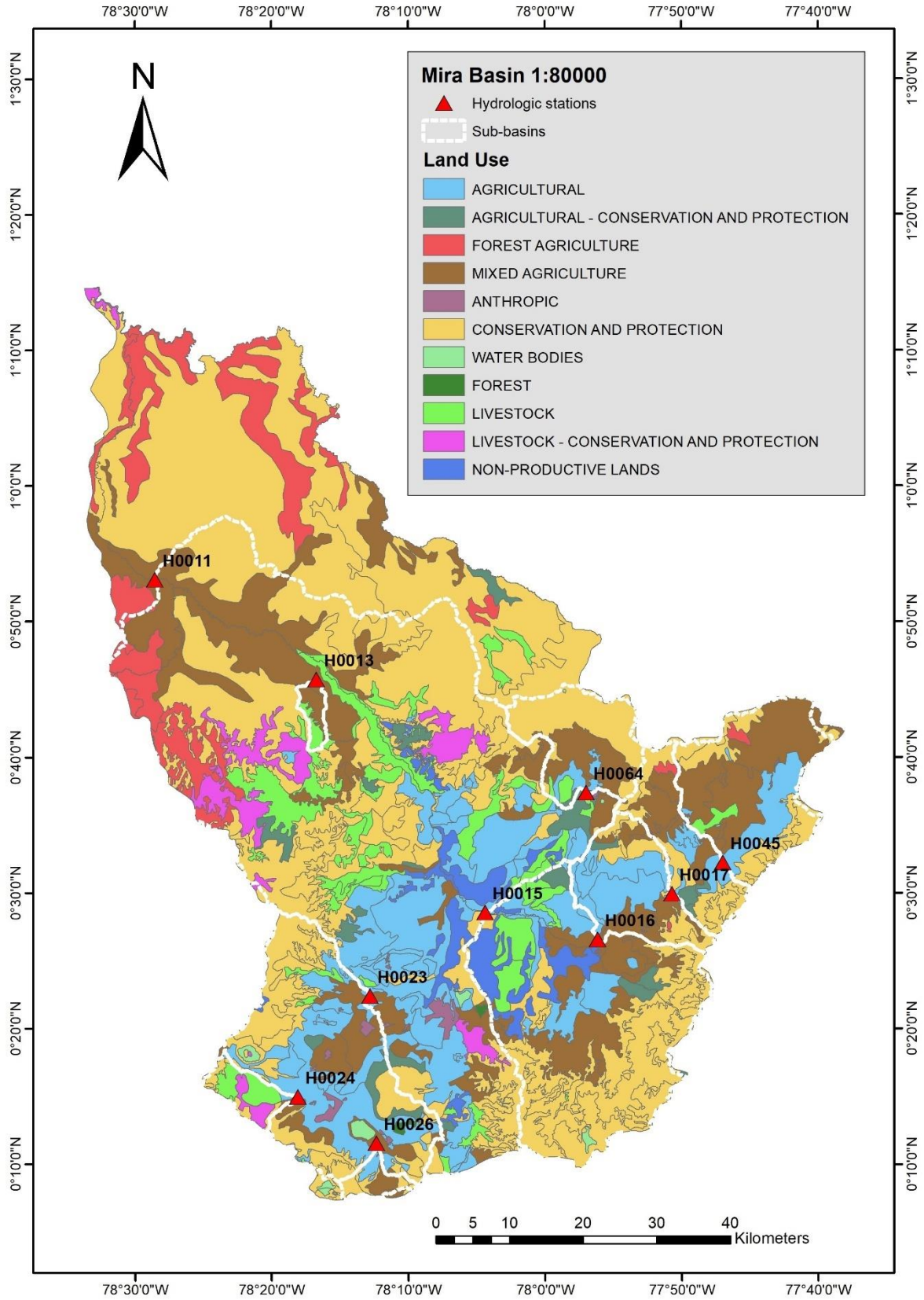


Fig. 5. Map of land use in the Mira river basin with sub-basins in the study area.

4.6 WATER RESOURCES

4.6.1 Catchment drainage

The main rivers draining the headwaters of the Mira river basin are Ambi in the southwestern and Apaquí in the northeastern edges of the basin. Other important tributaries are: the Ángel, Lita and Blanco rivers.

The annual hydrological regimen mostly follows the annual rainfall cycle variability. Streamflow in a river channel can be used as proxy to infer the different components of water flow over a catchment such as surface runoff, sub-surface and baseflow (Brodie & Hostetler, 2005). This last one representing the fraction of water flow infiltrating the soil. In the Mira catchment, streamflow is variable depending on the season and the monthly precipitation, increasing between April and May. Taking in consideration this annual regimen, it is possible to differentiate between highland catchments and valleys in the Mira watershed. In Carchi Province, upstream runoff is around 600-800 mm/year, while downstream, runoff values increase dramatically from 3000 to 3500 mm/year.

The studied area includes 10 micro-basins which are 5 to 30 km separated apart. The drainage configuration is governed by the geomorphology of the study area. Thus, the micro-basins H0016, H0017, H0045 and H0064 drain through the Apaqui and El Angel rivers to the south of the Mira basin, while the micro-basins H0023, H0024 and H0026 drain through the Itambi and Ambi rivers towards the North (see again Fig. 1.). These two large drainage groups are tributaries of the Chota river which downstream becomes the Lita river. On these last rivers micro-basin H0015, H0013 and H0011 are located, being the latter the largest one and the outlet point of this study.

V. MATERIALS AND METHODS

This section describes the hydrological characteristics of the study area, the data used and the methodology applied in the study (Table 1). The latter includes the analysis of hydrographs (separation of hydrograph components), computation of physiographic characteristics for each sub-basin and their corresponding flow indices or signatures. These

parameters are then analyzed using statistical regression techniques to study the importance of climatic and geological factors in the generation of runoff for each sub-basin.

5.1 MATERIALS

5.1.1 Data

5.1.1.1 Geographic Information

Table 1 Cartographic information used in this study.

Cartographic information	Format	Year	Scale	Description	Responsible agency
Lithological map	Vector	n.d	1:50000	Rock type division	MAGAP ¹
Contours	Vector	n.d	1:250000	Terrain level curves	IGM ²
Rivers	Vector	n.d	1:50000	Base layer with geographic information	IGM
Use/Cover map	Vector	n.d	1:250000	Soil use and coverage division	MAGAP
Hydro-meteorological network	Vector	n.d	1:250000	Hydrologic and meteorological stations	INAMHI ³
DEM	Raster	2018	1:80000	Digital elevation model	Japan Aerospace Exploration Agency

¹Ministerio de Ganadería, Agricultura y Pesca, ²Instituto Geográfico Militar,

³Instituto Nacional de Meteorología e Hidrología.

5.1.1.2 Hydro-meteorological information

Hydrometeorological (streamflow, precipitation, and temperature) information was used to characterize climate and river flows in the 10 selected sub-basins. Both meteorological and streamflow data was obtained from 10 hydrological stations of the Ecuadorian National Institute of Meteorology and Hydrology (INAMHI) (Table 2 and 7).

Table 2 Hydrological stations with daily information for the period 1985-2015.

Code	Name	Coordinates UTM WGS84 17S		Altitude (masl)
		x	y	
H0011	MIRA EN LITA	782299	10093951	475
H0013	BLANCO AJ	803375	10084283	890
H0015	CHOTA	825765	10052817	1515
H0016	APAQUI AJ	841074	10049013	1715
H0017	APAQUI LA PAZ	851176	10055411	2365
H0023	AMBI DJ	810143	10041214	2015
H0024	BLANCO	800343	10027542	2573
H0026	ITAMBI	810821	10021243	2648
H0045	APAQUI DJ	858100	10059439	2650
H0064	EL ANGEL	839654	10069610	2850

5.1.2 Characteristics of the study area

5.1.2.1 Location

The ten study sub-basins are placed on the southern region of Mira river basin and upstream of the hydrological station H0011 in Lita. Together they cover approximately 75% of the Mira river basin in the Ecuadorian side. Their catchment delineation corresponds with the drainage area at the catchment outlet for each gauge station. This allows to analyze the hydrological behaviors and relate them with climatic and geological factors.

5.1.2.2 Physiographic characteristics of the basin

In general, qualitative and quantitative methods are required to study a watershed. The factors considered in order to study the hydrological processes of the Mira river basin were: morphology (catchment shape, relief, drainage network, etc.), soil types, vegetation cover, geology, land use, etc. Table 3 shows the physiographic factors used in this study as reported by Guachamín et al. (2015).

Table 3 Physiographic factors used in this study.

Area	6904,23 km ²
Bottom level of the basin	92 masl
Upper limit of the basin	4863 masl
Length of the river to the point of closure	195,38 km
Coefficient of compactness (kc)	2,38
Form factor (kf)	0,46
Drainage density (Dd)	0,10 km / km ²
Sinuosity of the currents (S)	1,81
Average slope of the Basin	31%

Geomorphology, climatology, and pedology were considered important factors affecting hydrological behavior. The interaction among the runoff driving factors is complex since they operate in multiple time scales that affect the runoff generation mechanisms, influencing entry, accumulation and water basin outflow.

In order to quantify these factors this study used the following river basin characteristics:

a) Total length of the main river (Tl): The longest drainage path of the basin, expressed in Km.

b) Middle slope of the main river (Ms): The total difference of elevation on the main channel (maximum level – minimum level), divided by its total length (Eq. 1).

$$(Eq. 1) Ms = \frac{Hmax - Hmin}{Tl}$$

Where;
Ms= Middle slope of the main river
Hmax= Maximum height of the main channel
Hmin= Minimum height of the main channel
Tl= Total length of the main river

Taking into account that the slope has a direct relationship with the flow velocity, the higher the slope value, the higher the velocity of the overland flow. Thus, this index provides an idea about the transit time of water along a longitudinal profile of the river (Guachamín et al., 2015).

c) Basin perimeter (P): This parameter together with the area describes the shape of the basin. It is expressed in Km.

d) Drainage area of the basin (A_c): The horizontal projection of the entire drainage area system on the same natural channel. It is bounded by the water divide.

e) Average slope of the basin (S_b): The slope controls the speed of surface runoff. It limits the time range in which the rainwater concentrates in the fluvial beds representing the drainage network of the basins.

f) Shape of the basin: It is related with the time that water takes to concentrate on the basin borders until it reaches the outlet (Eq. 2).

- **Gravelius compactness coefficient (k_c):** This coefficient represents the relationship between the basin perimeter and the area of the circle enclosing the basin. It is determined by measuring the perimeter and surface, so that the result should be close to one if it is a circular basin, or failing to three if the basin is irregular shaped.

Where;

$$(Eq. 2) \quad k_c = 0,28 \frac{P}{A^{\frac{1}{2}}}$$

A = Basin drainage area [km^2]

P = Basin perimeter [km]

K_c = Gravelius compactness coefficient

The coefficient of compactness is directly related to the concentration time. This means that the basin with a high coefficient of compactness would also have a long concentration time. Thus, the magnitude of the runoff generated by a precipitation event in a basin with a high coefficient of compactness will be lower than the one generated in a basin that has a low coefficient.

g) Concentration time: It is the travel time in which rain falls on the most distant point of a watercourse in a basin until it reaches a determined section of that watercourse.

- **Kirpich:** The equation by Kirpich was developed empirically from the Soil Conservation Service (SCS) information in seven rural basins in Tennessee, USA, with well-defined channels and steep slopes (3 to 10%) (Eq. 3).

Where;

$$(Eq. 3) Tc = 0,39 \left(\frac{Tl^2}{H} \right)^{0.385}$$

Tc= Concentration time [hours]
Tl= Total length of the main river
H= difference of coordinates between the extreme points of the watercourse [m/m]

- California: This is equation was especially developed for low mountainous basins in California (Eq. 4).

Where;

$$(Eq. 4) Tc = 0,952 \left(\frac{Tl^3}{H} \right)^{0.385}$$

Ct= Concentration time [hours]
Tl= Total length of the main river
H= difference of coordinates between the extreme points of the watercourse [m/m]

- Delay equation: The SCS developed this equation from the sum of individual travel times for different regions. They could be wooden cover areas with steep slopes, plains and impermeable areas (Vélez & Gutiérrez, 2011). This equation was developed using data of urban areas with areas below 800 Ha, in addition to agricultural basins. Thus, it is suitable for the calculation of concentration time for small basins. Moreover, it usually performs well when the area is completely paved. However, in mixed areas it tends to overestimate the concentration time (Eq. 5).

Where;

$$(Eq. 5) Tc = \frac{100Ml^{0.8} \left[\left(\frac{1000}{CN} \right) - 9 \right]^{0.7}}{1900Sb^{0.5}}$$

Ct= Concentration time [hours]
Tl= Total length of the main river
CN= Curve number
Sb= Average slope of the basin [%]

h) Hypsometric curve of the basin: The hypsometric curve indicates, in percentage, the area occupied by the basin above a certain level. It relates the value of height in y-axis, with the percentage of accumulated area in the x-axis.

i) Basin Order: It reflects the branching rate of a drainage system. Thus, it is possible to classify different watercourses in a basin based on the following criteria:

- First order watercourses are those that do not have tributaries.

- Second order are formed by the union of two first order watercourses. In general, watercourses of n-order are formed when two n-1 watercourses join.
- When a watercourse joins a watercourse of higher order, the resulting channel downstream retains the largest order.
- Finally, the order of the basin is the same as the order of the main watercourse.

The higher the order of the basin, the more efficient the drainage system is.

j) Curve number: It is a technique widely used by operational hydrology due to its simplicity and ease of use in both medium and small watersheds. The curve number (CN) is an empirical parameter developed by the SCS. This method considers the humidity of the soil (which can be “dry”, “normal”, or “wet”) as a main parameter, focusing on the five previous days. It is represented by a number without dimension in standardized curves, which vary between 0 and 100. An area with CN = 0 means no runoff while a CN = 100 means fully impermeable conditions and all precipitation generates runoff.

The following equations are used to obtain CN values, depending if the previous days have been dry or wet (Eq. 6 and 7):

$$\text{(Eq. 6) } CN(I) = \frac{4.2CN(II)}{10 - 0,058CN(II)}$$

$$\text{(Eq. 7) } CN(III) = \frac{23CN(II)}{10 - 0,13CN(II)}$$

Where; *CN (I): For previous dry conditions, CN(II): For previous normal conditions, CN(III): For previous wet conditions.*

k) Drainage density: It indicates the capacity of a basin to evacuate water that flow through its surface. It relates the total length with the total area of the basin (Eq. 8).

Where;

$$(Eq. 8) Dd = \frac{\sum Lc_i}{Ac}$$

Dd= Drainage density [km/km²]
Ac= Drainage are of the basin [km²]
ΣLc_i= Total length of the water channels (km)

It is important to emphasize that the concentration time tends to decrease when the parameters associated with the drainage system tend to be greater. As a result, there will be greater production capacity of superficial flow in the basin. Finally, as a reference, the drainage density takes values between 0.5 km / km² for watersheds with poor drainage up to 3.5 km / km² for basins with very good drainage.

i) Water flow sinuosity: The sinuosity of a river represents water flows away from a straight line. It is possible to measure this activity by the relationship between the distance separating two points along the deepest part of the channel and the distance in a straight line between them. For this case, water flow sinuosity is only the relation of river length in front of valley length, measured through a curve or a line (Eq. 9).

Where;

$$(Eq. 9) S = \frac{L}{L_T}$$

S= Water flow sinuosity [km/km]
L = Length of the main channel [km]
L_T = Length of the principal channel measured in a straight line [km]

This parameter is very useful to measure runoff velocity. So, water flow density equal or less than 1.25 shows low sinuosity, defining a river with a nearly straight alignment.

Table 4 summarizes main geomorphological factors for each sub-basin in the study area and Fig. 10 shows the concentration time for each sub-basin which can be considered an indicator for catchment storage capacity.

Table 4 Main geomorphological factors for each of the 10 sub-basins in the study area. Adapted from Guachamín et al., 2015

Code	Name	Coordinates UTM WGS84 17S		Mean elevation (Me) [masl]	Area (A) [Km ²]	Perimeter (P) [Km]	Average slope (Sb) [%]	River length (Tl) [km]	Basin elevation [masl]		River slope (Ms) [%]	Compactness index (kc)	Concentration time (Tc) [hour]	Curve number (CN)	Drainage density (Dd) [Km ⁻¹]
		x	y						Upper	Lower					
H0011	MIRA EN LITA	782299	10093951	2693	2691,4	351,10	32,68	457	4885	500	0,018	1,89	16,36	73,2	0,170
H0013	BLANCO AJ MIRA	803375	10084283	2270	158,29	85,02	51,71	13,72	3638	901	0,104	1,89	1,84	74,12	0,087
H0015	CHOTA EN PTE.CARRET ERA	825765	10052817	2858	815,89	145,92	30,59	95,46	4195	1520	0,023	1,43	9,86	73,3	0,117
H0016	APAQUI AJ CHOTA	841074	10049013	2870	201,15	71,28	23,15	39,97	4025	1715	0,028	1,41	8,3	75,65	0,199
H0017	APAQUI D GRUTA LA PAZ #3	851176	10055411	3219	173,58	81,12	20,79	26,35	4025	2412	0,016	1,72	6,13	78,63	0,152
H0023	AMBI DJ CARIYACU	810143	10041214	3095	571,11	137,54	16,28	108,9	3754	2436	0,039	1,61	5,64	70,58	0,189
H0024	BLANCO EN PTE.CARRET ERA	800343	10027542	3210	58,68	41,03	23,03	18,23	3859	2561	0,057	1,50	4,86	61,48	0,311
H0026	ITAMBI EN L.S. PABLO	810821	10021243	3467	33,30	32,94	32,35	12,58	4254	2680	0,089	1,60	1,34	80,69	0,378
H0045	APAQUI DJ MINAS	858100	10059439	3355	342,01	92,88	19,73	70,39	4025	2684	0,02	1,41	5,01	78,91	0,206
H0064	EL ANGEL EN PTE.AYORA	839654	10069610	3561	199,85	76,32	18,48	28,40	4195	2926	0,061	1,51	3,44	79,52	0,142

5.2 METHODS

Time-series data and physiographic descriptors were analyzed through five stages which include: 1. Streamflow analysis, 2. Flow component separation analysis, 3. Computation of physiographic characteristics, 4. Computation of flow indices, 5. Correlation analysis.

5.2.1 Stream flow analysis and data processing

One fundamental characteristic of streamflow is that this hydrological variable summarizes the catchment response to meteorological forcing as well as geological and land cover characteristics. The river discharge is measured as a function of the water volume that flows through a stream in a certain period of time. This time series is very important for understanding the catchment runoff dynamics and to unveil what are the environmental and geological factors controlling and regulating runoff over a catchment.

This section describes the techniques used to analyze the streamflow data from a raw database collected at INAMHI all the way to hydrograph separation of flow components.

5.2.1.1 Time series data format and quality control

To convert raw data provided by INAMHI into ready tractable time series the statistical software R (R Foundation, n.d.) was used. The purpose of this conversion is to transform the native INAMHI-txt format into a format ready for the subsequent processing of time series. By breaking the series into a range of years is possible to plot the dataset and visualize the hydrological series to make a first quality control.

First, the time series data were imported. At this point, the time series data: precipitation and streamflow data were analyzed taking into account the entire time period (1985-2015). By using the code, the structure of the raw plain data is read to finally yield time-arranged data columns. It is necessary to convert them into a data-time classes with the objective to identify only the columns that have the pluvio/hydro information in terms of year and month, ignoring those columns that do not have information. Finally, a quality control was developed in order to verify if the data time series obtained was appropriately re-formatted.

Hydrological analysis relies on good quality data. One important criterion is that river flow time series are not affected by error measurements, change in gauge location or depth-to-discharge rating curve transformations. The time series selected in this study were quality controlled before the analysis. This quality control involves visual inspection of the hydrographs, mass balance checks and comparison with publish literature.

One other important criterion is that the time series do not show magnitude changes with time, namely they are stationary. Stationary series are much easier to analyze. If they behaved in a certain way in the past (with a certain mean and variance), we can assume that they will continue to behave in the same way in the future. Under the stationary assumption all the statistical analysis and inference out the time series are assumed to be valid.

5.2.1.2 Hydrological annual cycle

By averaging out monthly values of streamflow, it was possible to estimate the hydrological annual cycle and identify wet and dry seasons. Such events are associated with different dry and wet periods which are a fundamental factor in analyzing the water balance of micro-catchments.

With the objective to search for the climatic influence on the hydrological behavior the annual hydrograph was plotted (Fig. 6.). The annual hydrograph represents in which way the climate influences the availability and timing of runoff through the year. In more concrete terms, by analyzing the long-term mean and distribution of streamflow in a yearly basis it was possible to identify dry and wet periods in December – February (DJF), March – May (MAM), June -August (JJA) and September – November (SON) seasons.

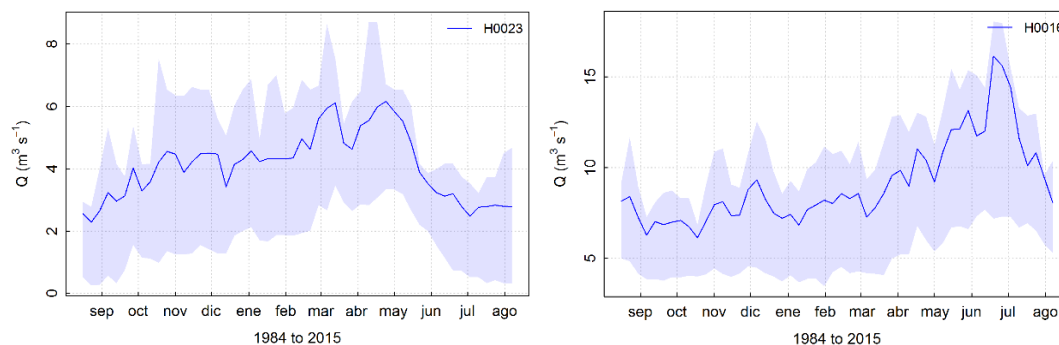


Fig. 6. Annual hydrograph of the stations H0023 (Ambi river) and H0016 (Apaqui river). Weekly mean of streamflow (blue line) with the lower and upper quartiles (blue shadow)

Fig. 6. shows two contrasting hydrological regimens in rivers Ambi (southern basin) and Apaqui (northeastern basin). In the annual hydrograph of the Ambi river (left), dry months have an average flow of approximately 2 to 4 m³/s in June - November, reaching the highest volumes of approx. 6 m³/s in March – May. By contrast, the annual hydrograph of the Apaqui river (right) has the highest volumes of approximately 15 m³/s that occur in July. Thus, the southern and northeastern basin showed two distinct hydrological regimes.

5.2.2 Hydrograph separation component

The analysis of hydrograph components provides important information concerning the flow process operating in each catchment zones. In a hydrograph separation graph is possible to see the rate of flow discharge in a specific time slide in a river, channel or conduit carrying the flow (Brodie & Hostetler, 2005) (Fig. 7.). The components of the hydrograph are:

- a) Fast flow: it is the immediate response to a rain event, including the terrestrial flow (overland flow), the lateral movement in the soil delineation (interflow) and the direct rain on the surface of the streamflow (direct precipitation), and;
- b) Base flow: the long-term discharge derived from natural storage (Brodie & Hostetler, 2005).

The relative rate of the fast flow and base flow components vary through the hydrographic record of the stream. The flood hydrograph (catchment area) is the classic response to a rain event and develops on three main stages (Fig. 7.):

1. The pre-conditions of low flow in the stream at the end of a dry period consists entirely of base flow (Brodie & Hostetler, 2005);
2. The increase in rainfall generates an increase in the streamflow, contributing mainly to the quick flow which is dominated by overland flow (runoff) and interflow. This stage starts in the *rising limb* towards the crest of the flood hydrograph (Brodie & Hostetler, 2005). The rapid increase in the level of the current in relation to the surrounding groundwater levels reduces or may even reverse the hydraulic gradient into the stream. This is expressed as a reduction in the base flow component at this stage;

3. Recession of quick flow component is represented by *recession limb* of the flood hydrograph. With the decrease of the current levels, the hydraulic gradient increases towards the current (Brodie & Hostetler, 2005). At this moment, base flow component begins to increase. At some point along the recession limb, the quick flow ceases and the streamflow is again composed entirely of base flow. Over time, the base flow decreases as the natural stores gradually drain during the dry period until the next significant rainfall event.

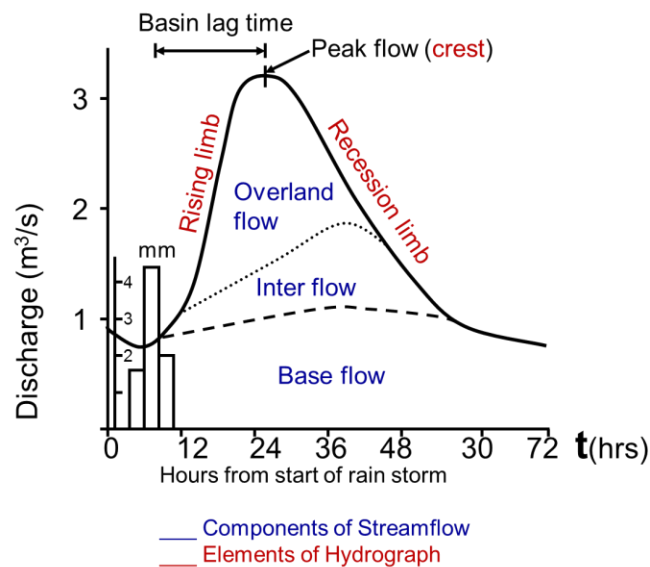


Fig. 7. Hydrograph component separation (AIHassoun, n.d.)

In this case study, the separation of hydrograph components was performed by using the open access tool called Water Engineering Time Series PROcessing (WETSPRO) developed by Willems (2009). This tool uses the Chapman filter which is derived from the general equation of a "low pass filter" (Willems, 2009). By applying this filter, it is possible to divide the total flow time series $q(t)$ into its components: slow flow $b(t)$ and quick flow time series $f(t)$. Chapman's original filter (1991) has one parameter: the recession constant k of the subflow to be separated. Willems (2000) shows that, in the original form of this filter, it is assumed that the long-term total volumes of the slow and quick flow series are identical (every 50% of the total runoff). The fractions of slow and quick runoff, however, vary strongly between watersheds depending on their characteristics i.e. topography, soil type, etc. Therefore, Willems (2000) proposed a generalization of the original Chapman filter where a new filter

parameter called reduction factor w (Fig. 8), is introduced which represents the case-specific average fraction of the quick flow volumes on the total flow volumes.

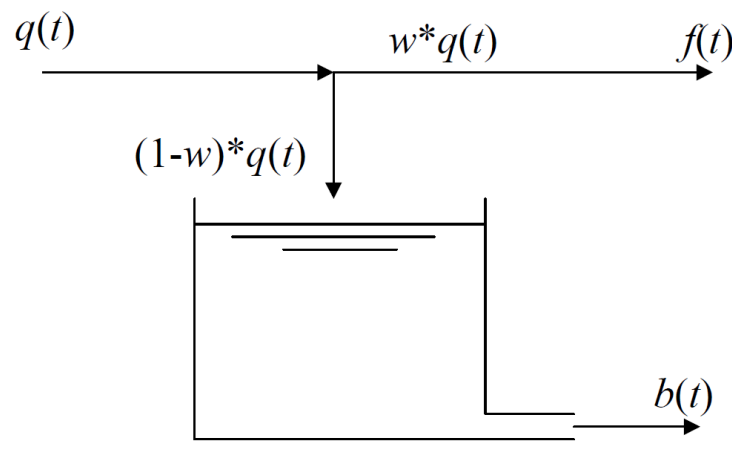


Fig. 8. Generalization of the Chapman-filter (Willems, 2000).

In a certain series of fluvial flows, discharges of independent maximum flows can be defined using criteria of independence (Willems, 2009). The dependence between the maximum flows is determined mainly by the recession of the basin, so the runoff peaks after rain can be considered largely independent if the time between events exceeds the recession time and if the lowest discharge between events falls below a specific low flow level.

The process to separate the slow flow, called in hydrology baseflow, is a graphical interactive method using the WETSPRO tool. This method consists in calibrate k and w filter parameter in order to separate the baseflow from the total flow. The k value can be assessed by analyzing the slope of the flow during recession periods (dry periods). The flow in exponential decreasing is plotted; on a hydrograph it has a linear decrease which is better visualized in a log scale. So, the mean of recession slope (yellow line, Fig. 9) must be aligned with the recession periods (blue curve, Fig. 9) looking all the dry periods in the time series. This gives an estimate of the k value based on a visual observation.

What it is aimed for the filtering is that the baseflow filter result is close to the real baseflow. That means the baseflow should follow the total flow as close as possible during the baseflow recession periods. On the other hand, w value is the fraction of total flow that belongs to the quick flow, for this reason the value calculated for the baseflow is $1-w$. So, the w value is

evaluated numerically for the quickflow to finally obtain the adequate visual alienation for the baseflow. For this alienation it is necessary to match the baseflow line (purple curve, Fig. 9) with the inflection point which separates the slope of the baseflow recession from the steeper slope of the quicker flow components by following the entire period in the time series.

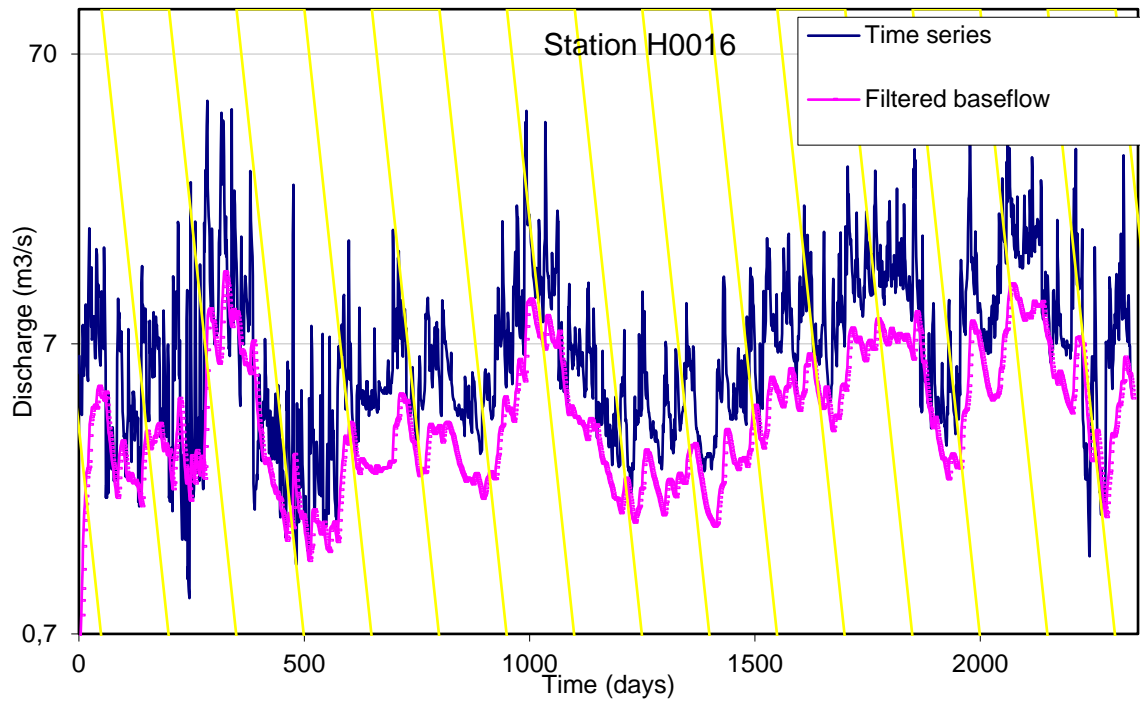


Fig. 9. Evaluation of the base flow recession constant and the results of the base flow filter based on the daily Mira river flow series, the first 10 950 days after 01-01-1985 (Graph presented to illustrate the separation component made in this study).

5.2.3 Computation of catchment physiographic characteristics

The computation of physiographic characteristics for the Mira basin was carried out through the analysis of soil types, topography, land use and climate descriptors as well as geology from free access data (Table 5). Thus, 74 descriptors were evaluated for each sub-basin upstream of their outlets, summarizing in this way the watershed physiographic properties (Kuentz et al., 2017).

The physiographic characteristics such as area, length, elevation and slope were calculated using the ARCGis software (ESRI, 2019). The types of parental rocks were provided by MAGAP whose database describe geological formations and lithology as well as deposition environments (Table 5). The soil type and land cover, also provided by MAGAP, describe the type, depth, infiltration and soil erosivity in addition to the use, the agricultural practices and the conditions in each land cover.

Table 5 Catchment descriptors and their data sources.

Variable	Unit	Data Source	Description
Area (T ¹)	km ²	Calculated using ArcGIS software	Total upward area of each sub-basin outlet
Elev(T)	masl	Provided by MAGAP	Elevation (DEM resolution 1:80000)
averSlope (T)	%	Calculated using ArcGIS software	Average slope (DEM resolution 1:80000)
Drainage density (T)	km ⁻²	Calculated from an equation	Drainage density was calculated dividing the total length of all streams by the area of the basin.
11 land cover variables (LC ²)	–	Provided by MAGAP	Percentage of catchment area coated by the subsequent land cover type: Agriculture; Agricultural - Conservation and Protection, Forest agriculture, Mixed agriculture, Anthropic, Conservation and Protection, Water bodies, Forest, Livestock, Livestock -Conservation and Protection and Non-productive lands
15 soil types variables (ST ³)	–	Provided by MAGAP	Percentage of catchment area coated by the subsequent soil types: andisols, calcisols, cambisols, durisls, fluvisols, inceptisol, kastanosems, leptosols, no data, phaeozems, regosols, solonetz, stagnosols, sixed land use and umbrisols

44 geological variables (G ⁴)	–	Provided by MAGAP	Percentage of catchment are coated by the subsequent lithologies: Andesite, feldspars, pyroxenes and iron oxides / Pyroxene Andesite with plagioclase / Basaltic Andesites / Basaltic Andesites, volcanic breccias and tuff / Andesites, tuff, breaches and agglomerates / Pyroxene Andesite, pyroclastic and laharitic flows / Andesites, breaches and agglomerates / Sand and gravel / Sand intercalated by silt and gravel / Sand, gravel and blocks / Sandstone, shale, chert, limestone and greywacke / Pillow basalt, lavas and breccias / Andesitic breccia, with lavas and sediments / Breccia, tuffs, pyroclastics and volcanic conglomerates / Ash and lapilli / Conglomerate / Volcanoclastic conglomerates, breaches and sandstones / Conglomerates and volcanic sandstones / Tuff, ash, pyroclastic, pumice and lapilli / Micaceous schists, quartzite and gneiss / Schist, garnet and graphite / Pyroclastic flows, lapilli, ash, lithics and pumice / Granodiorite / Andesitic pyroxene and lavas with plagioclase / Andesitic lavas with plagioclase and basalt / Andesitic lavas, agglomerates and laharic flows / Andesitic lavas, breccias and tuffs / Andesitic lavas, breccias, agglomerates and pyroclast / Andesitic lavas, volcanic and pyroclastics breccias / Andesitic lavas, agglomerates and volcanic breccias / Andesitic lavas, pyroclastics and dacitic domes / Lavas, pyroclastic material and volcanic breccias / Silt, clay, sand, gravel and blocks / Pyroclastic material, ash, lapilli and tuffs / Not apply / Pyroclasts, conglomerate and laharitic material / Volcanic tuff and ash / Andesitic tuff, ash and lapilli / Pelitic metamorphic rocks and metabasites / Volcanoclastics, lava and subvolcanic intrusions / Volcanic sediments, tuffs and silicified lavas / Tillites, sands, gravels and sedimentary blocks / Andesitic tuff, ash and lapilli / Undifferentiated volcanics
P _{mean} (C ⁵)	mm	Provided by INAMHI	Mean annual precipitation
SI (C)	–		Seasonality index of precipitation using the mean rainfall of month and the mean annual rainfall
T _{mean} (C)	°C	Provided by INAMHI	Mean annual temperature

¹T: topography; ²LC: land cover; ³ST: soil type; ³G: geology; ⁴C: climate

5.2.4 Computation of flow indices

The following sections describe the different parameters used and coefficients calculated in this study. A brief description of the parameters' and coefficients' rationale, common use, and relevance is included, followed by a description of how these were applied.

The flow indices or signatures were grouped using the daily time series from the databases of INAMHI. Those time series with continuous hydrological/meteorological data were selected to guarantee the reliability of the flow signature analysis, eliminating years with lack of data as well as signatures inconsistent with the rest of the data. In addition, data were taken from stations with a time range of 30 years (from 1985 to 2015). Missing data were eliminated in order to use continuous time series for each station. This means that some periods of time differ between the measurement stations, but descriptors consistent with the precipitation data provided by the INAMHI were used.

Eventually, all hydrographs of the resulting subgroup were visually verified over a period of 30 years. In order to guarantee quality, seasonal analyzes were carried out for wet and dry seasons, as mean to control time consistence in hydrographs by localizing missing time ranges.

For each catchment area, 15 flow signatures were calculated (Table 6). The selection of flow signatures follows Olden and Poff's (2003) criteria, which provides guidelines for the selection of seven indices that describe the flow regimes important for hydro-ecology. In addition, five flow signatures commonly used in hydrology were added for comparability (Qsp, Qcv, Q5, Q95, RBI).

Table 6 Description of the 15 signatures studied.

Component of flow regime		Variable	Unit	Description
Magnitude of flow events	Average flow conditions	skew	–	Skewness = mean/median of daily flow
		Qsp	Ls ⁻¹ km ⁻²	Mean specific flow
		Qcv	–	Coefficient of variation = SD/mean of daily flows
	Low flow conditions	bfi	–	Baseflow index: 7 days minimum flow divided by mean annual daily flow averaged across years
	High flow conditions	Q5	Ls ⁻¹ km ⁻²	5th percentile of daily specific flow
		HFD	–	High flow discharge: 10th percentile of daily flow divided by median daily flow
		Q95	Ls ⁻¹ km ⁻¹	95th percentile of daily specific flow

Frequency events of flow	Low flow conditions	lfs.freq	Year ⁻¹	Total number of low flow spells (threshold equal to 5 % of mean daily flow) divided by the record length
	High flow conditions	hf.count.v ar	–	Coefficient of variation in annual number of high flow occurrences (threshold 75th percentile)
Duration of flow events	Low flow conditions	lfdur.var	–	Coefficient of variation in annual mean duration of low flows (threshold 25th percentile)
	High flow conditions	mean.max 30d	–	Mean annual 30-day maximum divided by median flow
Rate of change in flow events		RBI	–	Richard-Baker flashiness index that sum absolute values of day-to-day changes in mean daily flow divided by the sum of all daily flows
Catchment response		RunoffCo	–	Runoff ratio: average of annual flow divided by average of annual precipitations
		AET	mm yr ⁻¹	Actual evapotranspiration: average of annual precipitation minus average of annual flow

5.2.5 Analysis of physiographic controls of flow characteristics

Hydrological signatures or indices are derived or calculated values from hydrological data sets such as rain, flow or soil moisture (McMillan et al., 2016). All of these are designed to represent relevant information on hydrological behavior, as well as to locate dominant processes and determine the spatiotemporal variability of the rain-runoff cycle (McMillan et al., 2016). An index is a scalar estimation from the streamflow, which includes the average flow, the base flow index or the slope of the flow duration curve (FDC). Recapitulating the history, these indices have been applied in the area of hydrology for a long time. However, the concept of hydrological signature was described as minimal representations of the relevant information contained in a set of hydrological databases (McMillan et al., 2016).

It should be emphasized that the link between the values of the indices compared with the behavior and hydrological processes is not always easy to analyze, which leads to the variability in the choice of the appropriate indices. According to Olden & Poff (2003), the task in hydrological analysis is to choose among a large number of hydrological indices in order to reduce computational effort and the redundancy of indices before statistical analyzes.

McMillan et al. (2016) and Olden & Poff (2003) offer a series of recommendations on how many and which indices should be used in hydrological studies. Both studies make the point that the best choice should deal with the selection of at least one index that describe each of the components of the flow regime. These are the magnitude, duration and frequency of the flow events (Kuentz et al., 2017). This ensures that the majority of the variation and redundancy will be minimized and that different aspects of the flow regimes are adequately represented in subsequent analyzes.

However, the indices manufactured for the analysis of each component of the flow regime are more than a dozen. The most successful approach would be to work with the indices that best describe that component. It was found that the asymmetry in the daily flows (Skew, Table 6) is one of the indices that most consistently describe the magnitude in all types of currents and can be a particularly important measurement of the daily flow conditions (Olden & Poff, 2003). The hydrological indices that represent the duration of flooding in streamflow are particularly important given the impact of flood events to maintain diversity through their influence on sediment dynamics (Olden & Poff, 2003). The hydrological indices that describe the monthly (30 days) and seasonal (90 days) duration of high and low flows (lfdur.var, mean.max30d) are good candidates for studies in high mountain regions. Finally, indices related to frequency (lfs.freq, hf.count.var) may be important for stable/super stable groundwater flows given their high information, their non-redundant nature and the importance of conditions during the critical life history of the river stages (Olden & Poff, 2003). In addition, quantifying the time of the floods would be important since there may be a correlation in linking the productive performance of the basin with the magnitude of the flood.

5.2.6 Correlation analysis

Correlation analysis shows the robustness of a relationship or level of association between two, numerically measured variables. It is estimated by a coefficient which describes both the robustness and the direction of the relationship.

5.2.6.1 Pearson correlation

The Pearson correlation evaluates the linear association between two variables. This linear relationship occurs when the change of one variable is proportional to change in another variable (Lehman et al., 2013) (Eq. 10). This is used to evaluate whether a change in catchment descriptors at the study zone is associated with progressive change in certain proposed flow index to study the runoff response.

Where;

$$(Eq. 10) \rho_{X,Y} = \frac{cov(X,Y)}{\sigma_X \sigma_Y}$$

cov = is the covariance

σ_X = *is the standard deviation of X*

σ_Y = *is the standard deviation of Y*

5.2.6.2 Spearman correlation

The Spearman correlation evaluates the progressive change between two variables. In this connection, the variables tend to vary together, but not necessarily at a constant rate (Eq. 11). The coefficient of the Spearman correlation is based on the values ranked for each variable instead of the gross data (Lehman et al., 2013).

This correlation is often applied to evaluate relationships that involve ordinal variables. It can be used to evaluate whether the number in which catchment descriptors influence the runoff process is associated with the number of indices that have been proposed to describe the area.

Where;

$$(Eq. 11) \rho_{rg_X,rg_Y} = \frac{cov(rg_X,rg_Y)}{\sigma_{rg_X} \sigma_{rg_Y}}$$

ρ = *denotes the usual Pearson Correlation coefficient, but applied to the rank variables.*

$cov(rg_X,rg_Y)$ = *is the covariance of the rank variables.*

σ_{rg_X} and σ_{rg_Y} = *are the standard deviations of the rank variable*

One way to examine the connection between variables is through the use of correlation matrix plots. In which the range of influence of each index is visually plotted with respect to the proposed catchment descriptors. Then, connections are made by studying the linear (Pearson) and progressive (Spearman) correlation coefficients.

VI. RESULTS AND DISCUSSION

In this section the overall catchment hydrological response is first discussed based on the catchment descriptors presented in section 5.2.3. Then, the hydrograph composition at each gauge station is presented and discussed to illustrate basin-wide micro-catchment differences. Finally, the analysis of the physiographic controls of the runoff response for the entire studied area is presented. Results are presented for different seasons.

6.1 CATCHMENTS DESCRIPTORS

The results of the water concentration time for the Mira basin are shown to be consistent with the rivers length and each sub-basin slopes. There is a greater time concentration for the basins with larger river lengths and moderately strong slopes. This is the case of the Sub-basin H0011 where the Mira river extends approximately 150 km and whose slope ranges between 25 to 50%, yielding a concentration time of approximately 15 hours (Fig. 10). On the other hand, sub-basins with small river lengths have shorter concentration time. It should be noted that the slope of each basin plays a significant role because it ranges from strong to very strong (25 - 70%). This is the case of the sub-basins H0013 and H0026 (from 31,35 to 51.71%), whose concentration time are very low ranging from 1 to 2 hours (Fig. 10).

6.2 QUICK/SLOW FLOW RATIO RELATIONSHIP

The analysis of the streamflow time series data on rain events reveals that the flow throughout the year is distributed fairly uniformly (Fig. 11). Two patterns related to the streamflow can be identified. The G1, located in the northeast of the studied area (H0015, H0016, H0017, H0045) and draining to the Apaqui river, and the G2 located in the south (H0023, H0024 and H0026) and draining to the Ambi river. In the G1, a quickflow increase can be observed, which remains constant during the year for the sub-basins H0045 and H0017. However, the sub-basin H0016 generates more baseflow during SON and DJF. This might be due to the increase in rainfall that happens during these months, which exceeds the storage capacity of the soil, circulating more water through the subsoil layer (see section 6.3). The opposite happens in the G2 since the baseflow exceeds the quickflow throughout the year. This is a clear sign of a high water-storing area. As the flow is directed downstream, quickflow increases through the course of the Ambi river.

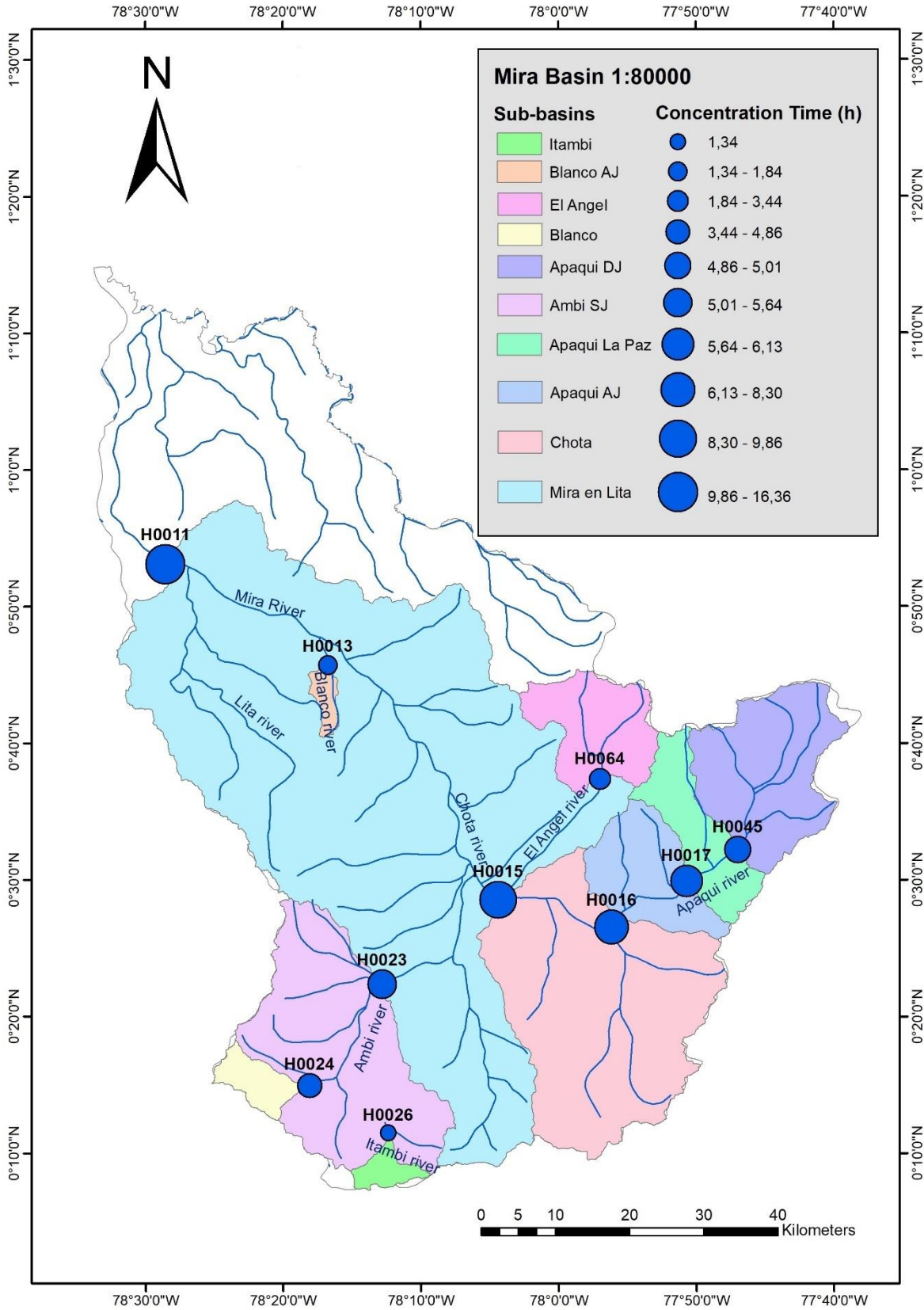


Fig. 10. Concentration time at each sub-basin outlet in the Mira basin.

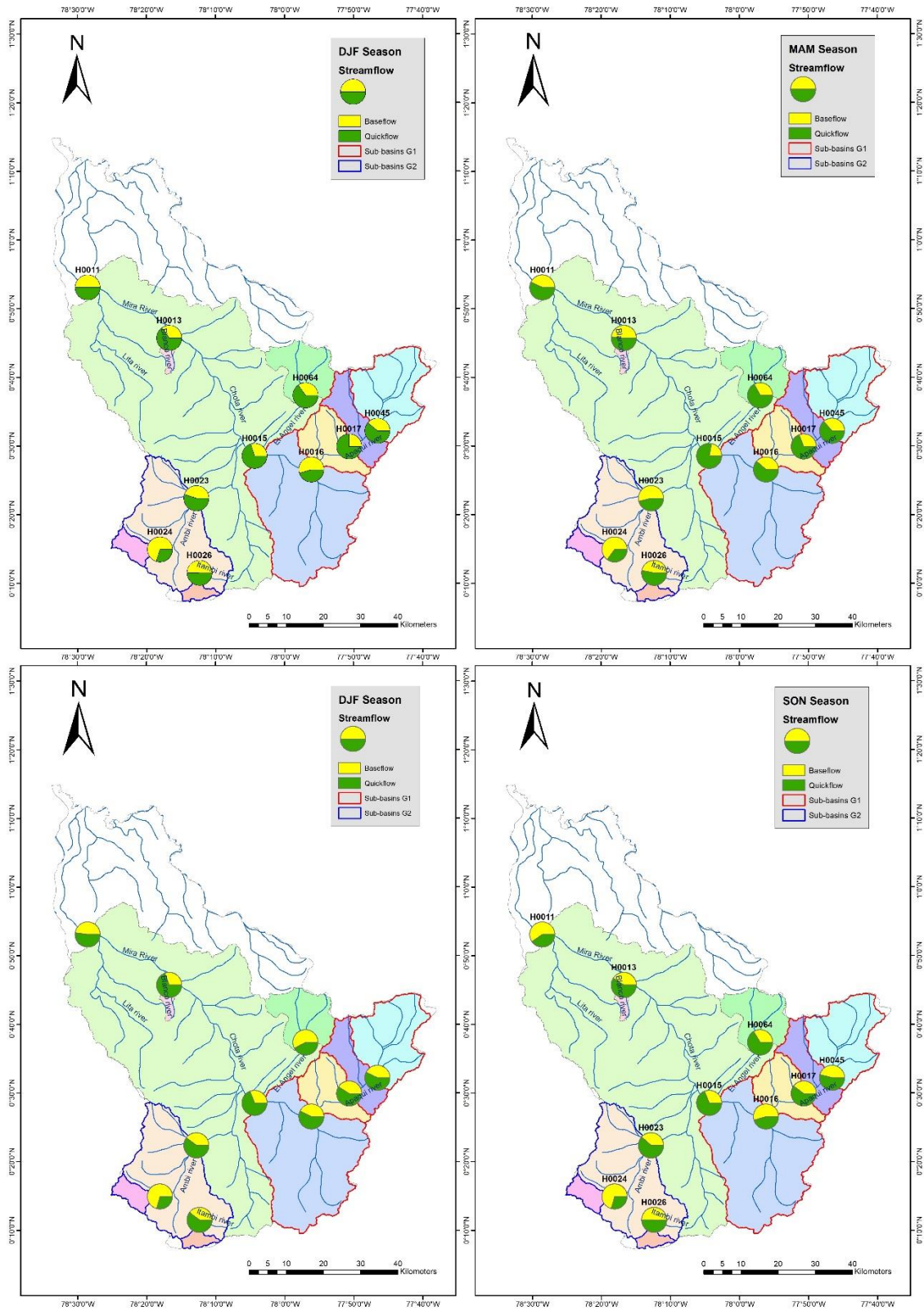


Fig. 11. Quick/Slow flow ratio relationship showed by season (DJF: December, January, and February; MAM: March, April, and May; JJA: June, July, and August; SON; September, October, and November)

6.3 PHYSIOGRAPHIC CONTROLS OF FLOW CHARACTERISTICS

After analyzing the response that each catchment descriptor showed in relation to the magnitude, duration and frequency of flow, as well as to the catchment response, for each group of sub-basins in the G1 (H0015, H0016, H0017, H0045) and the G2 (H0023, H0024, H0026), and after the linear and monotonic correlations, the main factors that affect each flow regime were identified. Those driving factors correspond to correlation coefficients (both Pearson and Spearman) greater than +0.7. The choice of the driving factors is based on a theoretical justification and meaningfulness (Shmueli, 2010) for the studied process rather than the statistical significance.

6.3.1 Group of sub-basins G1

In terms of climate, the G1 is a mountainous area characterized by year-round well-distributed rain, with a minimum in June to August (Fig. 16). Thus, actual evapotranspiration (AET) in the period following the precipitation deficit, SON and DJF, shows high Spearman correlation coefficients (around 0.9) with precipitations (P_{mean}) and seasonality (SI) (see appendix Fig. 19). From DJF towards the third quarter (JJA) of the year, frequency of the flow, particularly during MAM, increases with average precipitation (P_{mean} vs. $lfs.freq$). The same relationship can be observed in the remaining months, but with less intensity. Thus, precipitation shows to be an important factor for the frequency with which runoff occurs. Although much of this precipitation is lost through evapotranspiration.

The relationship between the topographic descriptors and the hydrological signatures of the flow is somewhat variant throughout the year. The magnitude of flows (Q_{mean}) correlates with the area and the slope of the sub-basins during DJF, highlighting a strong linear relationship between flow and the G1 basin's surface characteristics (Fig. 12 and 13). Out of this inference, the magnitude of the flow is associated with the land-form of the G1, which controls the temporal dynamics of the basin's response. In the following quarters, MAM, JJA and SON, there is an increase in the correlation patterns between the frequency of low flow ($lfs.freq$) and the duration events ($lfdur.var$, $mean.max30d.med$) with the area and especially with the average slope (Fig. 12 and 13). Sharp and elongated slopes in the G1 help the runoff generation process through quick flows, resulting into a rapid basin response.

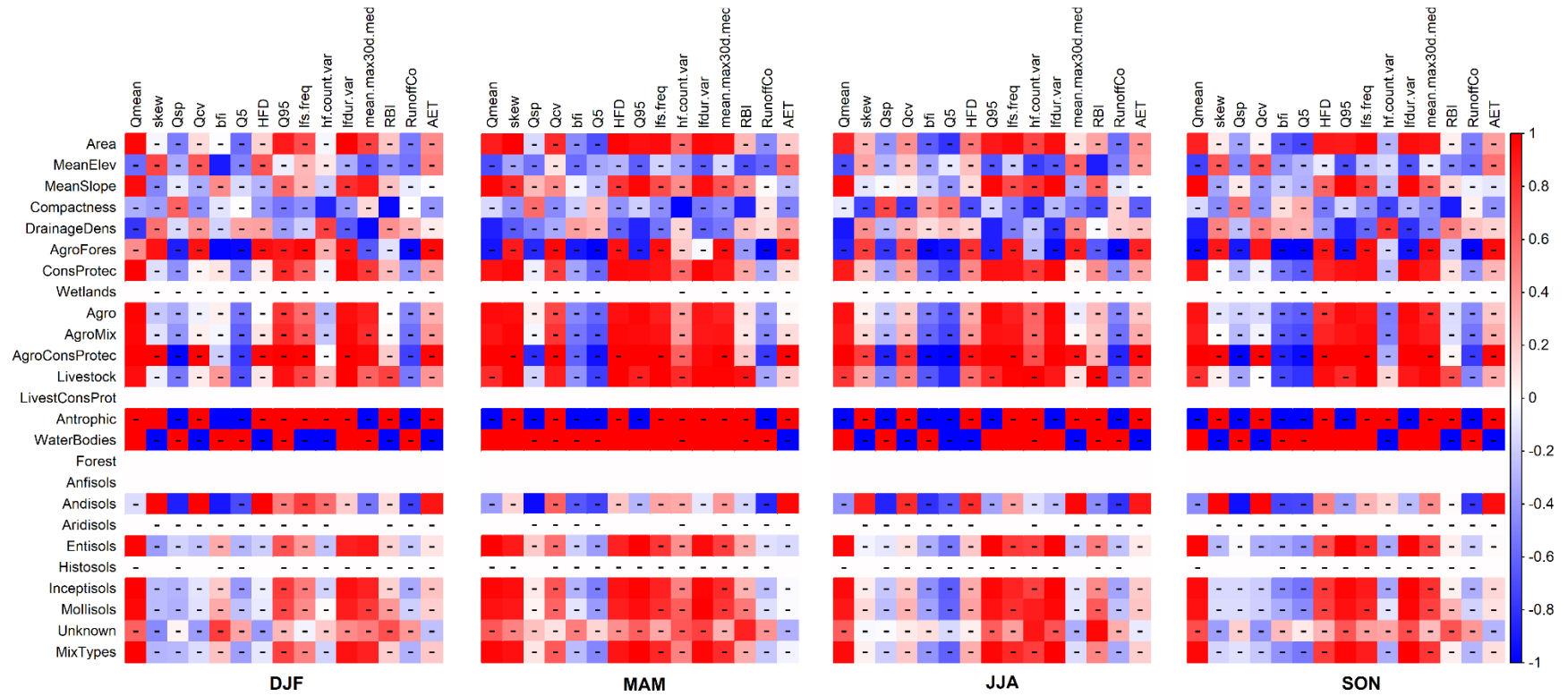


Fig. 12. Pearson correlation matrix of the G1 between proposed flow signatures and catchment descriptors related to topography, land cover, and soil type. Non-significant correlation according to the significance test are indicated with a dash (-).

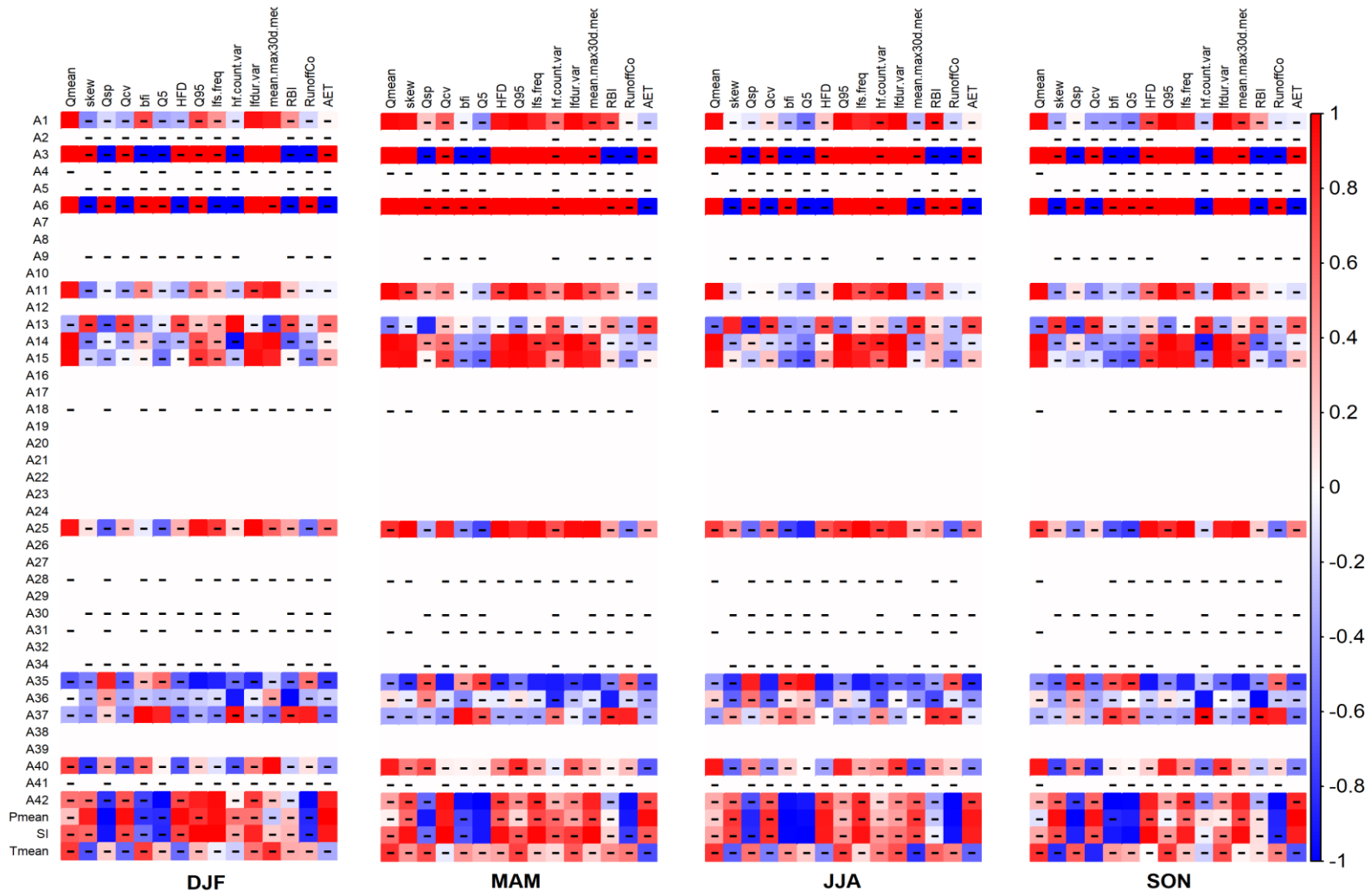


Fig. 13. Pearson correlation matrix of the G1 between proposed flow signatures and catchment descriptors related to geology, and climate. Non-significant correlation according to the significance test are indicated with a dash (-).

On the other hand, the land uses in the G1 show a strong correlation (more than 0.8 of Pearson coefficients) (Fig. 12) with the magnitude, frequency, and duration of the flow. During MAM, this influence is accentuated especially in conservation areas, and livestock areas with a high index of vegetative thickness, and water bodies (Fig. 12 and 13). Dense vegetation increases permeability in agricultural, conservation, and protection land uses benefiting infiltration, which is consistent with the low concentration time of the steeper and short river-length sub-basins in the G1. Low concentration time together with sharp slopes and high infiltration levels suggests a lateral movement of the flow following an Hortonian-like mechanism. Once the wet period has elapsed, correlation levels decrease, as well as rainfall decreases. However, the magnitude indices (HFD, Q95), frequency (lfs.freq) and duration (lfdur.var, mean.max30d.med) remain constant throughout the end of the year.

In soil types, relationships of magnitude and duration of flow (Qmean and lfdur.var respectively) with Entisols, Inceptisols, Mollisols and mixed-type are reflected throughout the year (Fig. 12 and 13). This suggests that dry quarters SON and DJF reflect high correlations between these types of soils and the indices of flow duration (lfdur.var, mean.max30d.med) due to the high storage of water related with its organic composition and fine grain. These soils can hold large volumes of water; however, the slope and vegetation of the G1 favors rapid flow becoming an Hortonian-like pattern that might move laterally through the subsoil layer. On the other hand, in MAM and JJA the correlation between signatures and descriptors of the basin favors the frequency of the flow, which shows a linear relationship between rainfall and the presence of Entisols, Inceptisols and Mollisols (Fig. 12).

Something similar happens with lithology in the G1 group. Magnitude and duration of the flow (Qmean, lfdur.var, mean.max30d.med) strongly correlates with pyroclastic lithologies with a low percentage of coarse-grained sands (A1, A3, A6, A11, A14, A15, and A25) (see appendix Table 8). Due to its high index of consolidation and granulometry, these rocks make infiltration difficult, causing the greatest amount of flow to remain in the vadose zone. With the growth of rainfall, the relationship between these lithologies with the frequency, magnitude and duration indices increases (Fig. 13). This happens in MAM, especially with the presence of superficial granodiorite, corroborating that the subsurface flow moves laterally due to excess of water in the humid months.

6.3.2 Group of sub-basins G2

The annual total rainfall contribution in the sub-basins of the G2 group (H0023, H0024, H0026) is lower than in G1 (H0015, H0016, H0017, H0045). Despite its ephemeral character (Appendix 11.2, Sub-basin; H0023, H0024, H0026), the average rainfall and its temporality (P_{mean} and SI respectively) are highly correlated (> 0.9 Pearson and Spearman coefficients) with components of magnitude and flow rate (Fig. 14 and 15). The annual precipitation distribution, which leads streamflow availability, limits the generation of surface runoff in the driest season (JJA). The magnitude of the high flow (HFD) and the frequency of the low flow (lfs.freq) correlates strongly with the average temperature in DJF. This quarter is characterized by the decrement of rainfall after an increase in temperature. With this, the evapotranspiration (AET) is accentuated, in this time period limiting the superficial infiltration of the flow. In addition, there is no correlation between rainfall and baseflow which supports the idea that the volume of rainfall in humid quarters, partially evaporates but also infiltrates. This fact contradicts the idea of lateral flow, since the greater amount of water exceeds the vadose zone to become groundwater recharge.

Area and compactness index of the basin seem to have a strong relationship, (> 0.9 for Spearman coefficient) throughout the year, with signatures of magnitude of flow (Q_{mean} and Q_{95}) on the one hand, and the response of the catchment's area through evapotranspiration (AET) on the other. The G2's shape controls the temporal dynamics of baseflow (see again Fig. 11) which is limited by active evapotranspiration in the drier seasons (JJA, SON and DJF). In addition, a constant correlation can be observed throughout the year between the runoff coefficient (RunoffCo) and elevation, as well as with slope. This suggest that the baseflow moves slowly, due to gravity, increasing the concentration time in the G2 (Fig. 10). Partially a strong correlation is shown (> 0.8 Pearson coefficient) between these topographic descriptors with the duration of the baseflow during DJF and MAM. This reflects the increase in soil-humidity during these months.

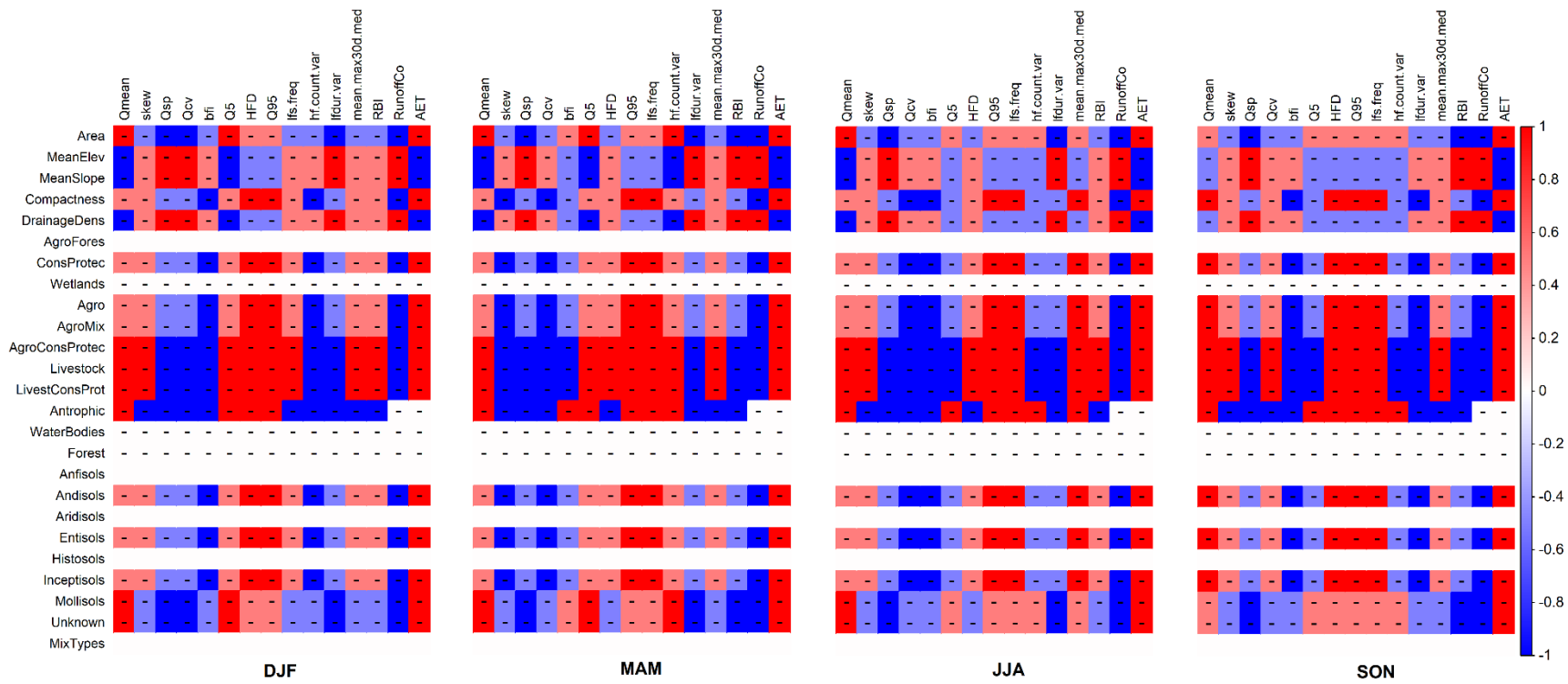


Fig. 14. Spearman correlation matrix of the G2 between proposed flow signatures and catchment descriptors related to topography, land cover, and soil type. Non-significant correlation according to the significance test are indicated with a dash (-).

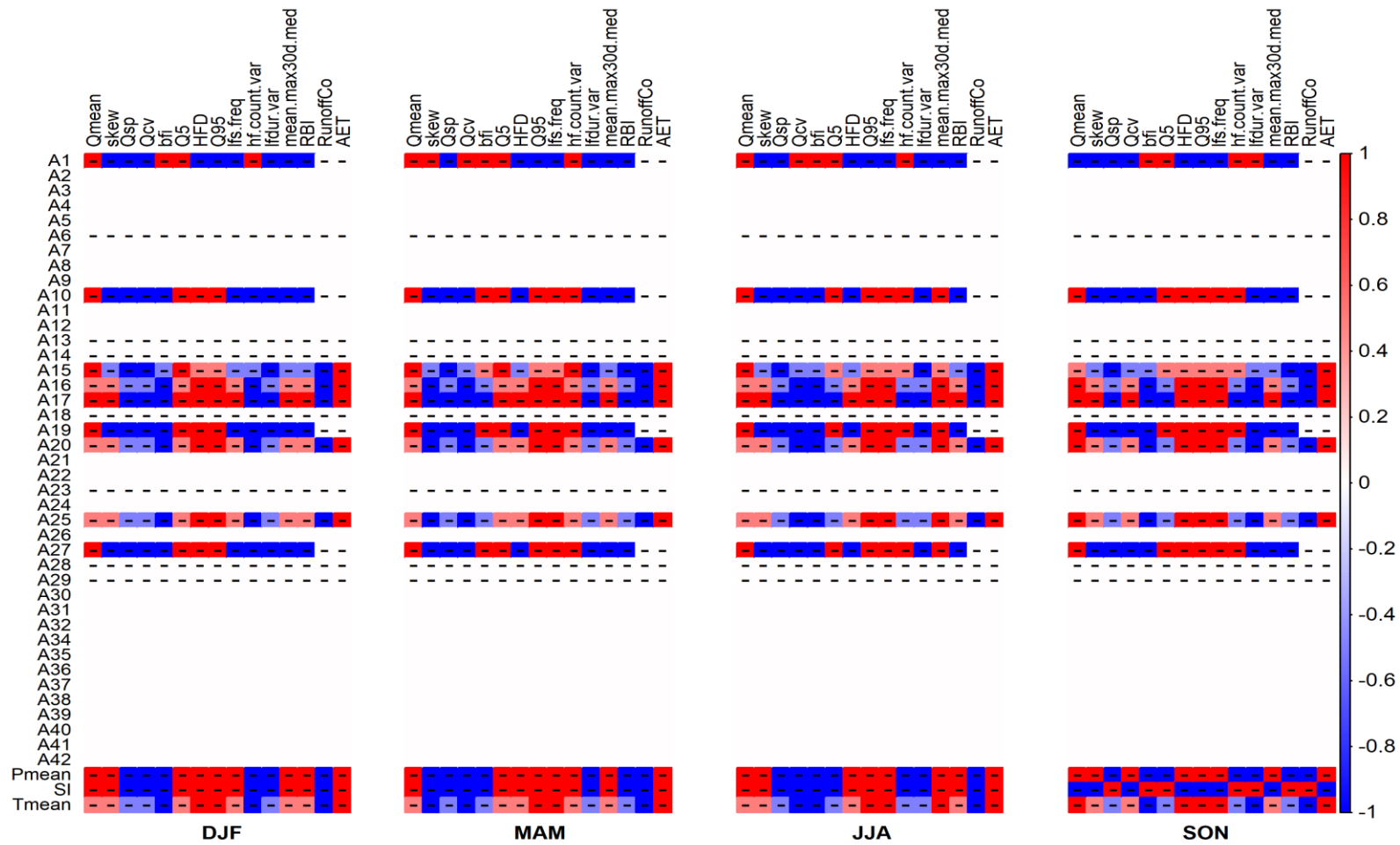


Fig. 15. Spearman correlation matrix of the G2 between proposed flow signatures and catchment descriptors related to geology, and climate. Non-significant correlation according to the significance test are indicated with a dash (-).

In general, land degraded by agriculture generates surface runoff shortly after a rain event. Thus, agriculture has a very rapid and sharp hydrological response on slopes (mean slope), since surface flow is the dominant runoff generation mechanism (Fig. 14).

Conversely, croplands and pastures do not allow surface runoff because they favor infiltration. This is the dominant factor in the G2 area since its soils are characterized by a high infiltration capacity. Results strongly suggest that the generation of runoff in degraded ecosystems is controlled primarily by surface vegetation and land management. Dense vegetation, combined with gentle slopes contributes to streamflow from which the baseflow is the main component.

Flow magnitude indices strongly correlate with all land uses, as shown by the mean flow (Q_{mean}), the skewness (skew), the 5th and 95th percentile of the daily specific flow (Q_5 and Q_{95}) and the high discharge rate (HFD). Regarding the frequency of the flow, there is a correlation only with the low flow index, highlighting the scarcity of rainfall in the area (Fig. 14). However, during MAM a more extensive correlation pattern is seen which suggest an increase in soil humidity. Finally, the indices of duration and rate of change (mean.max30d.med and RBI respectively) show high correlation with conservation and livestock areas which are characterized by poorly worked soils suitable for surface flow.

All soil-types that show significant correlation (andisols, entisols, inceptisols and mollisols) are compatible with the components of the flow regime (Fig. 14). The most outstanding are: average flow (Q_{mean}), 5th and 95th percentile of the daily specific flow (Q_5 and Q_{95}), and AET. As the year progresses from January to December, stronger correlations can be seen, including low flow rate indices (lfs.freq) and high flow duration (mean.max30d.med), suggesting conservation of the flow hydrograph characteristics in the year. These soils are characterized by having a great infiltration capacity, which in combination with the shortages of precipitations result in base flow over quickflow.

A similar pattern can be observed in the lithology descriptors at the level of correlation (>0.8 for the Pearson coefficient) between all the significant lithologies and flow magnitude signatures: the mean flow (Q_{mean}) and the 5th and 95th percentiles of the daily specific flow (Q_5 and Q_{95}). The frequency and duration of the flow is remarkable during MAM and SON, quarters in which two large precipitation pulses are observed.

Finally, AET is well related to pyroclastic flows and andesitic lavas (A15, A16, A17, A20, A25) throughout the year (see appendix Table 8). These types of rocks are characterized by a large permeability due to their consolidation, thus contributing to surface flow. However, this flow is affected by evapotranspiration so that the actual flow is diminished (Fig. 15).

6.4 FLOOD HYDROGRAPH ANALYSIS

6.4.1 Group of sub-basins G1

The increase in precipitation generates high correlation between basin descriptors with magnitude and frequency signatures of the flow (Fig. 16). This can be seen during MAM where the soil type and land use show a Spearman correlation coefficient greater than +0.9 (see appendix Fig. 18). The increase in rainfall results in a greater volume of total flow generating around 35 m³/s towards JJA, suggesting that the slopes of the sub-basins in G1 are a main factor for quickflow generation. During JJA, soil type and land use are dominant factors for streamflow infiltration, which is most likely moving laterally through the vadose zone. In August there is a drastic decrease in the amount of precipitation. However, this dry period is short since rains increase towards the fourth quarter (SON) generating a fairly high correlation between soil types with frequency and duration of the flow. The bimodal character of the regime establishes a region where rapid flow exceeds baseflow, due to the continuous supply of rainwater. The Hortonian movement by infiltration excess is due to organic soils with a high vegetation index. The presence of soils of volcanic origin help infiltration diminishing the storage of high-water volumes. Impermeable granodiorite seems to be a relevant rock for this process, maintaining water in the vadose zone.

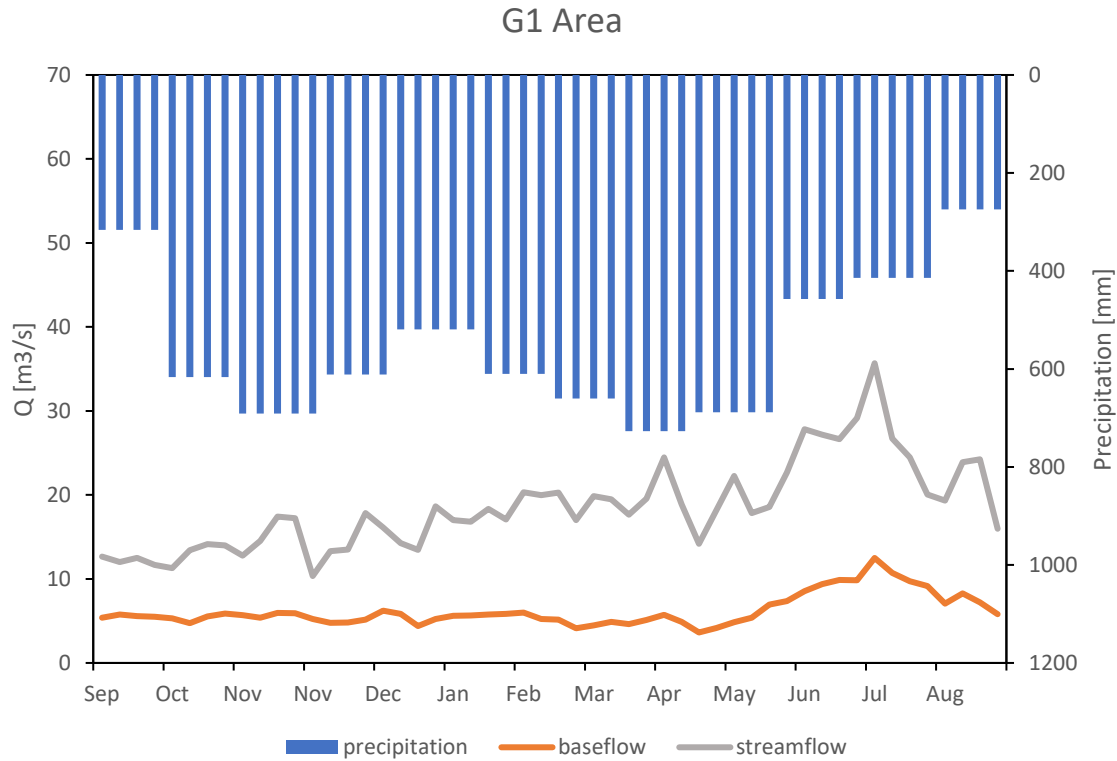


Fig. 16. Flood Hydrograph corresponding to north-east flow regime in the G1 sub-basin group.

6.4.2 Group of sub-basins G2

The increase in the total flow during MAM is the result of intense rains (about 1.200 mm) in the G2 (Fig. 17). Large amount of streamflow becomes fast flow. The runoff in this section is dominated by the elevation and slope factor (see appendix Fig. 20), generating an increase in base flow which travels through the organic soil horizons where the Andisols, Entisols and Inceptisols stand out. The bimodal character of the rains generates two pulses, the highest in MAM and the other one during SON. These two floods result in a progressive increase of the streamflow which is transferred to the subsurface level through pyroclastic deposits with little consolidation, facilitating the infiltration (see appendix Fig. 21). This results in an increase of the baseflow in G2, whose transport is conditioned by the lithology of the area as well as by the high-ranking slopes present in this group of sub-basins.

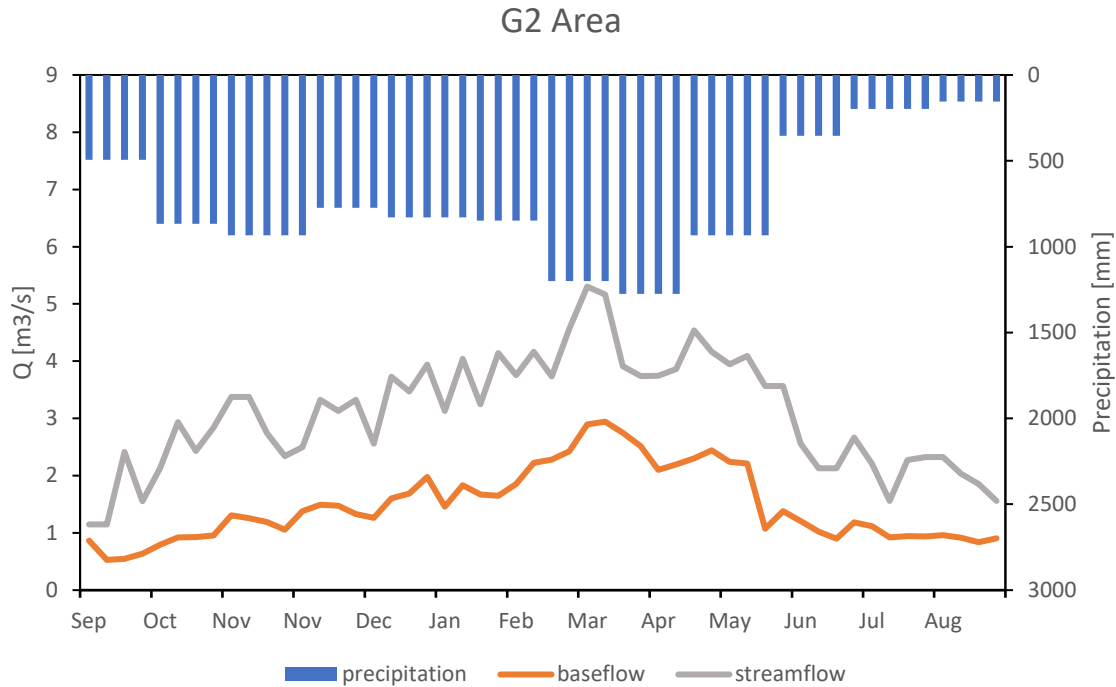


Fig. 17. Flood Hydrograph graph corresponding to south-west flow regime in the G2 sub-basin group.

VII. CONCLUSION

The generation of runoff in the studied area is controlled by several climatic and physiographic characteristics of the Mira river basin. One of these features that results to be highly variable in the Andes is elevation as a main factor, and with it the spatial and temporal distribution of the atmospheric water and the hydric gradients. As the surface temperature decreases rainfall increases, affecting the streamflow regime which is associated with the temporal distribution and dynamics of runoff over each sub-catchment group.

7.1 SPATIAL VARIABILITY OF RUNOFF

At the southwestern side of the Mira basin, in the Ambi sub-basins group, the annual baseflow (low component) is more prominent than the quickflow. Therefore, runoff is likely originated from sub-surface flow, related with the high surface evapotranspiration throughout the year and the high infiltration that exceeds the vadose zone driven by gentle slopes and long dry periods.

By contrast, at the northeastern side in the Apaqui sub-basins group the quickflow is the dominant component of the hydrograph throughout the year. Therefore, climatic factors are to be likely the main driver of runoff. In addition, constant precipitations over the year maintain the level of water supply and consequently the infiltration. The latter is favored by the abundance of vegetation and sharp slopes.

7.2 AT CATCHMENT SCALE

Through the study of selected sub-basin's flow regimes, it was possible to analyze its temporal dynamics describing two different flow regimes, which relate to areas G1 and G2 (see again Fig. 11). The perennial behavior in the G1 area is associated with an abundance of rainfall during the year, showing constancy between high and low rainfall pulses (see again Fig. 16). By contrast, the ephemeral behavior of G2 (see again Fig. 17) shows a decrease in rainfall towards SON and DJF, and only one large rainfall pulse on April.

The rainfall volume in the northeast of the Mira river basin is an essential factor of the frequency and final amount of runoff. The magnitude of the flow is associated with the landforms in the northeast section of the Mira basin, which controls the temporal dynamics of the basin's runoff response. The steep and elongated slopes help the process of runoff generation through rapid flows, which results in a rapid basin's response. The livestock and conservation areas have a high index of foliage which benefits permeability of the area and the generation of runoff. The organic composition and fine grain of the soil elevates the groundwater storage index. Moreover, the low concentration time together with the steep slopes and the high levels of infiltration through densely vegetated areas suggest a lateral movement of the flow following a Hortonian-like mechanism. In addition, the infiltration is limited when reaching the saturation limit of the vadose zone. There are granodiorite deposits with a high index of consolidation and granulometry, corroborating the infiltration of the flow at the subsurface level, where it moves laterally due to the excess of water in the humid months.

The annual precipitation distribution that determines the availability of streamflow in the southwest of the Mira watershed, conditions the generation of surface runoff in the drier season (JJA). The decrease in rainfall, after an increase in temperature accentuates the active evapotranspiration in the drier seasons, limiting the surface infiltration of the flow. In

addition, pyroclastic deposits and andesitic lavas which are characterized by having high rates of permeability due to their consolidation, restrict surface flow infiltration. However, this flow is affected by evapotranspiration, which decreases sub-surface flow.

The shape of the basin controls the temporal dynamics of the sub-surface flow which is affected by the evaporation during dry periods. This fact contradicts the idea of lateral flow since the rest of non-evaporating water exceeds the vadose zone by the action of dense vegetation and gentle slopes. This ultimately becomes part of the groundwater recharge, resulting in a major base flow over quickflow.

In conclusion, the rainfall-runoff cycle in the Mira basin is mainly conditioned by topographic and climatic factors. These two are related since the high-elevation terrain in the study area cause sharp hydro-climatic gradients that modify the precipitation pattern. This, coupled with the steep slopes and dense vegetation of the paramo, result in different behaviors in terms of basin response. Through this study, it has been detected that water availability in the catchment areas of the Mira basin fluctuates due to the variability in the rainfall-runoff cycle. With this premise, it is possible to identify the major water sources in order to improve the sustainable management of this basic resource for human consumption, agriculture, and industrial activities.

VIII. FURTHER RESEARCH

Since different hydrological behaviors have been identified in the Mira basin, it would be necessary to focus studies in sub-basins of the G1 and G2 groups. With the use of soil moisture sensors, soil-water column experiments could be set to understand the hydro-physical process of soil and the vadose zone. In addition, the application of geophysical methods such as electrical resistivity measurements and magnetic resonance will help to understand the relationship between the latter and the underlying aquifers. There are non-invasive methods which minimize the damage to the environment and in practice they generate reliable results.

IX. ACKNOWLEDGEMENTS

I wish to express my sincere gratitude to all the people who, through their scientific and human support, have collaborated in the development of this research. First, I want to thank the Ecuadorian public institutions that made possible this work through data provision: Instituto Nacional de Meteorología e Hidrología (for hydro-meteorological data). The Ministerio de Agricultura, Ganadería y Pesca (for thematic maps) and the Instituto Geográfico Militar (for cartographic information).

I am highly indebted to my thesis advisor, Dr. Luis Eduardo Pineda Ordóñez, for the academic orientation, support and critical discussion that allowed me to undertake this research work, which finally came to a successful conclusion. Finally, I wish to thank my family for their understanding, constant communication, and daily support. To my parents who have always been by my side sharing my happiness and anguishes, and in a very special way, to my brother for the encouragement to overcome myself day by day; and being the unconditional support where I found the strength to get to the end of this road.

X. BIBLIOGRAPHY

AlHassoun, S. (n.d.). *Hydrograph Analysis* [PPT].

Albán, M., & Argüello, M. (2004). *Un análisis de los impactos sociales y económicos de los proyectos de fijación de carbono en el Ecuador. El caso de PROFAFOR-FACE* (Vol. 7). IIED.

Alvarado, A. (2012). *Néotectonique et cinématique de la déformation continentale en Equateur*. Doctoral Thesis, University of Grenoble, 259 p.

Boland, A. M., Jerie, P. H., Mitchell, P. D., Goodwin, I., & Connor, D. J. (2000). *Long-term effects of restricted root volume and regulated deficit irrigation on peach: II. Productivity and water use*. *Journal of the American Society for Horticultural Science*, 125(1), 143-148.

Brodie, R. S., & Hostetler, S. (2005). *A review of techniques for analysing baseflow from stream hydrographs*. In *Proceedings of the NZHS-IAH-NZSSS 2005 conference* (Vol. 28). Auckland New Zealand.

Environmental Systems Research Institute (ESRI). (2019). *ArcGIS Release 10.5*. Redlands, CA.

Chapman, T., 1991. Comment on “evaluation of automated techniques for base flow and recession analyses” by R.J. Nathan and T.A. McMahon. *Water Resources Research* 27 (7), 1783–1784.

Consejo Nacional de Recursos Hídricos. (2002). *Gestión de los Recursos Hídricos del Ecuador – Políticas y Estrategias*. Ecuador.

Crespo, P. J., Feyen, J., Buytaert, W., Bücker, A., Breuer, L., Frede, H. G., & Ramírez, M. (2011). *Identifying controls of the rainfall–runoff response of small catchments in the tropical Andes (Ecuador)*. *Journal of Hydrology*, 407(1-4), 164-174.

Guachamín, W., Cadena, J., Carvajal, J., & García, F. (2015). *Cuenca Rio Mira Mapa De Escurrimiento* (Ecuador, INAMHI). Quito: INAMHI.

Gutscher, M. A., Malavieille, J., Lallemand, S., & Collot, J. Y. (1999). *Tectonic segmentation of the North Andean margin: impact of the Carnegie Ridge collision*. *Earth and Planetary Science Letters*, 168(3-4), 255-270.

Hughes, R., & Bermúdez, R. (1997). *Geology of the Cordillera Occidental of Ecuador between 0 00' and 1 00' S*: Quito, Ecuador, Proyecto de Desarrollo Minero y Control Ambiental. Programa de Información Cartográfica y Geológica Report, 4, 75.

Instituto Nacional de Estadísticas y Censos, INEC. (2000). *III Censo Nacional Agropecuario*. Instituto Nacional de Estadísticas y Censos de Ecuador. Quito: INEC/MAG. [access 2006 Jul 03]. <http://www.inec.gov.ec/interna.asp>.

Instituto Nacional de Meteorología e Hidrología, INAMHI. (2005). *Anuario meteorológico 2005*. INAMHI. Ecuador

Kuentz, A., Arheimer, B., Hundecha, Y., & Wagener, T. (2017). *Understanding hydrologic variability across Europe through catchment classification*. *Hydrology and Earth System Sciences*, 21(6), 2863-2879.

Lehman, A., O'Rourke, N., Hatcher, L., & Stepanski, E. (2013). *JMP for basic univariate and multivariate statistics: methods for researchers and social scientists*. Sas Institute.

MAGAP, S. (n.d.). *Geomorfología*. Retrieved November 12, 2018, from <http://geoportal.agricultura.gob.ec/index.php/metadatos>

McCourt, W., Duque, P., & Pilatasig, L. (1997). *Geology of the Western Cordillera between 1°-2°S*, Proyecto de Desarrollo Minero y Control Ambiental, Programa de Información cartografica y Geológico. Informe No. 3, CODIGEM-BGS, Quito, Ecuador.

McMillan, H., Westerberg, I., & Branger, F. (2016). *Five guidelines for selecting hydrological signatures*. *Hydrological Processes*, 31(26), 4757-4761.

Molina, A., Govers, G., Vanacker, V., Poesen, J., Zeelmaekers, E., & Cisneros, F. (2007). *Runoff generation in a degraded Andean ecosystem: Interaction of vegetation cover and land use*. *Catena*, 71(2), 357-370.

Olden, J. D., & Poff, N. L. (2003). *Redundancy and the choice of hydrologic indices for characterizing streamflow regimes*. *River Research and Applications*, 19(2), 101-121.

Pardo-Casas, F., & Molnar, P. (1987). *Relative motion of the Nazca (Farallon) and South American plates since Late Cretaceous time*. *Tectonics*, 6(3), 233-248.

Podwojewski, P. (1999). *Los suelos de las altas tierras andinas: los páramos del Ecuador*. *Bol Soc Ecuador Cie Suelo*, 18(9), 14.

R Foundation (n.d.). *The R Project for Statistical Computing*. Retrieved from <https://www.r-project.org/>

SIGTIERRAS, Sistema Nacional de Información y Gestión de Tierras Rurales e Infraestructura Tecnológica (2017). *Memoria explicativa del Mapa de Órdenes de Suelos del Ecuador*. Quito, Ecuador.

Shmueli, G. (2010). *To explain or to predict?*. *Statistical science*, 25(3), 289-310.

Spencer, N. (2011). *Mapa Geológico de la República del Ecuador*, map, scale 1:000.000, INIGEMM, Ecuador.

Spikings, R. A., Winkler, W., Seward, D., & Handler, R. (2001). *Along-strike variations in the thermal and tectonic response of the continental Ecuadorian Andes to the collision with heterogeneous oceanic crust*. *Earth and Planetary Science Letters*, 186(1), 57-73.

Spikings, R. A., Winkler, W., Hughes, R. A., & Handler, R. (2005). *Thermochronology of allochthonous terranes in Ecuador: Unravelling the accretionary and post-accretionary history of the Northern Andes*. *Tectonophysics*, 399(1-4), 195-220.

Tosse, O., & Iza, C. (2017). *Plan binacional para la gestión integral de recurso hídrico de las cuencas transfronterizas Carchi-Guáitara, Mira y Mataje Colombia – Ecuador: Síntesis*. Bogotá, D.c.-, Quito: Colombia. Ministerio de Ambiente y Desarrollo Sostenible; Ecuador. Senagua.

Vallejo, C., Spikings, R. A., Luzieux, L., Winkler, W., Chew, D., & Page, L. (2006). *The early interaction between the Caribbean Plateau and the NW South American Plate*. *Terra Nova*, 18(4), 264-269.

Vallejo, C., Winkler, W., Spikings, R., & Luzieux, L. (2009). *Evolución geodinámica de la cordillera occidental (cretácico tardío-paleógeno)*.

Vélez Upegui, J. J., & Botero Gutiérrez, A. (2011). *Estimation of the time of concentration and the lag time at San Luis creek basin, Manizales*. *Dyna*, 78(165), 58-71.

Willems, P. (2000). *Probabilistic Immission Modelling of Receiving Surface Waters*. PhD Dissertation, Department of Civil Engineering, K.U. Leuven, Leuven, Belgium, 347pp.

Willems, P. (2009). *A time series tool to support the multi-criteria performance evaluation of rainfall-runoff models*. *Environmental Modelling & Software*, 24(3), 311-321.

XI. APPENDIX

11.1 TABLES

Table 7 Meteorological information with daily information for the period 1985-2015.

Code	Name	Coordinates UTM WGS84 17S		Altitude [masl]
		x	y	
M0001	INGUINCHO	789319	10028583	3140
M0021	ATUNTAQUI	808388	10038764	2200
M0084	BOLIVAR-CARCHI INERHI	847626	10058917	2790
M0085	SALINAS-IMBABURA INERHI	817142	10050878	1730
M0086	SAN VICENTE DE PUSIR	829118	10054327	1891
M0102	EL ANGEL	840093	10068513	3000
M0103	SAN GABRIEL	853808	10066399	2860
M0104	MIRA-FAO GRANJA LA PORTADA	830662	10060845	2275
M0105	OTAVALO	806422	10026927	2550
M0106	LITA	783606	10095675	720
M0107	CAHUASQUI-FAO	810207	10056962	2335
M0110	SAN PABLO DEL LAGO	812074	10023364	2700
M0282	TANGALI	795486	10027941	2860
M0301	FF CC CARCHI	818527	10066957	1280
M0302	MIRA	829115	10060814	2410
M0303	BOLIVAR-CARCHI INAMHI	844470	10055563	2800
M0304	MONTE OLIVO	843608	10045478	2040
M0305	JULIO ANDRADE	864521	10072242	2890
M0307	GRUTA LA PAZ	851962	10054983	2470
M0309	SAN JUAN DE LACHAS-RIO BLANCO	805149	10082811	950
M0310	MARIANO ACOSTA	835780	10033023	2980
M0311	CAHUASQUI	810207	10056962	2340
M0312	PABLO ARENAS	812250	10055211	2340
M0314	AMBUQUI	832866	10046796	1880
M0315	PIMAMPIRO	840533	10043138	2090
M0316	ZULETA	824454	10022352	2910
M0317	COTACACHI-HDA.ESTHERCITA	803809	10033383	2410
M0319	SAN RAFAEL DEL LAGO	806999	10021765	2790
M0320	HDA.LA VEGA	813808	10020352	2700
M0321	TOPO-IMBABURA(ANGLA)	815231	10023026	2860
M0322	CAMBUGAN	790349	10029784	3160
M0323	ACHUPALLAS-IMBABURA	791865	10031659	3205

M0324	SAN FRANCISCO DE SIGSIPAMBA	843581	10032625	2230
M0328	HDA.LA MARIA-ANEXAS(LETICIA)	803684	10038178	2600
M0333	INGUINCHO # 8	788060	10028831	3300
M0334	INGUINCHO # 9	788091	10028954	3410
M0554	ALTO TAMBO	776305	10095056	750
M0562	RIO BLANCO INECEL	802952	10083855	950
M0604	SIGSICUNGA-HDA.	791093	10027694	3200
M0692	TOBAR DONOSO	776123	10130367	220
M0693	BUENOS AIRES-IMBABURA	797267	10069036	2200
M0694	MALDONADO-CARCHI	820950	10100221	1550
M0910	MORASPUGRO-IMBABURA	795610	10029724	2860
M0911	RIO BLANCO (CUENCA EXP.)	800345	10027511	2550
M1199	HUACA HACIENDA-UPEC	861490	10067996	2837
M1201	CHIRIYACU	811386	10048663	2262
M1240	IBARRA	819241	10036493	2256
M1248	EL CRISTAL	780051	10091985	435
M1250	LA CONCEPCION - GRANJA ALFONSO TADEO UPEC	819146	10066127	1436

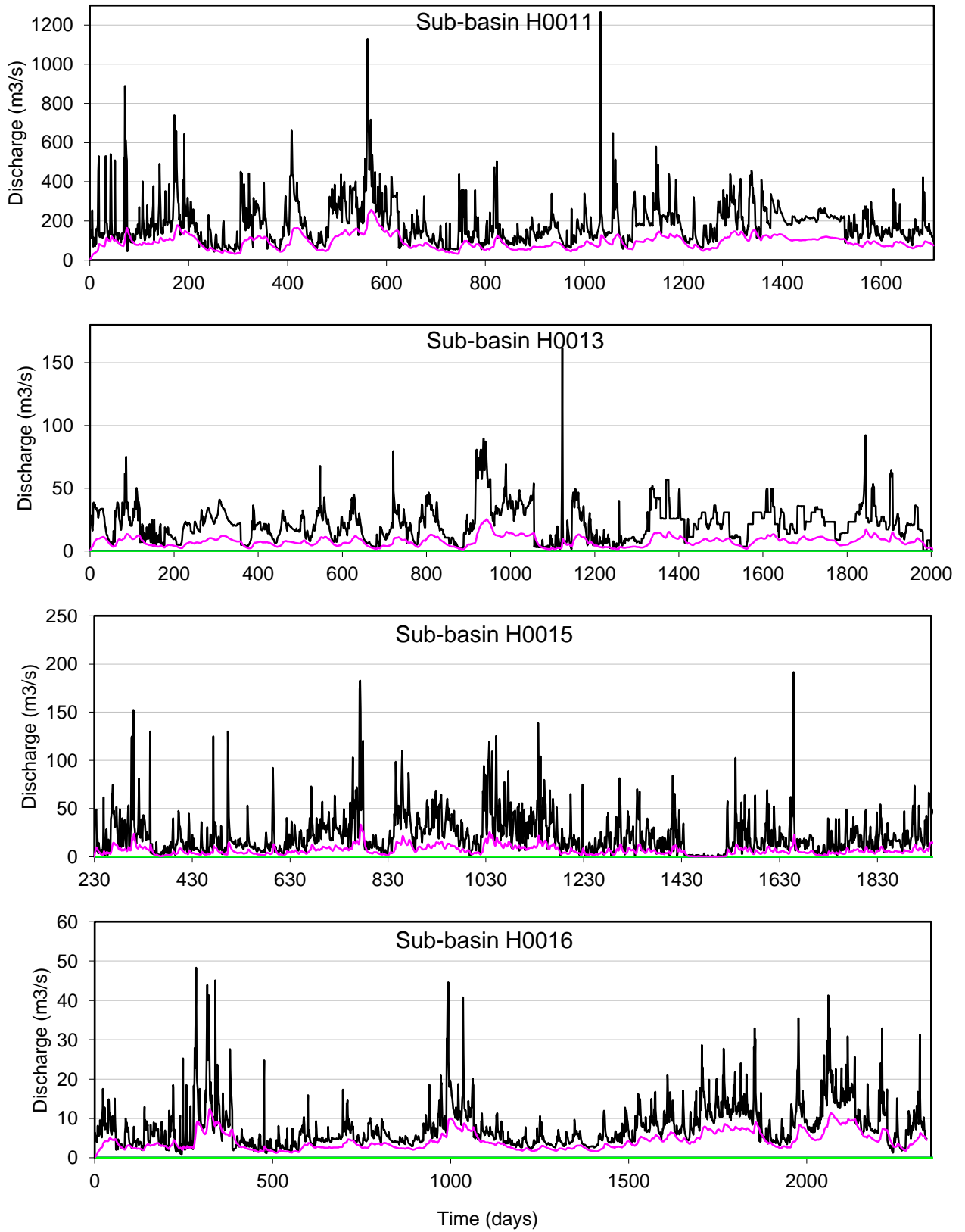
Table 8 Original source of lithologies of the study area with their corresponding abbreviation (MAGAP, n.d).

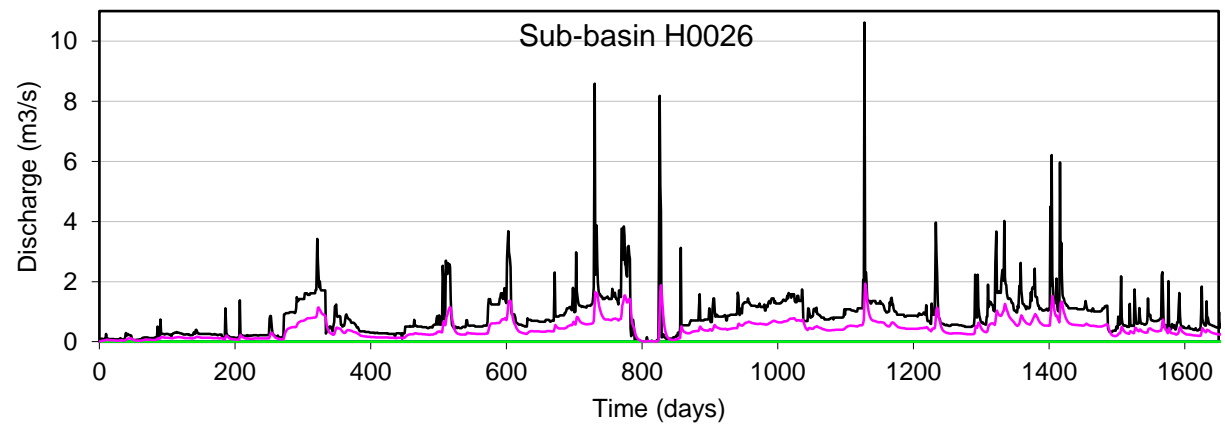
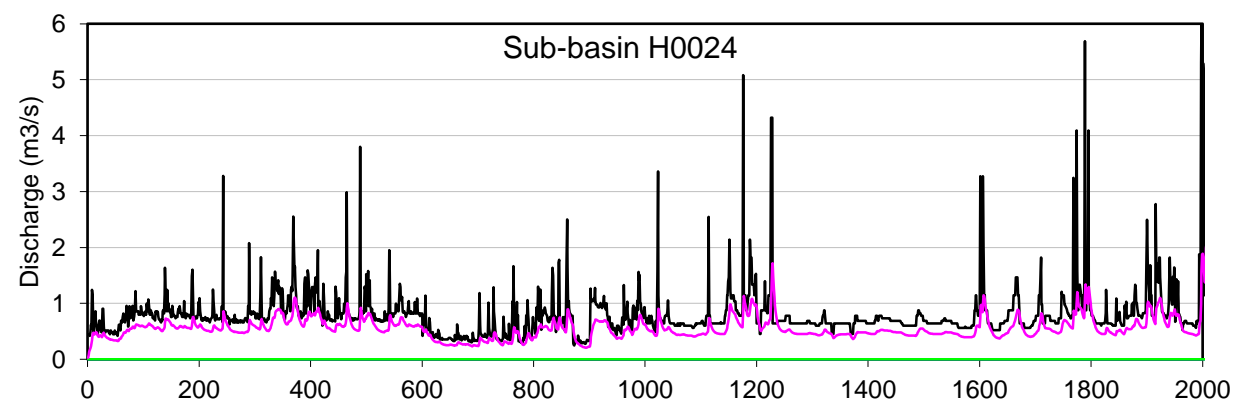
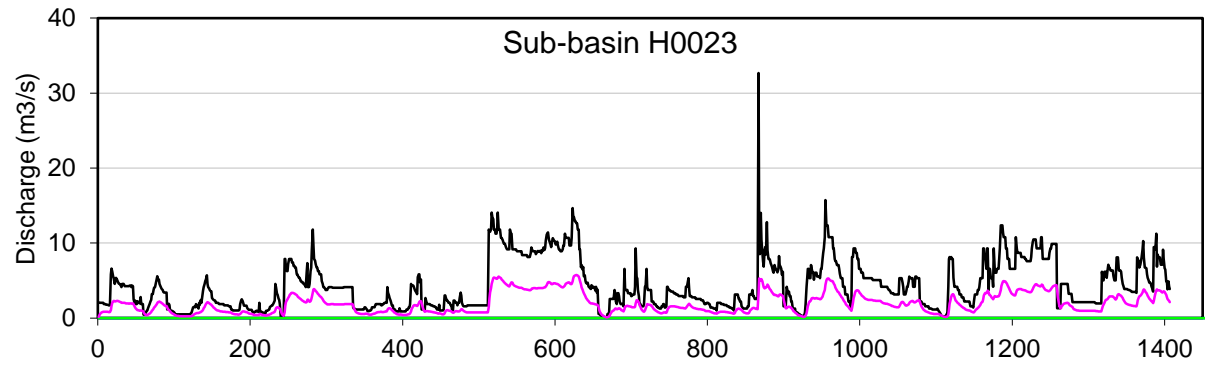
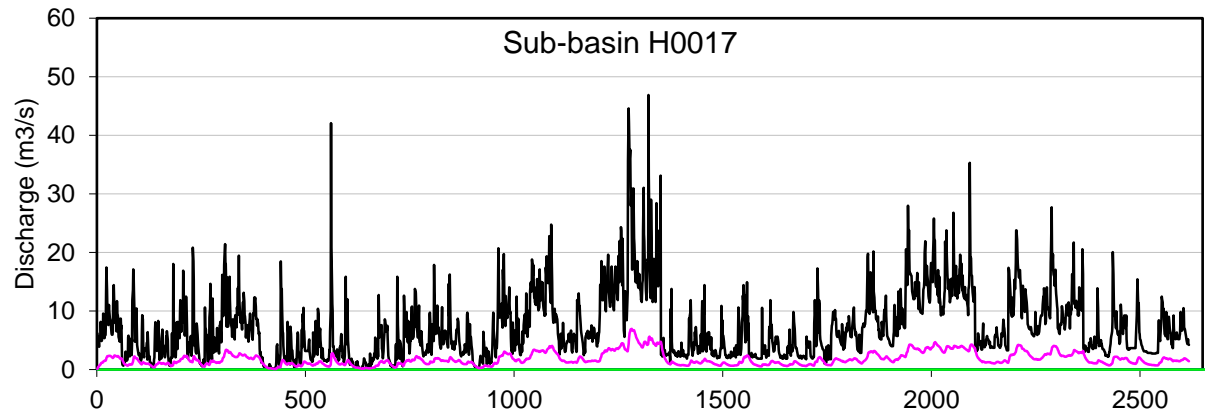
Abbrev.	Lithology	Abbrev.	Lithology
A1	Andesitas, brechas y aglomerados	A22	Sedimentos volcánicos y tobas silicificadas intercaladas con lavas silicificadas
A2	Esquistos, moscovita, granate y grafito	A23	Lavas andesíticas y brechas volcánicas con productos piroclásticos flujos de lava y piroclastos
A3	Conglomerados volcánicos, areniscas volcánicas y sedimentos tobáceos	A24	Brechas andesíticas con lavas y sedimentos
A4	Volcánicos indiferenciados	A25	No aplica
A5	Limos, arcillas, arenas gravas y bloques en proporciones variables	A26	Conglomerado compacto compuesto por fragmentos subangulares milimétricos a centimétricos
A6	Granodiorita	A27	Lavas andesíticas de grano fino a medio, aglomerados y flujos laharíticos

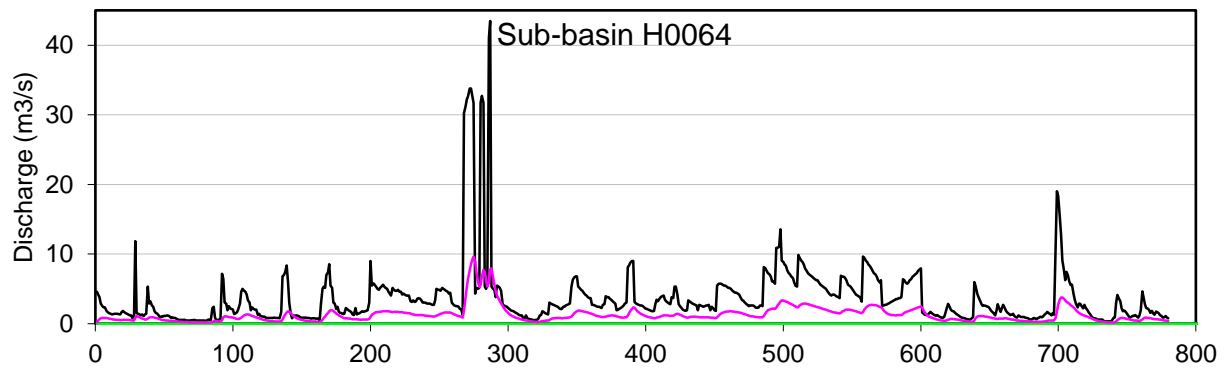
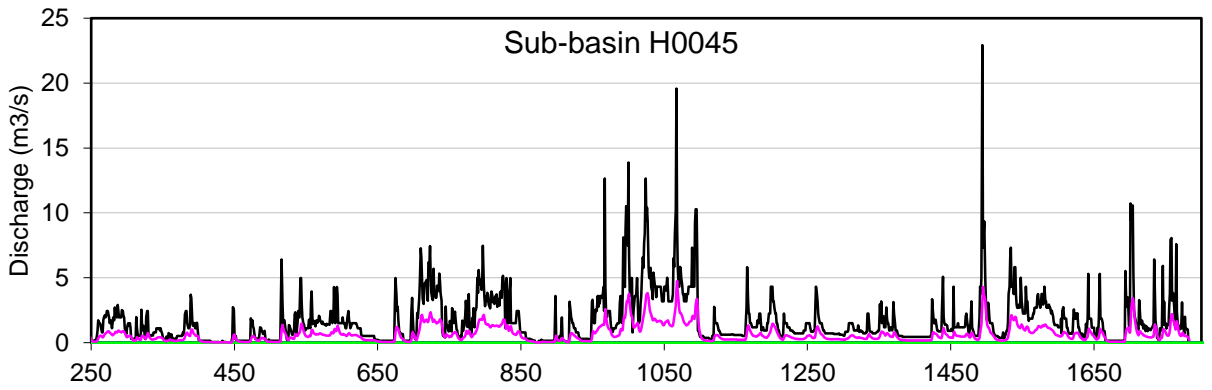
- | | | | |
|-----|---|-----|---|
| A7 | Andesitas basálticas de color gris verdusco | A28 | Toba andesítica de color café claro, ceniza y lapilli |
| A8 | Areniscas, lutitas chertosas, calizas y grauvacas | A29 | Tilitas, arenas, gravas y bloques sedimentarios de composición variable |
| A9 | Rocas volcanoclásticas con lavas e intrusiones subvolcánicas | A30 | Lavas grises con material piroclástico y brechas volcánicas |
| A10 | Depósito de toba volcánica y ceniza, en la base se encuentran piroclastos pómez y lapilli | A31 | Brechas, tobas, productos piroclásticos y conglomerados volcánicos |
| A11 | Arenas de grano medio a grueso, gravas y bloques | A32 | Lavas andesíticas verdosas, brechas y tobas |
| A12 | Basaltos en almohadillas, lavas y brechas | A34 | Lavas andesitas piroxénicas con abundantes fenocristales de plagioclasa |
| A13 | Arenas de grano medio a fino con intercalación de limos y gravas | A35 | Andesitas grises claras y oscuras, tobas, brechas y aglomerados |
| A14 | Arenas de grano de medio a grueso, gravas con cantos subangulares a angulares | A36 | Esquistos micáceos, cuarcitas y gneis |
| A15 | Flujos piroclásticos y depósitos de caídas, lapilli, ceniza, líticos y pómez blanca amarillenta | A37 | Andesita gris oscura constituida de feldespatos piroxenos olivinos y óxidos de hierro |
| A16 | Lavas de composición andesítica, depósitos piroclásticos y domos dacíticos | A38 | Lavas andesíticas con plagioclasas y basaltos |
| A17 | Lavas de composición andesítica, aglomerados y brechas volcánicas | A39 | Andesita piroxénica de color gris, plagioclasa alterada en matriz de vidrio |
| A18 | Ceniza y lapilli | A40 | Andesitas basálticas, brechas volcánicas y tobas |
| A19 | Depósitos de toba volcánica y ceniza, en la base se encuentran piroclastos pómez y lapilli | A41 | Material piroclástico tipo ceniza, lapilli y tobas |
| A20 | Andesitas piroxénicas, depósitos de avalancha, flujos piroclásticos y flujos laharíticos | A42 | Rocas metamórficas pelíticas intercaladas localmente con metabasitas |
| A21 | Conglomerados masivos volcanoclásticos, brechas, areniscas, limolita y cherts | | |
-

11.2 SEASONAL BASEFLOW ANALYSIS

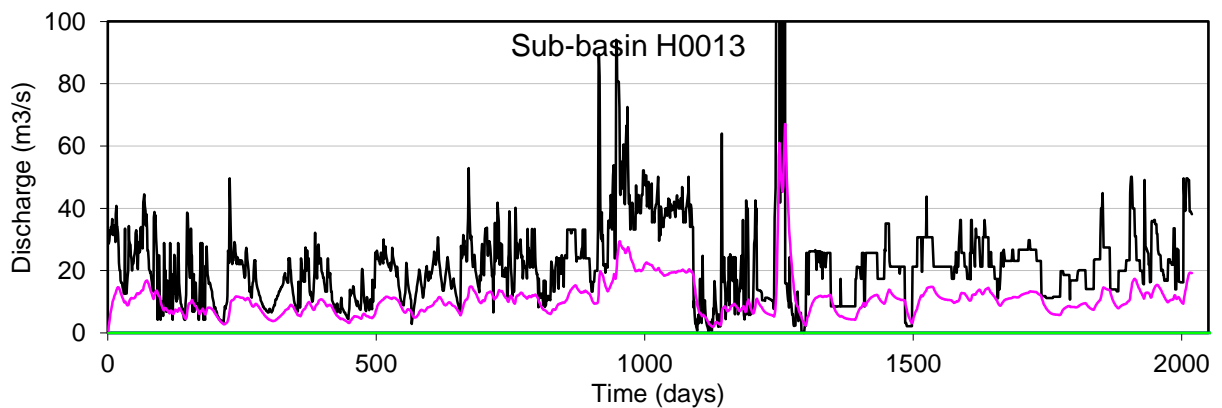
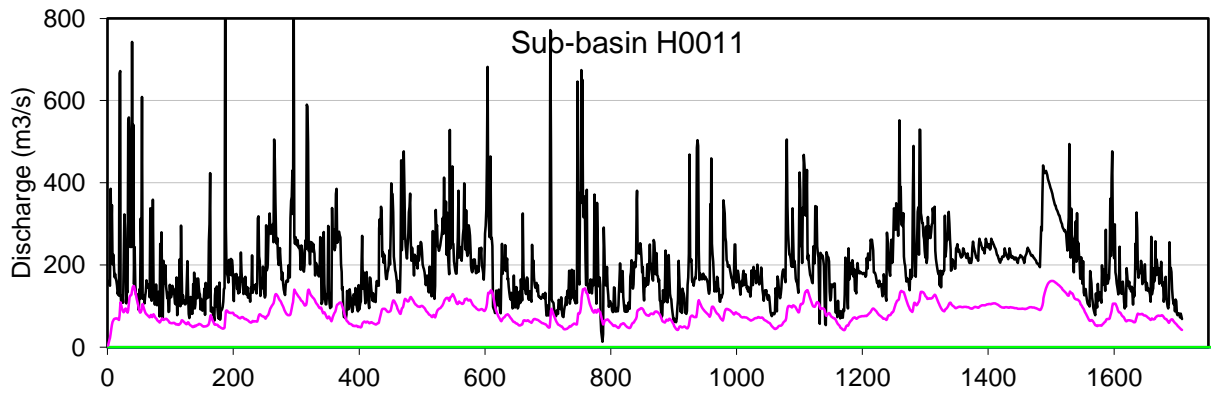
Seasonal baseflow (purple) separation component of the total discharge (black) for DJF

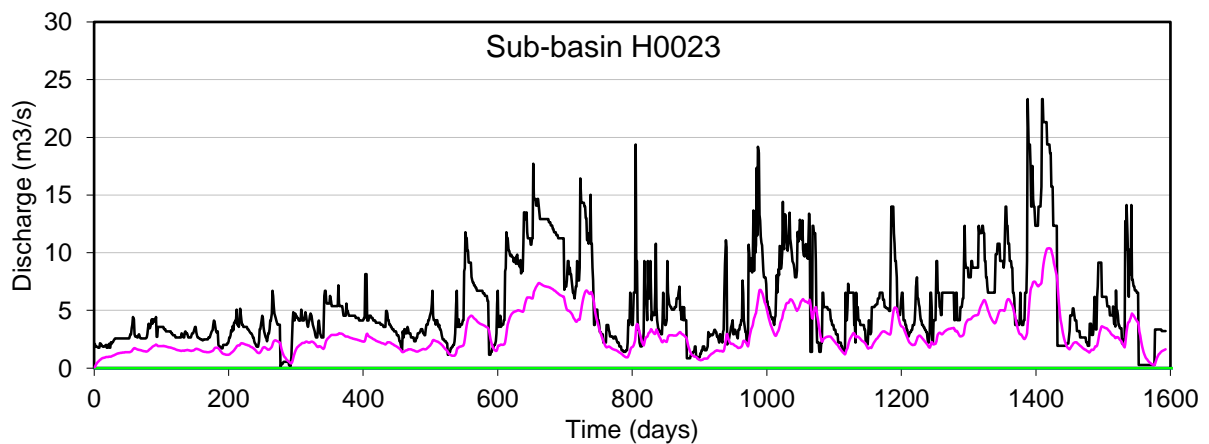
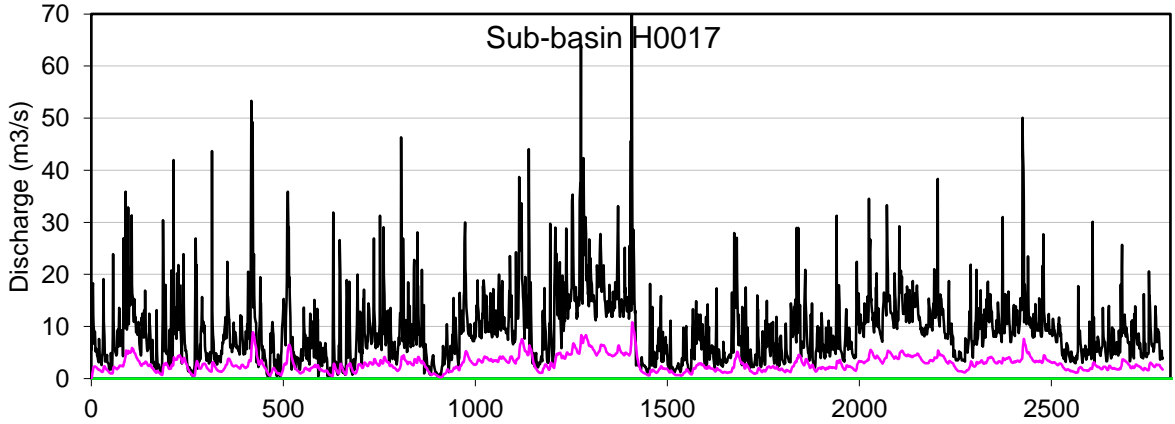
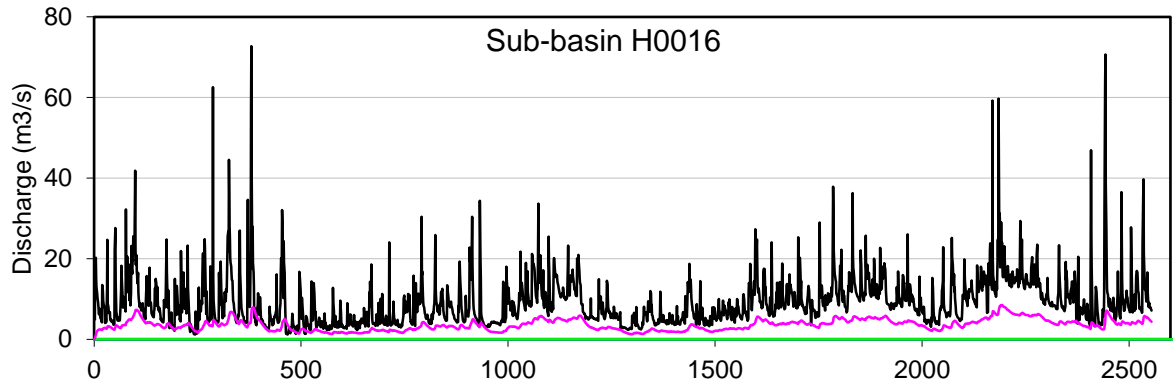
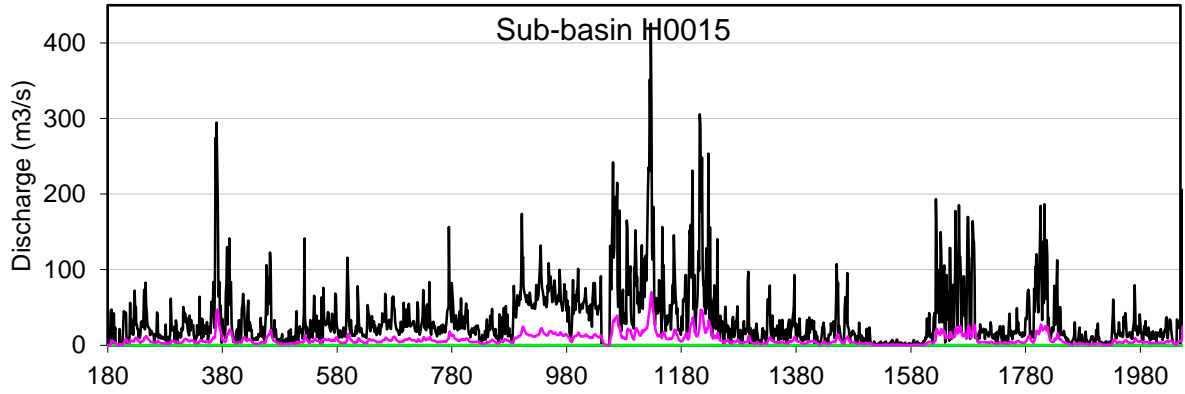


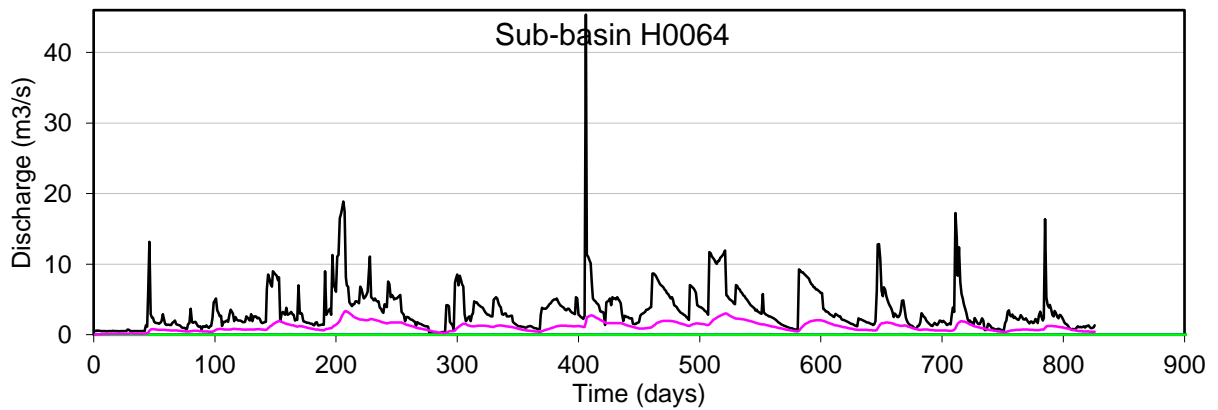
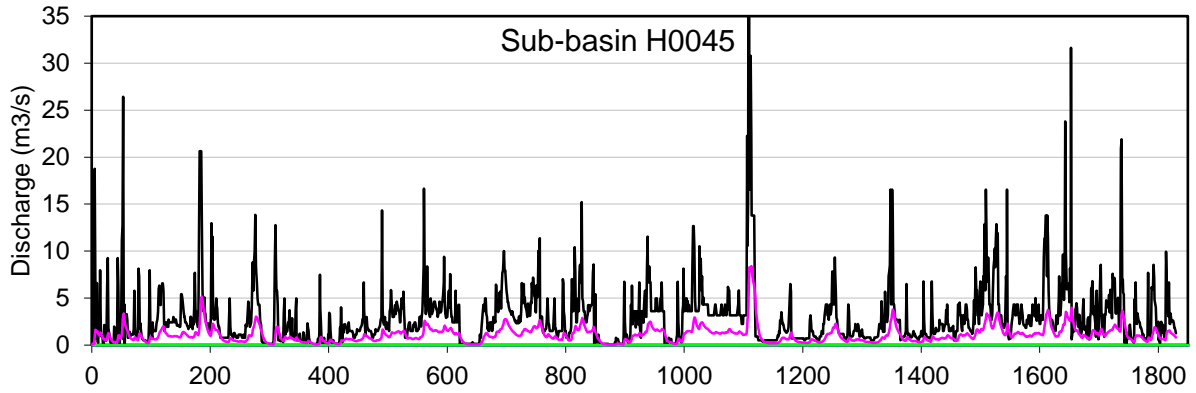
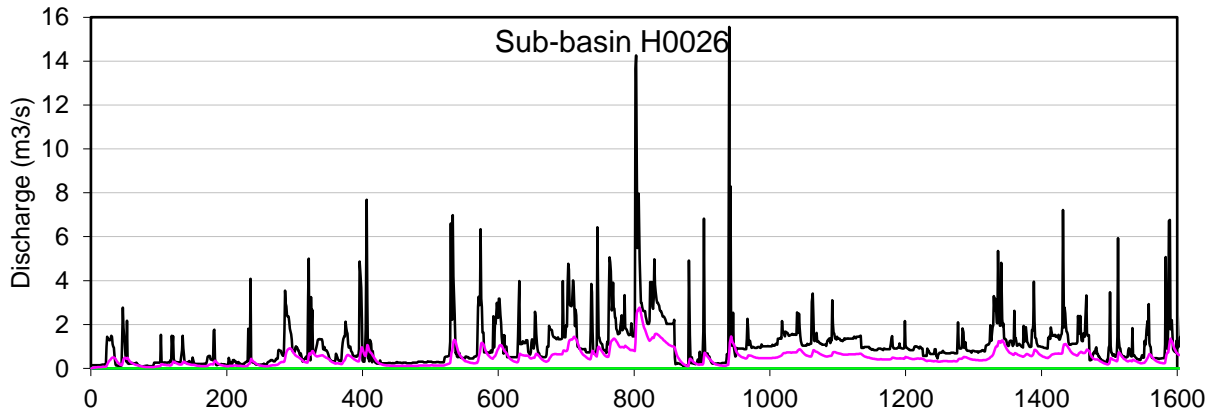
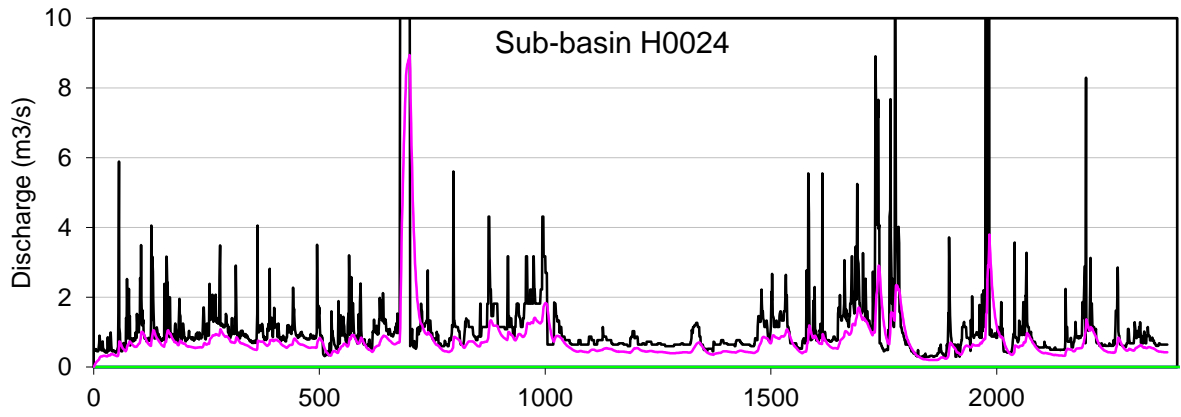




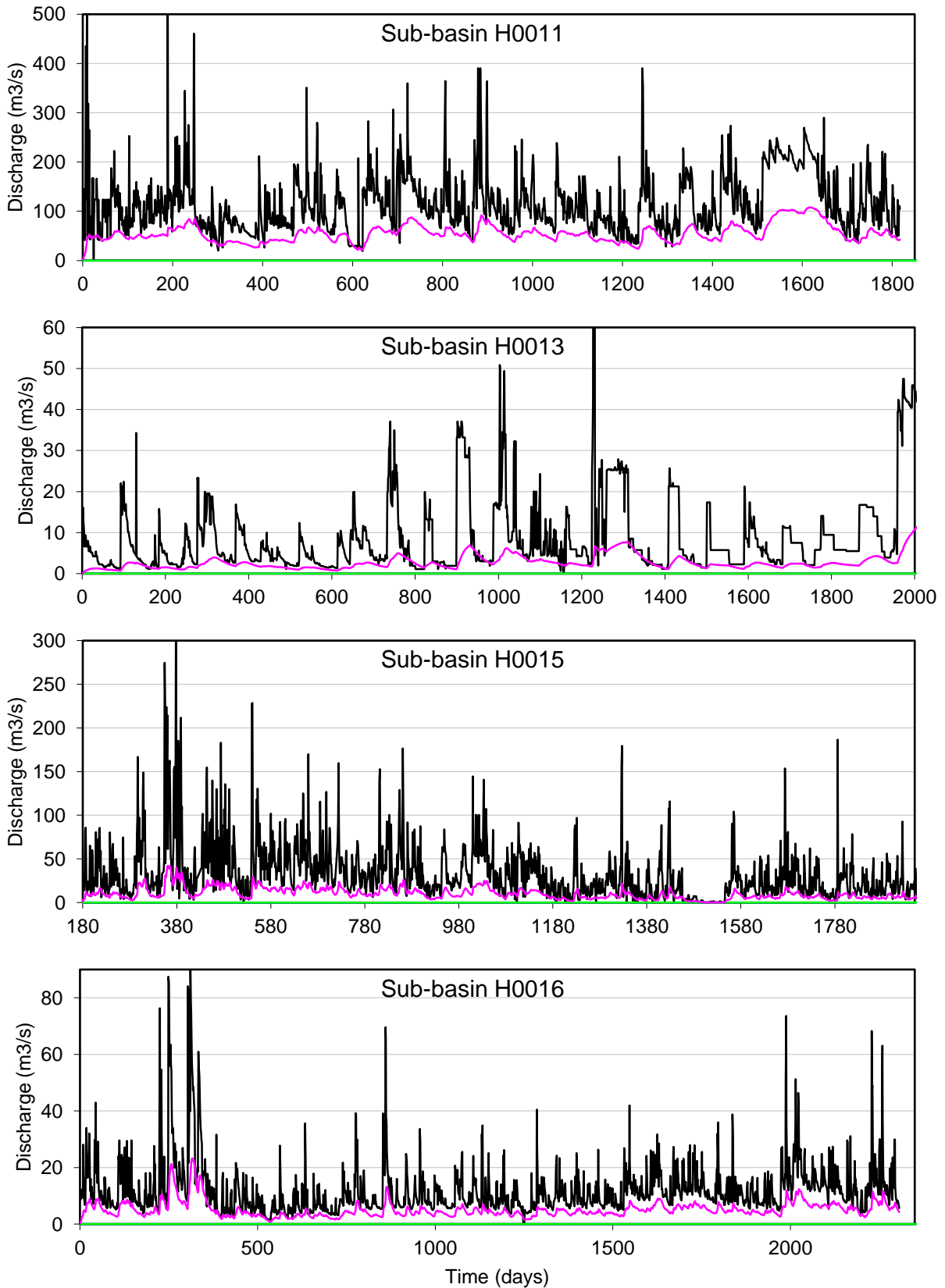
Seasonal baseflow (purple) separation component of the total discharge (black) for MAM

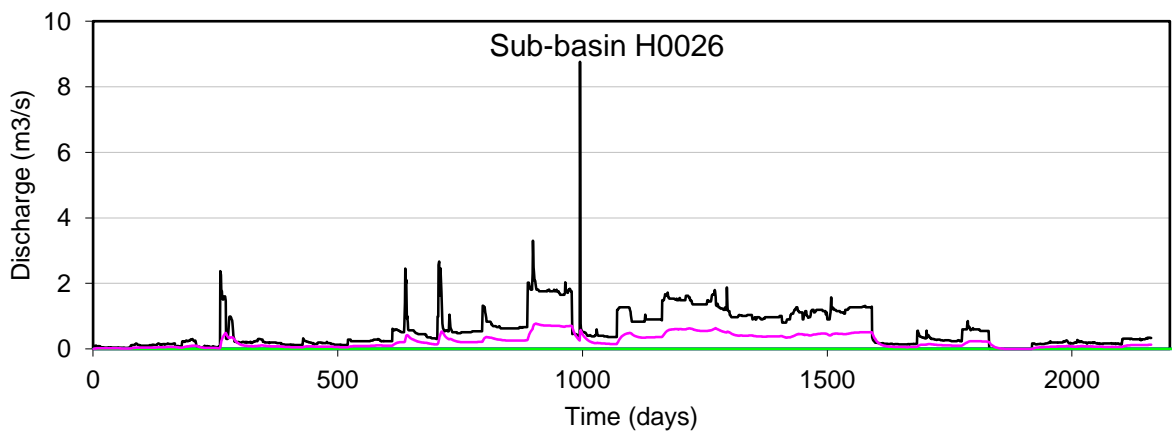
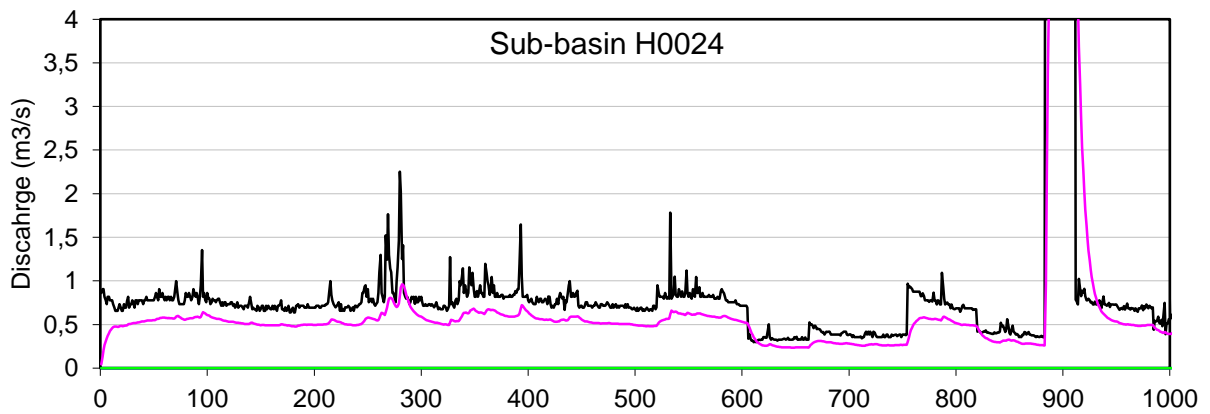
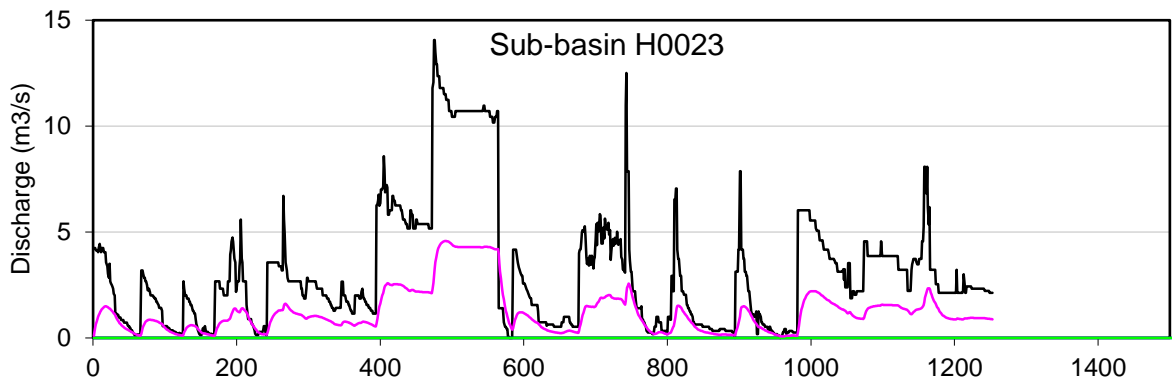
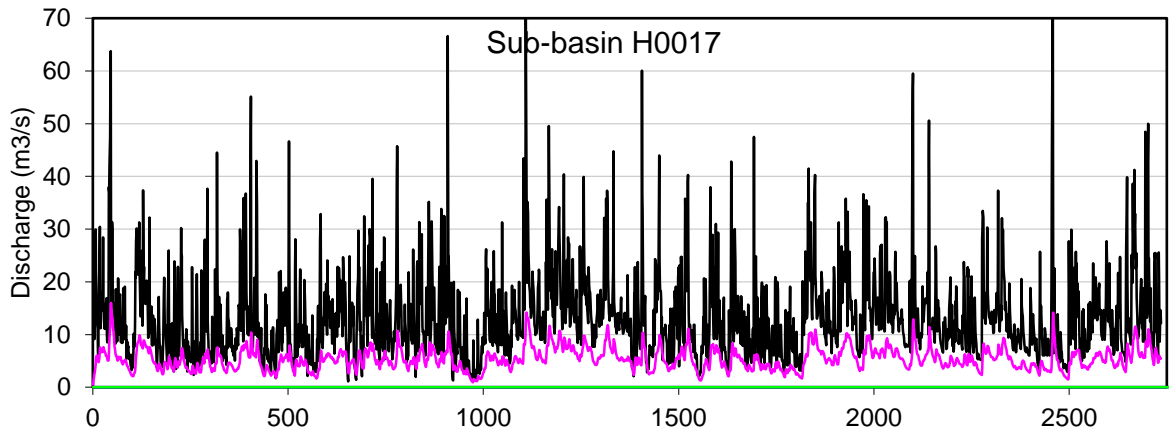


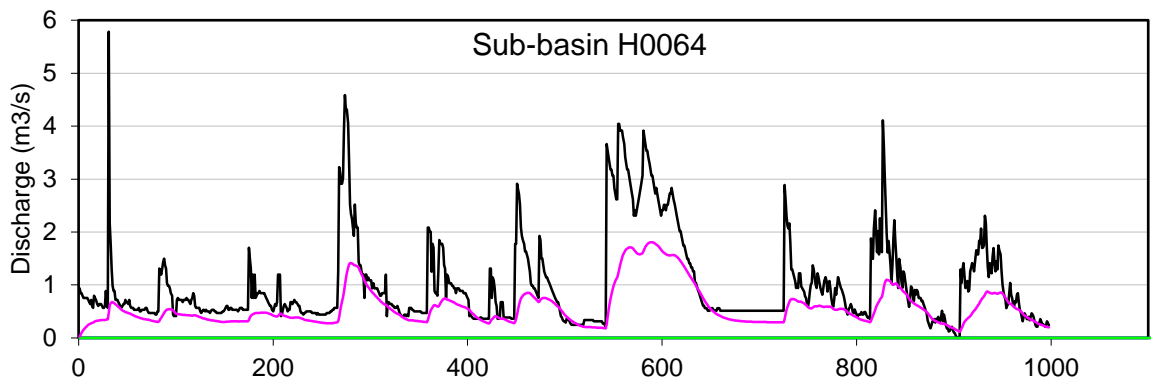
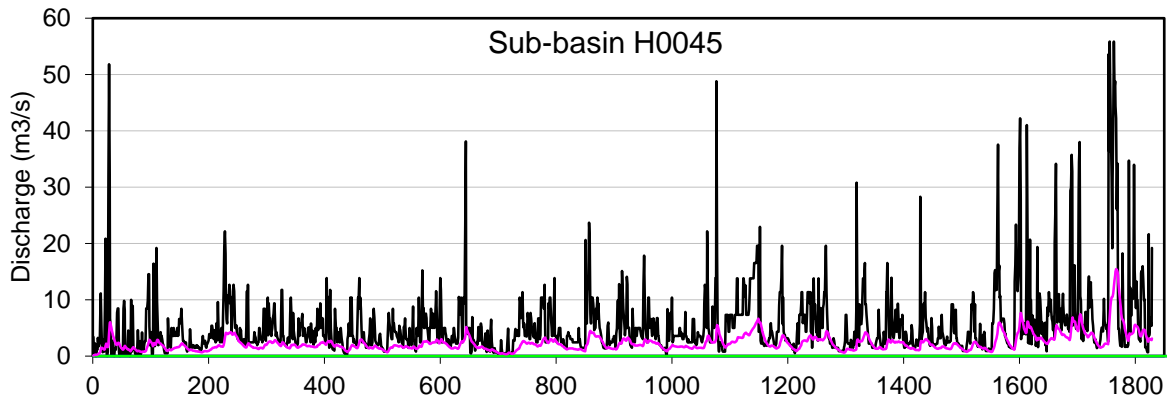




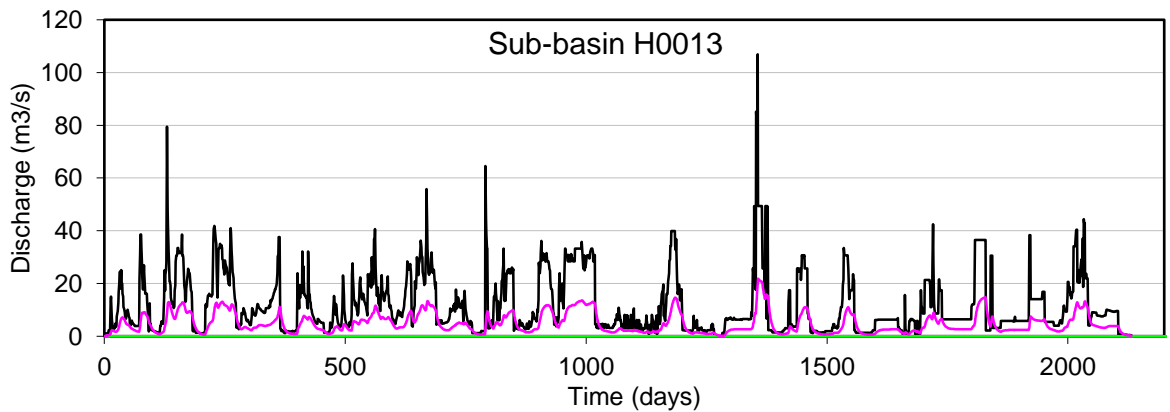
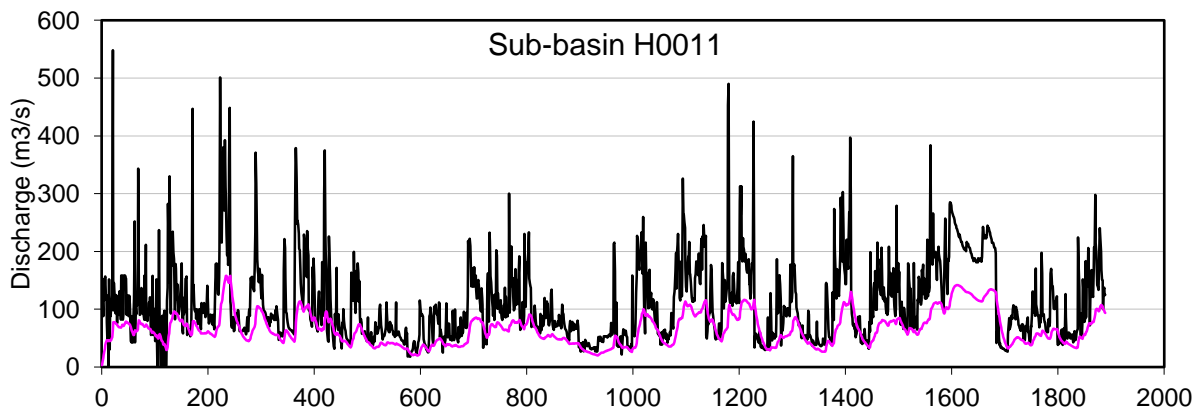
Seasonal baseflow (purple) separation component of the total discharge (black) for JJA

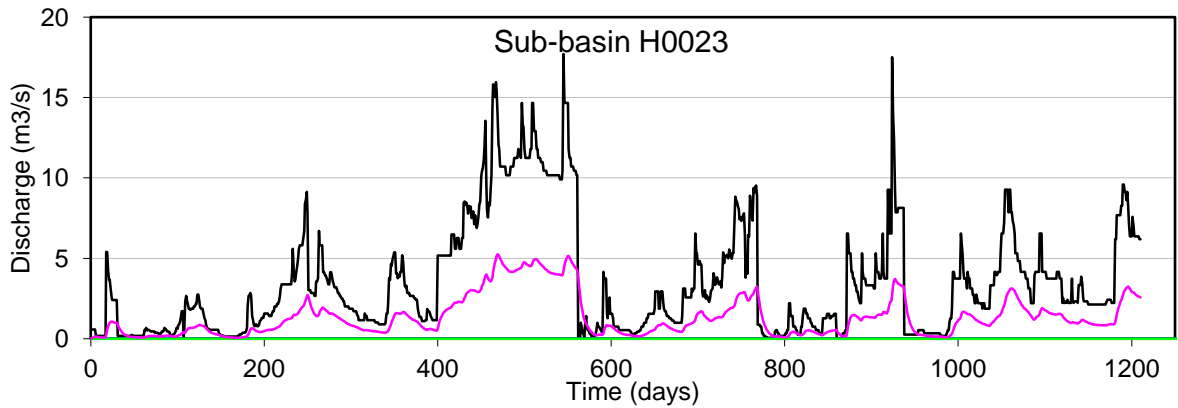
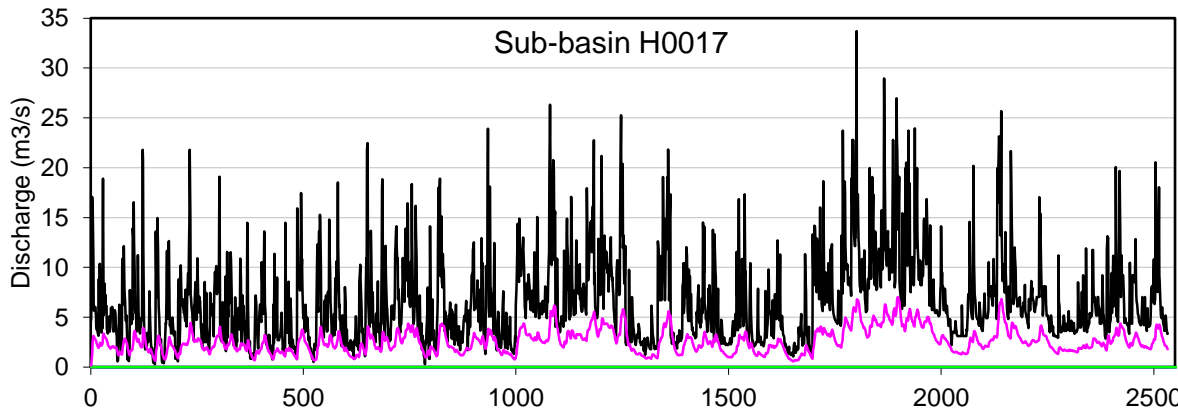
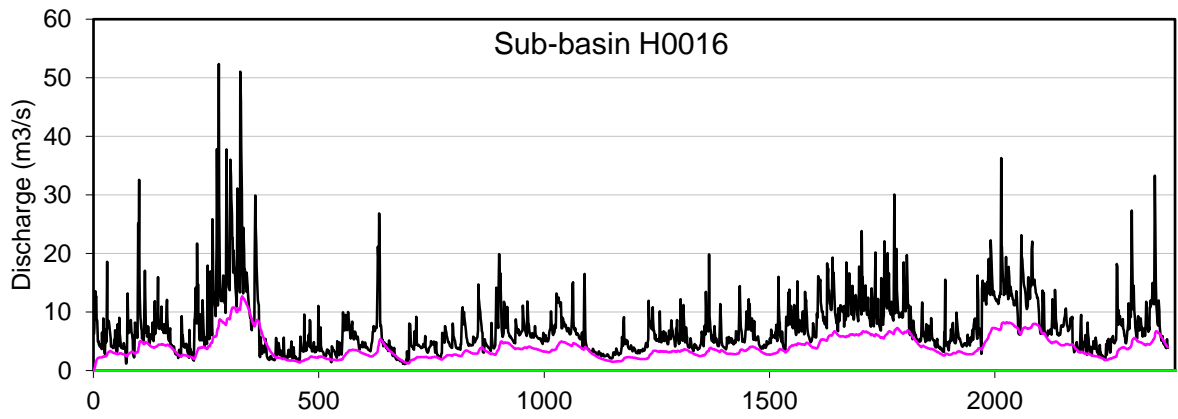
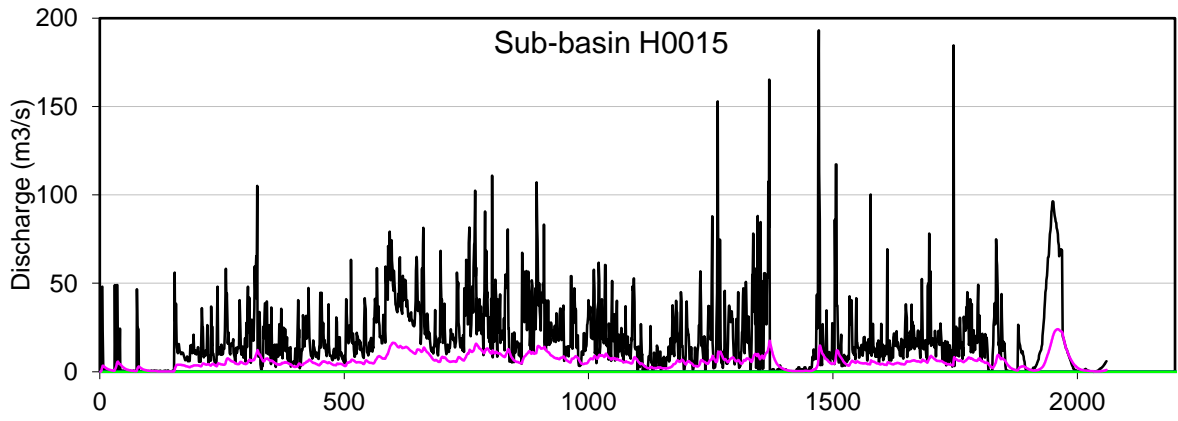


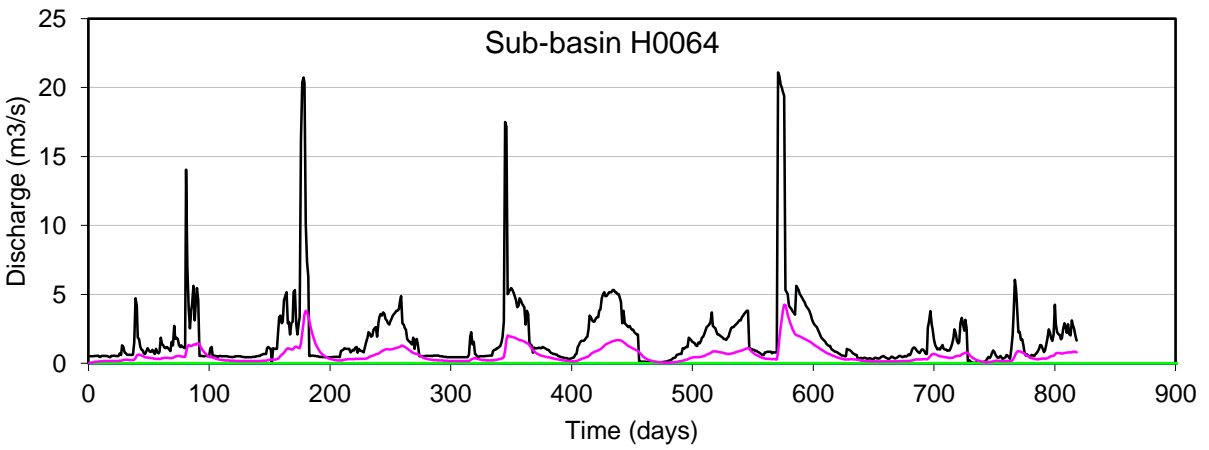
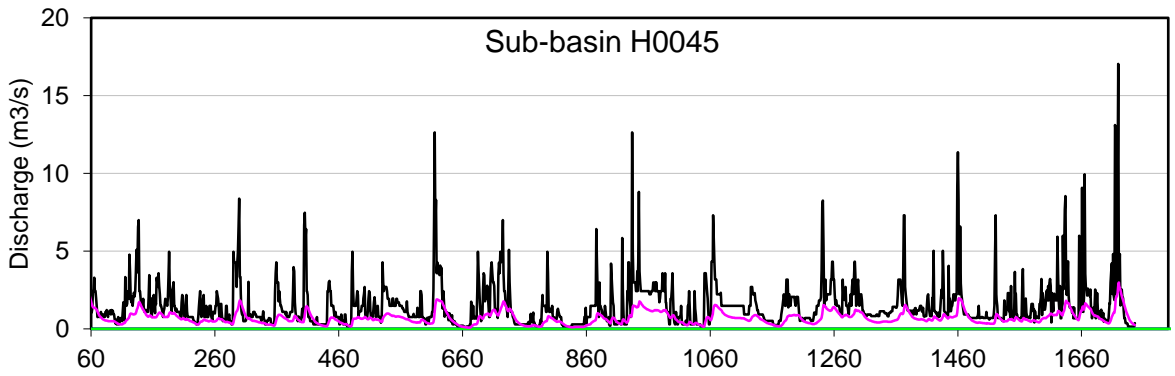
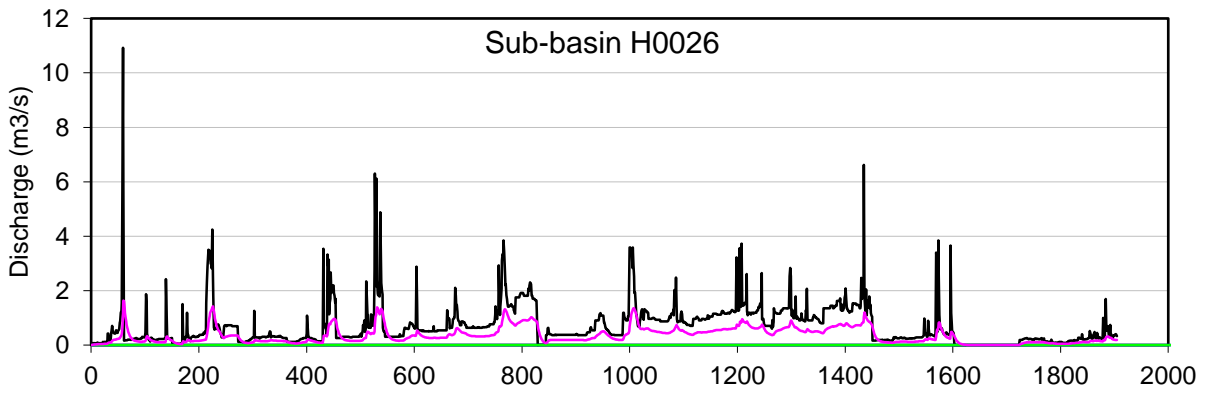
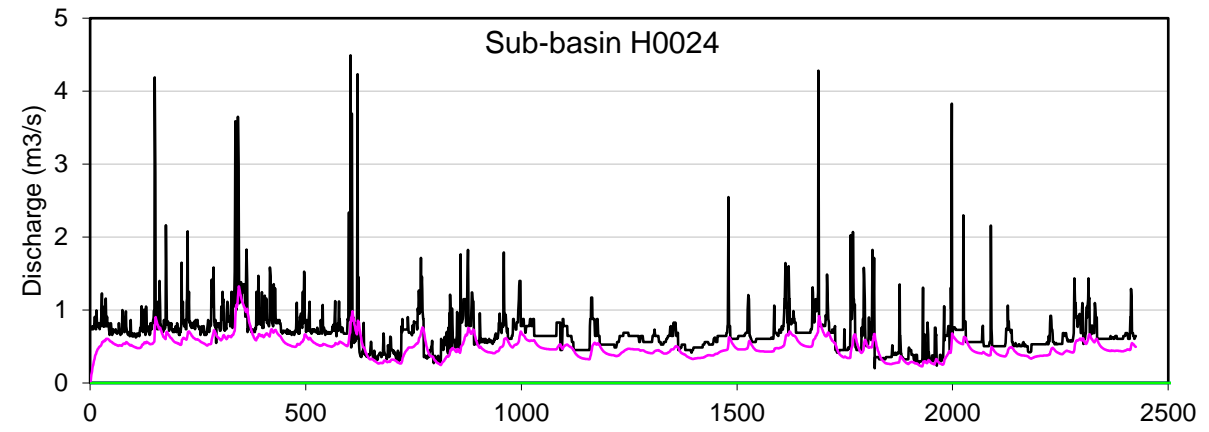




Seasonal baseflow (purple) separation component of the total discharge (black) for SON







11.3 CORRELATION MATRICES

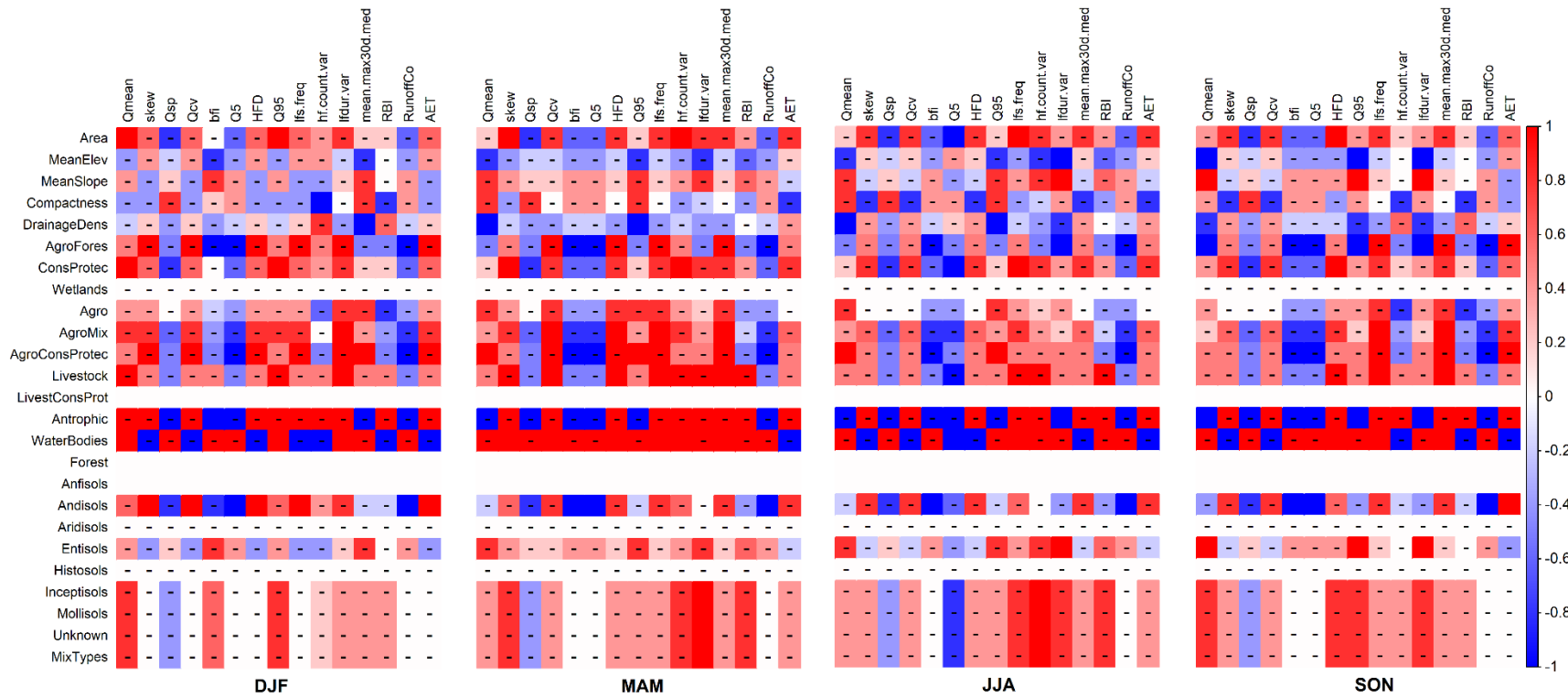


Fig. 18. Spearman correlation matrix of the G1 between proposed flow signatures and catchment descriptors related to topography, land cover, and soil type. Non-significant correlation according to the significance test are indicated with a dash (-).

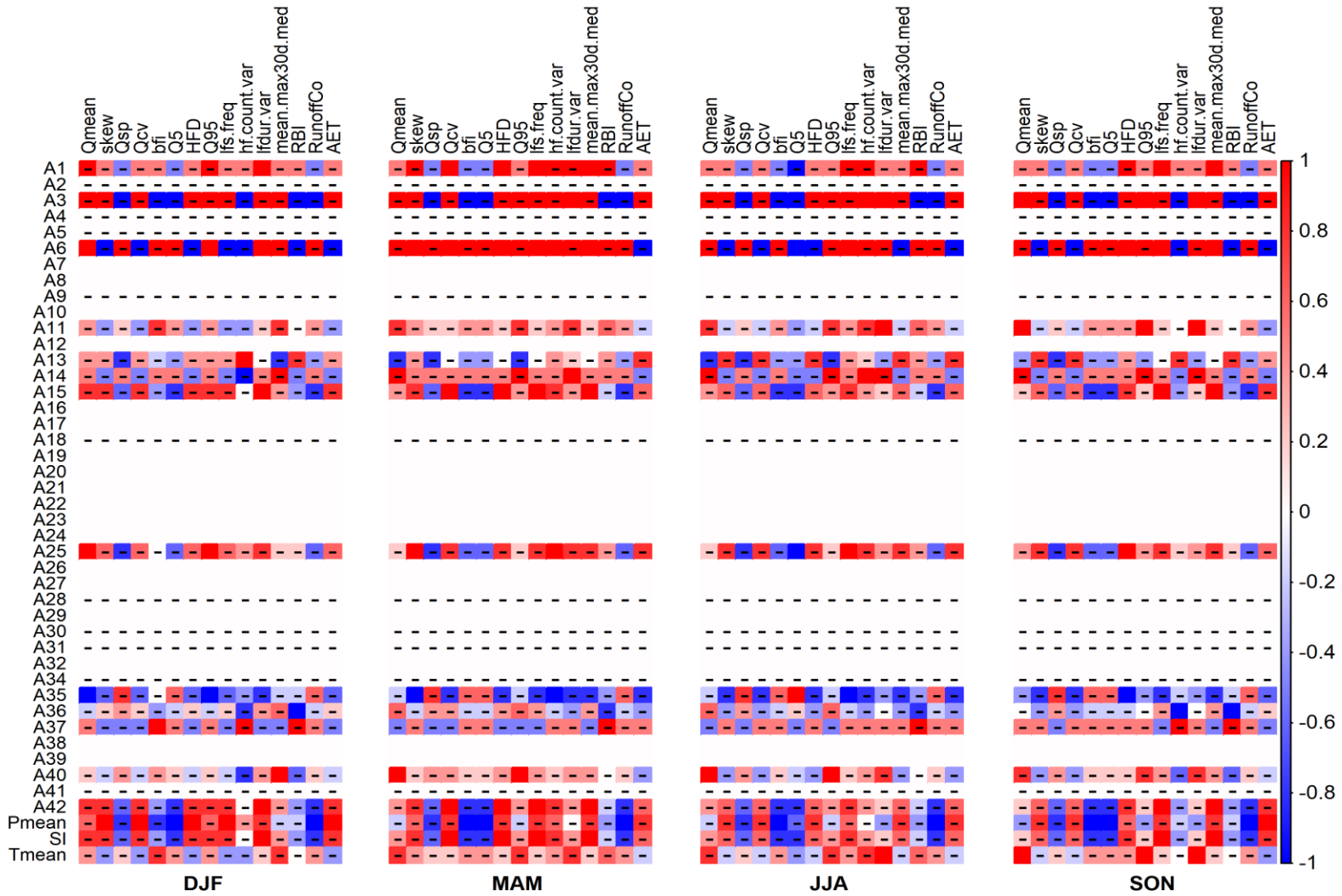


Fig. 19. Spearman correlation matrix of the G1 between proposed flow signatures and catchment descriptors related to geology, and climate. Non-significant correlation according to the significance test are indicated with a dash (-).

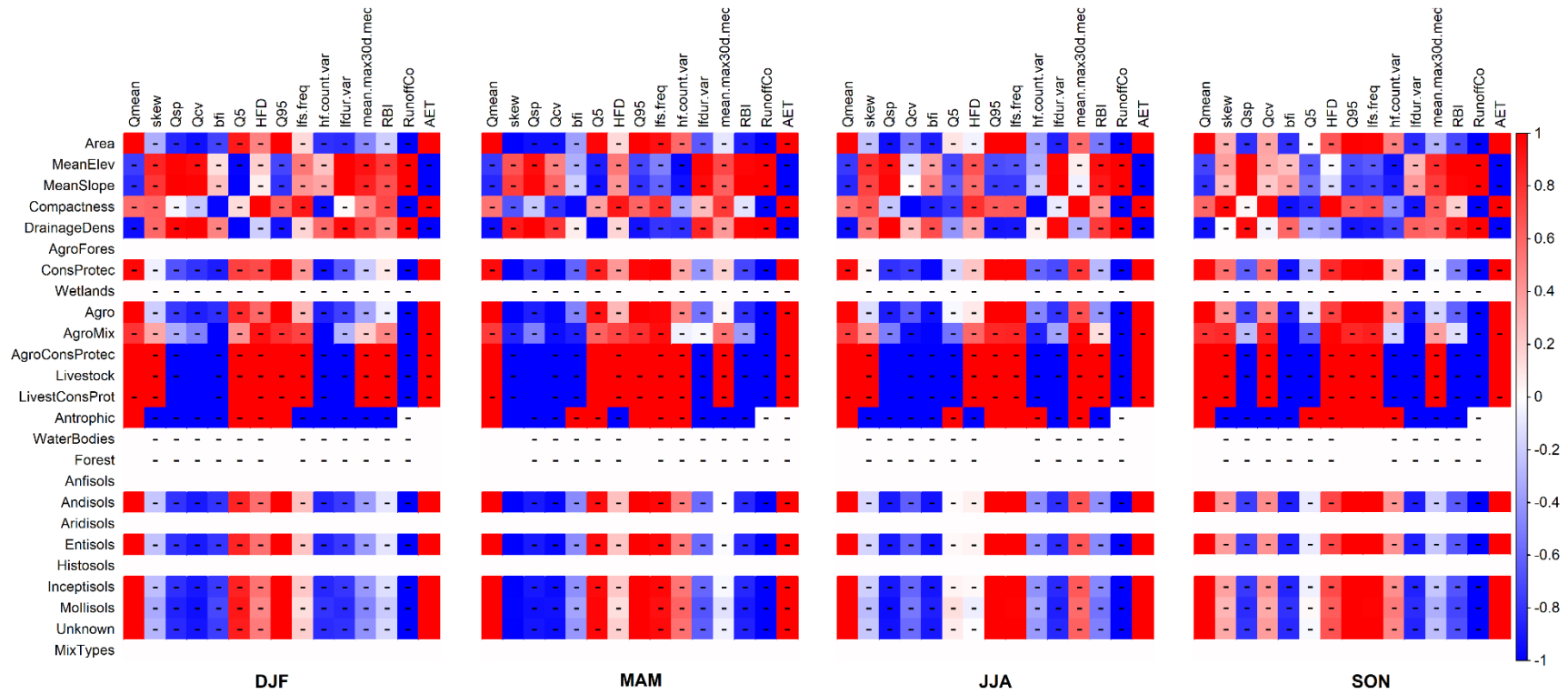


Fig. 20. Pearson correlation matrix of the G2 between proposed flow signatures and catchment descriptors related to topography, land cover, and soil type. Non-significant correlation according to the significance test are indicated with a dash (-).

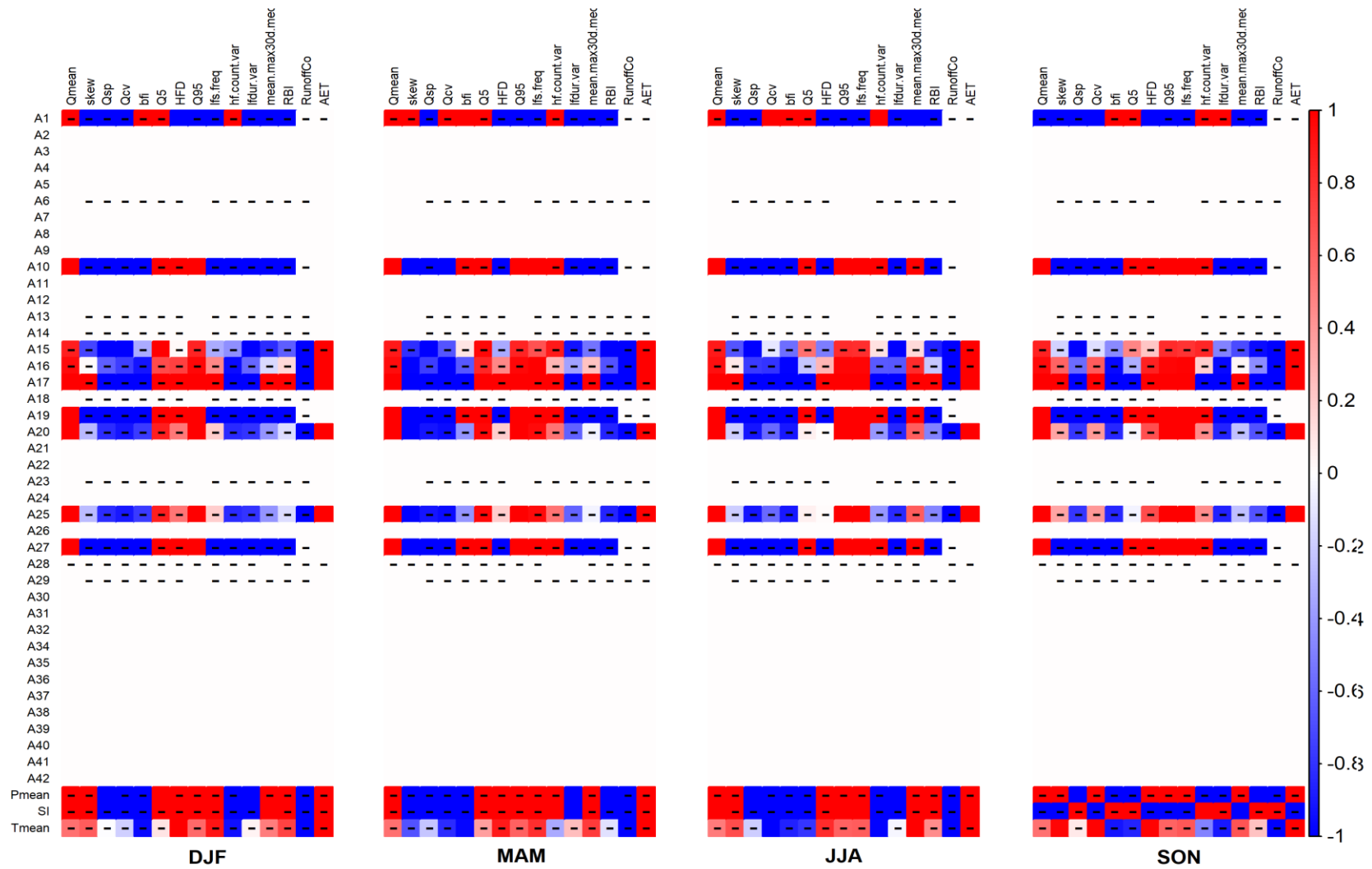


Fig. 21. Pearson correlation matrix of the G2 between proposed flow signatures and catchment descriptors related to geology, and climate. Non-significant correlation according to the significance test are indicated with a dash (-).

